

GENETIC ANALYSIS OF PHOTOSYNTHESIS *psbO*  
AND *psbV* GENES IN CYANOBACTERIA  
*SYNECHOCYSTIS*  
SP PCC6803

By

SUFIAN F. AL-KHALDI

Bachelor of Science  
University of Baghdad  
Baghdad, Iraq  
1985

Master of Science  
Oklahoma State University  
Stillwater, Oklahoma  
1992

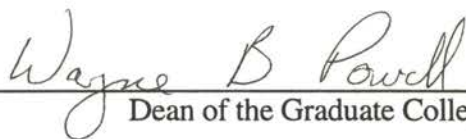
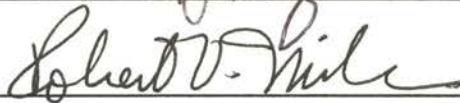
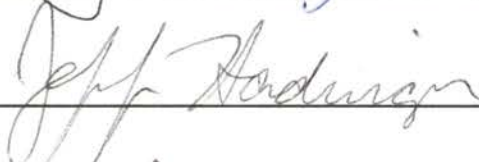
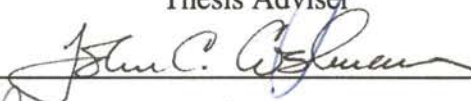
Submitted to the Faculty of the  
Graduate College of the  
Oklahoma State University  
in partial fulfillment of  
the requirements for the Degree of  
DOCTOR OF PHILOSOPHY  
May, 1998

GENETIC ANALYSIS OF PHOTOSYNTHESIS *psbO*  
AND *psbV* GENES IN CYANOBACTERIA  
*SYNECHOCYSTIS*  
SP PCC6803

Thesis Approved:



Thesis Adviser



Dean of the Graduate College

## ACKNOWLEDGMENTS

I would like to express my gratitude to my adviser Dr. Robert Burnap. He was a friend and a model for me as he showed me how to conduct scientific research. I would also like to thank my committee members Dr. Robert Miller, Dr. John Cushman, Dr. Jeff Hadwiger, and Dr. William Henley.

My deepest thanks go to my wife Sara Mabie and my son Sharif. They were the light that guided me in my work. Their love and warmth sustained me through the long process of conducting scientific research. I also want to thank my father Fawzi Al-Khaldi and my mother Intisar Shaat. They were always there when I needed them the most. My thanks also go to my mother-in-law Sallie Mabie for her constant encouragement during my work. My brothers, my sister, and my friends were always beside me when I needed someone to talk to. I would like to thank all my friends in NABS (Native Americans in Biological Sciences) for supporting me and giving me a worthwhile experience. Finally, the dream comes true, the Ph.D.

## TABLE OF CONTENTS

Chapter	Page
CHAPTER I.....	1
INTRODUCTION.....	1
Purpose of the Research.....	4
Goal and Strategies of the Research .....	4
CHAPTER II.....	5
LITERATURE REVIEW.....	5
Structure and Function of MSP.....	9
Calcium Requirements.....	11
Cytochrome C-550.....	15
Expression of MSP.....	18
CHAPTER III.....	21
MATERIAL AND METHODS.....	21
Strains and Plasmids.....	21
Media and Buffers.....	24
Random Mutagenesis of the MSP of <i>Synechocystis</i> sp. PCC6803.....	24
Growth and Storage of Bacterial Strains amd Transformation.....	26
Enzymes and Chemicals.....	27
Gel Electrophoresis and Westen Blotting Analysis.....	27
MSP-Binding Assay.....	29
Flash O <sub>2</sub> Yield Measurement.....	30
Oxygen-Evolving Activity.....	30
Heterologous Expression of MSP.....	30

Cyanobacterial DNA Isolation .....	31
DNA Sequencing.....	32
CHAPTER IV.....	33
ISOLATING CALCIUM-DEPENDENT MUTANTS.....	33
Introduction.....	33
Results.....	35
Cloning the 6.4 kb <i>Hind</i> III fragment of the <i>psbO</i> -km cassette from SS6803.....	35
Random Mutagenesis of the <i>psbO</i> Gene.....	39
Hydroxylamine Mutagenesis.....	39
<i>E. coli</i> Mutator Strain.....	42
Determination of the Calcium Requirement of <i>Synechocystis psbO</i> Deletion mutant S425.....	44
Enrichment of Calcium-Dependent Mutants.....	44
Growth Rate of Calcium-Dependent Mutants.....	52
Cloning the 6.4 kb <i>Hind</i> III Fragment Containing <i>psbO</i> from the 39A and 43A Calcium-Dependent Mutants.....	54
The MSP Binding of Calcium-Dependent Mutants.....	55
Oxygen-Evolving Activities of the Random Mutants Using Whole Cells and Membranes.....	55
Spectroscopic Characterization .....	59
The Kinetics of Oxygen Release.....	59
Sequence Analysis.....	65
Discussion .....	70
Sequence Analysis of 39A and 43A Calcium-Dependent Mutants.....	72
CHAPTER V.....	75
INTERACTION BETWEEN MSP AND CYTOCHROME C-550.....	75
Introduction .....	75
Results.....	77

Introduction of Site-directed Mutants of MSP in the Absence of Cyt c-550.....	77
Growth in the Absence of Glucose.....	78
Immunoblot Analysis of the Mutants.....	84
Characterization of Oxygen-Evolution (VO <sub>2</sub> , max).....	88
Comparison Effect of Stress-inducing Agents on the Phenotype of Wild Type SS6803, $\Delta psbV$ and $\Delta psbO$ .....	88
Discussion.....	92
CHAPTER VI.....	96
HETEROLOGOUS EXPRESSION OF MSP.....	96
Introduction.....	96
Results.....	98
Discussion.....	104
CHAPTER VII.....	104
CONCLUSION AND RECOMMENDATIONS.....	106
Isolating Calcium-Dependent Mutants.....	106
Interaction Between MSP and Cytochrome c-550.....	107
Heterologous Expression of MSP.....	108
REFERENCES.....	109

## LIST OF TABLES

Table	Page
1- <i>Synechocystis</i> sp PCC6803.....	3
2- Metal Ions Effects on Calcium-Activated Oxygen Evolution.....	14
3- <i>Synechocystis</i> sp PCC6803 Mutant Strains.....	22
4- <i>E. coli</i> Strains and Recombinant Plasmids.....	23
5- Antibiotic Cassette Markers.....	28
6- Calcium Depletion-Medium in Microtiter Plate.....	45
7- Site-Directed Mutants of MSP.....	79
8- Oxygen-Evolving Activities of the <i>psbV</i> Derivative Mutants.....	89
9- Effect of Stress Oxidative-Inducing Agents of Different <i>Synechocystis</i> Strains.....	91

## LIST OF FIGURES

Figures	Page
1- The PSII Complex and the Electron Transfer Sequence in the Complex.....	6
2- Homologous Recombination of pRB81 and pSSO5 with S425 <i>psbO</i> Deletion Mutant.....	37
3- The Cloning Strategy for the 6.4 kb <i>HindIII</i> Fragment Containing the <i>psbO</i> gene and Kanamycin Cassette.....	38
4- 6.4 kb <i>HindIII</i> Fragment of pSSO5.....	40
5- Transformation frequency difference between pRB81 vs pSSO5.....	41
6- The Strategy of Conducting Random Mutagenesis of the 6.4 <i>HindIII</i> Fragment Using an <i>E.coli</i> Mutator Strain.....	43
7- Viable Count of the SS6803 Wild Type and S425 Deletion Mutants in Calcium-Depletion Medium.....	47
8- S425 Deletion Mutant Inoculated in Two Plastic-Polycarbonate Flasks Containing Calcium-Depletion Medium.....	48
9- Viable Count of the SS6803 Wild Type and S425 Deletion Mutants in Calcium-Depletion Medium Supplemented with 150 $\mu$ g of Cycloserine.....	49
10- Selection Strategy of Isolating Calcium-Dependent Mutants Using Microtiter Plates, Plastic Tubes, and Plastic-Polycarbonate Erlenmeyer Flasks.....	51
11- Growth Curve of the Random Calcium-Dependent Mutants 39A, 43 in Calcium-Depletion Medium.....	53
12- Immunoblot Analysis of MSP in Whole Cells Containing Lysate, Pellet and Post Centrifugal Supernatant in Lanes Designated L, P, and S Respectively.....	56
13- Immunoblot Analysis of MSP in Membrane Containing Pellet and Postcentrifugal Supernatant in Lanes Designated P and S, Repectively.....	57
14- Maximal Light-Saturated rate of O <sub>2</sub> Evolution (VO <sub>2</sub> , max) of Whole Cells Expressed as a Percentage of the Rate Observed for the Wild Type SS6803.....	60
15- Oxyen-Evolving Activities of the Wild Type SS6803 and Calcium-Dependent Mutants.....	61



16- The Mean of the Maximal rate of O <sub>2</sub> Evolution(VO <sub>2, max</sub> ) of Membrane Expressed as a Percentage of the Rate Observed for the Wild type SS6803.....	62
17- Maximal Recovery of Oxygen Evolution VO <sub>2, max</sub> membrane/ VO <sub>2, max</sub> cells isolated membrane .....	63
18- Absorption Spectra of the Whole Cells and Cell Membranes of the 39A, 39B,43A, 43B Calcium-Dependent Mutants and the Wild type SS6803.....	64
19- Time- Resolved O <sub>2</sub> Release Signal from the Bare Platinum Oxygen Electrode.....	67
20- Rise Time of the Calcium-Dependent Mutants Which Measures the Kinetic Release of Oxygen upon Flash in the Sample with Light.....	68
21- Sequence Deduced Alignments of the <i>psbO</i> of the pSSO39, pSSO43 and Wild Type.....	69
22A- Amino acid sequence of MSP and the Conserved Sequence in <i>Anabaena</i> , <i>Arabidopsis</i> , <i>Chlamydomonas</i> , Pea, Potato, <i>Synechocystis</i> sp. PCC6803, <i>Synechococcus</i> sp. PCC7942, Selong, Spinach, and Wheat.....	80
22B-Possible Interaction between the Asp and Arg in the Turn which Formed by Pro..	81
23- Growth Rate of Delta <i>psbV</i> -D159N , Delta <i>psbV</i> -R163L, Delta <i>psbV</i> -D159N-R163L Mutant Strains in BG11 at 30 <sup>0</sup> C in the Absence of Glucose.....	82
24- Growth rate of Delta <i>psbV</i> -D159N and Delta <i>psbV</i> -R163L Mutant Stains in BG11 at 30 <sup>0</sup> C in the Presence and Absence of Glucose.....	83
25- Growth Rate of D159N, R163L, and D159N-R163L Mutant Strains in BG11 at 30 <sup>0</sup> C in the Absence of Glucose.....	85
26- Growth Rate of Wild type SS6803, Delta <i>psbV</i> , Delta <i>psbO</i> (S425), Delta <i>psbO</i> and Delta <i>psbV</i> Mutant Strains in BG11 at 30 <sup>0</sup> C in the Absence of Glucose.....	86
27- Immunoblot Analysis of Anti-MSP in Whole Cell Lysate.....	87
28- Immunoblot Analysis of Heterologous MSP.....	100
29- Immunoblot Analysis of Heterologous MSP at Different Tme Intervals.....	101
30- Immunoblot Analysis of Site-Directed Mutants of Heterologous MSP.....	103

## CHAPTER I

### INTRODUCTION

Photosynthesis is clearly one of the most important biochemical processes on earth. We hardly look around in our environment without seeing the importance of photosynthesis. The air we breathe, the food we eat, and the energy we consume are direct or indirect products of photosynthesis. Ultimately, the studies of photosynthesis may be translated into practical application such as better energy sources and better crop yields . Additionally, understanding the detailed mechanisms of photosynthesis may lead to the design of extremely selective and environmentally benign herbicides. Oxygenic photosynthesis is a biological reaction carried out by plants, algae, and cyanobacteria. My focus in this chapter will be exploring cyanobacteria as a good model to study photosynthesis.

Cyanobacteria are excellent models to study oxygenic photosynthesis, the biogenesis of photosynthetic membranes, and metabolic pathways. The metabolic pathways of cyanobacteria are restricted not only to photosynthesis, but also include fermentation, dinitrogen fixation, aerobic and anaerobic respiration, hydrogen uptake, carbon dioxide fixation, and cellular differentiation. These diverse metabolic pathways have also created very interesting research challenges for different specialists such as physiologists, biochemists, geneticists, and biophysicists.

Because certain species of cyanobacteria can tolerate high temperatures, high UV radiation, desiccation, and free sulfide, their distribution in the environment is very diverse. One of the major environments inhabited by cyanobacteria is the ocean. Carpenter

et al. (12) suggest that one-quarter of the world's total oceanic nitrogen fixation is performed by cyanobacteria. Because of the emerging importance of studying oceanic productivity, the capability of cyanobacteria to fix nitrogen in the ocean has become a very important scientific issue (13).

Cyanobacteria are oxygenic photosynthetic prokaryotes which are divided into two groups: unicellular and multicellular (filamentous). An extensively studied example of the unicellular cyanobacteria is *Synechocystis* sp. PCC6803. *Synechocystis* sp. PCC6803 was isolated from freshwater and it has amorphous capsular material. As with other cyanobacteria and in contrast to purple and sulfur bacteria, *Synechocystis* sp. PCC6803 uses water as a source of electrons and fixes CO<sub>2</sub> by the Calvin cycle similar to plants. For a more detailed physiological characterization of *Synechocystis* sp. PCC6803, please see Table 1. (For complete review see (21)).

A key step in any genetic manipulation strategy of cyanobacteria is the ability to introduce genetic information to cells. Several methods have been developed to introduce a new or altered DNA sequence in cyanobacteria, including transformation, electroporation and conjugation. The most common method of introducing DNA into cyanobacteria is transformation. Several reports indicate that *Synechocystis* sp. PCC6803 has the ability to take up DNA naturally at a low frequency of 10<sup>4</sup> to 10<sup>7</sup> transformants per microgram of DNA (14). Electroporation was also explored for transforming cyanobacteria, especially in the strains which could not take up DNA by natural transformation. Thus, the transformation frequency using electroporation was not as high as it was in natural transformation (30).

The importance of cyanobacteria as a genetic model was also obvious when the *Synechocystis* sp. PCC6803 genome was totally sequenced (25, <http://www.kazusa.or.jp/cyano/cyano.html>).

TABLE 1

<i>Synechocystis</i> sp. PCC6803	
Cell Diameter	2-3 $\mu\text{m}$
Gas vacuole	none
Facultative Photoheterotroph	Yes
Glucose Metabolism	Yes
Sucrose Metabolism	No
Glycerol Metabolism	No
Nitrogen fixation	No
Toxin production	No
Maximum growth temp	39 °C
Mol%G+C	47.5

Table 1: *Synechocystis* sp. PCC6803 physiological characteristics (23).

### Purpose of the Research

The focus of our work is to explore the structural-functional relationships of the proteins of the H<sub>2</sub>O-splitting portion of the Photosystem II (PSII) complex. These proteins are the extrinsic manganese-stabilizing protein (MSP) and cytochrome c-550. Understanding the relationship between these proteins and the PSII complex represents an important step toward exploring photosynthesis. In this research, we investigated three problems: 1) the localization of possible calcium-binding sites affected by MSP, 2) the interaction between MSP and cyt c-550, and 3) the assessment of the heterologous expression of MSP in *E. coli*.

### Goals and Strategies of the Research

We used the following strategies to explore the oxidizing side of PSII in *Synechocystis* sp. PCC6803.

- 1- Isolate calcium-dependent mutants which might identify the calcium-binding sites of MSP in *Synechocystis* sp. PCC6803.
- 2- Localize and construct different mutants of *psbO* and *psbV* which exhibited interaction between the two genes.
- 3- Express MSP in *Escherichia coli* heterologously and explore the similarity of the transport mechanism into the periplasmic space between *E. coli* and *Synechocystis*.

## CHAPTER II

### LITERATURE REVIEW

The Photosystem II (PSII) complex in the cyanobacterium *Synechocystis* sp. PCC6803 is composed of at least five intrinsic membrane proteins and three extrinsic proteins. These intrinsic proteins are CP47, CP43, D1, D2, and cytochrome *b559*. On the other hand, the extrinsic proteins are the Mn-stabilizing protein (MSP encoded by *psbO*), cyt *c-550*, and 12 KDa. MSP is believed to be strongly bound and is associated with the luminal H<sub>2</sub>O splitting domain of the photosystem II complex. Cytochrome *c-550* encoded by *psbV* is also associated with the luminal domain and can effectively bind to the PSII complex in the absence of MSP. The cyt *c-550* and 12 KDa extrinsic proteins are replaced by the 23 and 17 KDa proteins respectively in the PSII complex of higher plants (Figure 1).

Biochemical analysis using spinach PSII particles has indicated that MSP stabilizes two of the four Mn atoms that are present at the catalytic center of the water-splitting enzyme (28). This was observed when the PSII particles of spinach were treated with concentrated salts which remove MSP. In the presence of 10 mM NaCl, the Mn contents decreased from about 3.6 to 2 atoms per reaction center and the presence of two Mn atoms per reaction center II produced a complete loss of oxygen evolution (28).

The PSII reaction center is defined by the minimal unit which is able to perform light-induced charge separation and electron transport (but not to evolve O<sub>2</sub>). This core is now agreed to contain the following proteins: four to six Chl<sub>a</sub>, two Pheophytin, two β carotene, one D1-D2 heterodimer, one (or 2) cytochrome *b559* and one 10 KDa

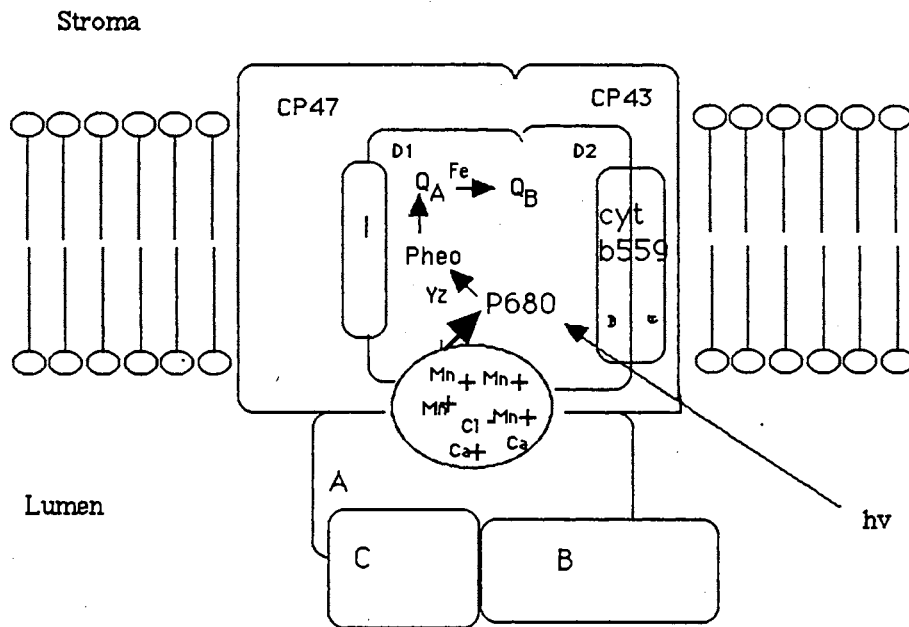
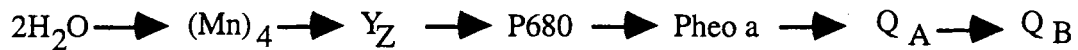


Figure 1. The PSII complex and the electron transfer sequence in the complex. In plants A: 33 KDa MSP; B: 24 KDa; C: 17 KDa. In cyanobacteria A: 33 KDa MSP, B- 17 KDa cyt c-550; C: 12 KDa . (For more details, refer to 17,46) .

polypeptide (I) per P680. No quinone(Q<sub>A</sub>) is present in the PSII reaction center unit.

In the water-splitting reaction, light excites an electron to a higher energy state creating a hole in the P680<sup>+</sup> in the reaction center. The excited electron transfers to an intermediate acceptor, a pheophytin-a (pheo a) molecule. From the pheo-a, the electron is transferred to a tightly bound molecule of plastoquinone (Q<sub>A</sub>) and the electron then is transferred to a plastoquinone (Q<sub>B</sub>) which occupies an exchangeable binding site, (Fig. 1). The doubly reduced, protonated form of Q<sub>B</sub> is replaced at its binding site by an oxidized plastoquinone molecule:

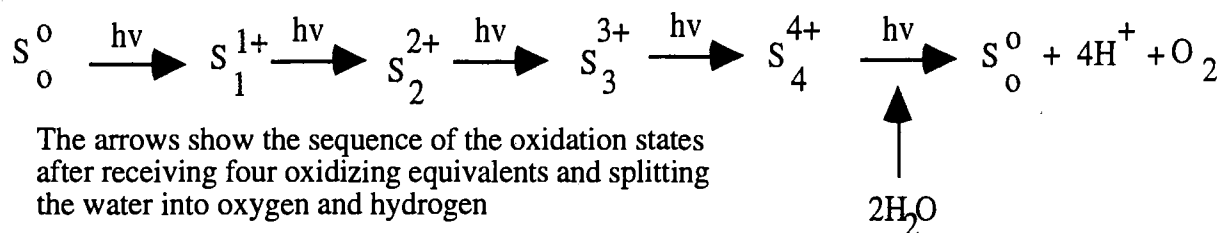


This represents the sequence of electron transfer after splitting two molecules of water.

As a result, the photooxidized reaction center, P680<sup>+</sup>, oxidizes a tyrosine residue denoted Y<sub>Z</sub> which mediates electron transfer between P680 and cofactors that catalyze the oxidation of water. When Y<sub>Z</sub> is oxidized, it extracts electrons from the H<sub>2</sub>O oxidative complex. The oxidative complex advances one step through a cycle of oxidation states named S<sub>0</sub>-S<sub>4</sub> (see below).

In the early seventies, Joliot and Kok (52) presented a model of photosynthetic oxygen production by indicating that the photosynthetic reaction consists of a linear, four-electron oxidation process that produces a gush of oxygen on every fourth light flash excitation of PSII. In this Kok model (demonstrated in the figure below), it was suggested that a set of S states (of undefined molecular composition) are associated with the reaction centers. Each S state represents a particular oxidation state of an oxygen-evolving system.





In this model the S state mechanism works as a charge-accumulating device, with H<sub>2</sub>O undergoing oxidation only after photochemical removal of four oxidizing equivalents of an oxygen-evolving enzyme.

**Photoactivation:** It was suggested that in the primary stages of assembling the Mn<sup>+2</sup> cluster, the three extrinsic polypeptides influence the kinetics of assembly. The assembly of Mn<sup>+2</sup> into the active site of the H<sub>2</sub>O oxidation complex is a light-dependent process called photoactivation (15). The oxidative complex of the Mn cluster advances one step through a cycle of oxidation states named S<sub>0</sub>-S<sub>4</sub>. In these S states and during photoactivation only, two photons of light lead to the binding of Mn to the oxygen-evolving center of PSII and production of O<sub>2</sub>. In further work (50) photoactivation was defined as a two-quantum process in which two Mn<sup>+2</sup> atoms are sequentially bound, photooxidized, and ligated by the Mn cluster of PSII. This process facilitates the ligation of the two additional Mn atoms to form four Mn atoms in the water-oxidizing complex. Burnap et al. (9) have suggested the two quantum series model of photoactivation where the photooxidation of the second Mn<sup>+2</sup> is affected by the absence or presence of MSP in *Synechocystis* sp. PCC6803. The MSP deletion mutant of *Synechocystis* sp. PCC6803 (8) was found to photoactivate faster than the wild type in hydroxylamine-treated cells and continuous illumination (39).

## Structure and Function of MSP

The Mn-stabilizing protein is encoded by the single copy *psbO* gene in *Synechocystis* sp. PCC6803. This gene is believed to be involved in photosystem II water oxidation. The *psbO* gene is 831 bp in length and encodes for a polypeptide containing 274 amino acid residues. Although the apparent molecular weight of MSP was originally estimated to be approximately 33 KDa using SDS polyacrylamide gel electrophoresis, the predicted molecular weight is 26 KDa (38). Philbrick et al. (38) sequenced the *psbO* gene and found that the amino acid sequence is 43% identical and 63% conserved regions with the spinach and pea MSP. The regions of high sequence identity were found to vary in length from 1 to 10 consecutive residues. These conserved regions are distributed throughout the sequence of the *psbO* gene, Figure 21.

The sequence data also revealed the presence of two cysteine residues (at position 20 and 45, excluding the 28 amino acids of the signal peptide). In further work, Burnap et al. (10) indicated that changing cysteine 20 to serine using site-directed mutagenesis resulted in the decrease of the accumulated MSP protein, although the mutant accumulated *psbO* mRNA transcripts. One possible explanation for the lack of MSP accumulation is proteolytic degradation in the absence of an intramolecular disulfide linkage. In addition, the lack of a disulfide bridge may interfere in the processing of the transport of the nascent MSP protein across the thylakoid membrane (10).

The role of MSP in photosynthesis in different systems has been investigated in past years (5, 42, 51, 52). A complete understanding of the function of MSP in *Synechocystis* sp. PCC6803 in water oxidation remains to be established. It was found that deleting MSP from the genome of *Synechocystis* sp. PCC6803 resulted in a 2/3 reduction in the rate of O<sub>2</sub> evolution compared to the wild type (8) in the presence of an artificial electron acceptor system 2, 6 dichloro-p-benzoquinone (DCBQ) plus potassium ferricyanide (K<sub>3</sub>Fe(CN)<sub>6</sub>). Under these conditions, the rate of oxygen evolution

approaches its maximum. Furthermore, the MSP deletion *Synechocystis* mutant S425 was also capable of autotrophic growth. Low temperature fluorescence spectroscopy 77K fluorescence (8) provides an indication of the organization of chlorophyll in the membrane where PSI emits at 720 nm and PSII emits at 685, 695 nm. The PSII emission is believed to be associated with CP43 and CP47, respectively. The reduction of the 77K fluorescence signal at 695 nm in the MSP deletion mutant indicated that MSP might bind to the luminal portion of the PSII complex altering the conformation of CP47 or even altering the conformation of other PSII proteins resulting in slow electron transfer between the PSII protein complex.

For the  $\Delta psbO$  *Synechocystis* mutant S425, the photoactivation time requirement ( $t_{1/2}$ ) was 0.8 min. in continuous light or (approximately 80 flashes), whereas the photoactivation of the wild type needed  $t_{1/2}$  3.5 min. or approximately 300 flashes indicating the MSP deletion mutant has a four fold greater relative quantum yield of photoactivation rate compared to the wild type. This finding with the wild type was comparable to the results obtained by Cheniae et al. (15) in measuring the number of the flashes which photoactivate the wild type *Synechococcus*.

There are a variety of reasons might explain the increased photoactivation of MSP deletion mutants compared to the wild type in *Synechocystis* sp. PCC6803. For example, MSP might form a diffusional barrier hindering the access of  $Mn^{+2}$  to the binding/photooxidation site(s). This is consistent with findings that MSP lowers reactivity of the Mn cluster towards exogenous reductants. This indicates that MSP reduces the accessibility to the catalytic site. Another possibility is that the binding of the MSP to the intrinsic portion of PSII modifies the complex in such a way that it affects the availability of Mn to its site of ligation or the affinity of its binding (9).

## Calcium Requirement

In addition to manganese, calcium is an absolute requirement for PSII enzyme activity. The requirement for calcium following biochemical deletion of the extrinsic proteins 23/ 17 KDa and 33 KDa MSP (extracting the proteins by washing the PSII with different chemicals) has been observed in plants and cyanobacteria, respectively. Nakatani (34) indicated that the addition of calcium in spinach can restore the oxygen-evolving activity in the absence of the 17 and 23 KDa extrinsic proteins (not 33kDa MSP). In *Synechocystis*, the addition of calcium to the *psbO* deletion *Synechocystis* mutant in autotrophic BG11 calcium-depletion medium resulted in restoration of the oxygen-evolving activity. It should be indicated that the two extrinsic proteins 17 and 23 KDa are not found in cyanobacteria and these proteins in eukaryotic PSII may be replaced by the cyt c-550 and 12 KDa proteins in cyanobacteria, respectively.

It is believed that spinach PSII has two calcium-binding sites per reaction center (11). This was observed by low pH citrate treatment of the spinach PSII membrane, which removed one of the two calcium atoms per unit of PSII and produced a complete loss of oxygen-evolving activity. Adding calcium to the low pH extracted spinach membrane of PSII restored 80% of the oxygen evolution. This indicated that only one calcium atom is involved in the oxygen-evolving activity in spinach, while the second calcium atom which was not affected by the treatment of the low pH citrate buffer is probably essential for the electron transport from YZ to P680 in PSII (see below).

The cyanobacterium *Synechococcus* contains one calcium atom per PSII which is tightly bound and, in addition, many loosely bound calcium atoms (27). Kashino et al. (27) were able to exhaustively remove all calcium and other cations from the suspending medium of the oxygen-evolving particles of *Synechococcus* using the cation-chelating resin, Chelex 100. However, this treatment did not remove the only tightly bound calcium located in the PSII reaction center. Harsher treatments with reductant resulted in a loss of

active site Mn and the accompanying release of this remaining calcium but with concomitant loss.

Although the exact functional role of calcium in PSII is still far from being understood, it is believed that calcium not only protects the Mn cluster from being overreduced by endogenous reductants, but also affects the conformation of the luminal side of the intrinsic PSII subunit (9).

Calcium affinity sites for PSII in plants are divided into two groups: high-affinity sites and low-affinity sites. In order to remove calcium ions from high-affinity sites,  $\text{La}^{+3}$  (lanthanide) is required. Lanthanide is a trivalent ion which can compete with calcium for binding sites on the oxidizing side of the PSII spinach membrane. Using EPR spectroscopy (1), it was possible to detect that lanthanide binds to the PSII membrane much more strongly than calcium.

To remove the calcium ions from low-affinity sites in PSII, an ionic solution such as NaCl, and an ion chelater such as EDTA, Chelex 100, and/or EGTA are required (27). Furthermore, it is believed that low-affinity sites for the calcium are created during the formation of the functional Mn complex where continuous illumination was an absolute requirement for complete extraction of calcium from the binding sites of PSII. This leads to the conclusion that the affinity of PSII for calcium depends on the redox state (17). Boussac et al. (3) indicated that faster calcium binding occurs in the S<sub>3</sub> state than in the S<sub>2</sub> state and the absence of calcium in the PSII membrane resulted in a system which is unable to proceed to a higher S state. This calcium binding to the S<sub>3</sub> state was observed after depleting PSII enriched spinach membranes of calcium by treating the membrane with NaCl and EGTA. In the same study, it was shown that the 17 and 23 KDa polypeptides did not have any calcium-binding sites.

Many competitive studies between calcium and metal ions were conducted to explore the binding of calcium to PSII in plants (3, 17, 52). It was indicated that Strontium  $\text{Sr}^{+2}$  and Vanadyl ion  $\text{Vo}^{+2}$  can substitute for calcium and can support the oxygen-evolving activities (3). Moreover, replacement of calcium by  $\text{Sr}^{+2}$  resulted in the perturbation of the Mn cluster indicating that the calcium-binding site is close to the functional Mn cluster in PSII. The addition of  $\text{K}^+$ ,  $\text{Cs}^+$ ,  $\text{Na}^+$  to PSII particles which are depleted of calcium exhibited a reduced oxygen-evolving activity due to the competition with the calcium on the binding site(s). More work indicated that  $\text{Cd}^{+2}$  and  $\text{Mn}^{+2}$  exhibit stronger inhibition than  $\text{K}^+$ ,  $\text{Cs}^+$ ,  $\text{Na}^+$  for oxygen-evolving activities. Please see Table 2 for the effect of other metal ions on calcium-activated oxygen evolution (52). For complete review, see (17).

Despite the evidence of calcium involvement in MSP binding, the presence of the calcium-binding sites in MSP is still controversial. One prediction indicated that the calcium-binding sites, if they exist, should have low-affinity and they should be in the unconserved C-terminal end of MSP (42). This prediction remains to be explored in my work.

TABLE 2

METAL IONS EFFECTS ON CALCIUM-ACTIVATED OXYGEN EVOLUTION			
Metal	Ionic radius	effect on oxygen evolution activity	$K_I$ (mM)
$\text{Ca}^{2+}$	0.99	activator	none
$\text{Sr}^{2+}$	1.13	activator	none
$\text{Ba}^{2+}$	1.35	weak inhibitor	none
$\text{Mg}^{2+}$	0.65	no effect	none
$\text{Mn}^{2+}$	0.8	weak inhibitor	none
$\text{Cd}^{2+}$	1.03	competitive inhibitor	0.3
$\text{La}^{3+}$	1.04	competitive inhibitor	0.05
$\text{Na}^3$	0.98	competitive inhibitor	5
$\text{K}^+$	1.33	competitive inhibitor	8
$\text{Cs}^+$	1.65	competitive inhibitor	10

Table 2: A summary of competitive studies of different metal ions with calcium and the effect of the competition on oxygen evolution.  $K_I$  is an inhibitory constant. High  $K_I$  indicates low competition and low  $K_I$  indicates high competition. This table was taken from Charles F. Yocum (52).

### Cytochrome C-550

Cytochrome c-550 is a c-type cytochrome (has a heme group attached covalently to the protein) with an apparent molecular weight of 17 KDa. cyt c-550 is also a low potential extrinsic protein which is believed to interact with MSP and D2 proteins of the PSII complex (44). cyt c-550 is encoded by a single copy gene *psbV* and it has 160 amino acid residues including a 25 signal peptide at the N-terminus. The N-terminus of *psbV* functions as a leader sequence which has Arg-Asn-Arg immediately before the putative cleavage site similar to the signal peptides found in other prokaryotes. This 25 signal peptide is proposed to direct cyt c-550 to the luminal space of the thylakoid membrane.

In previous studies, it was suggested that cyt c-550 works as an electron acceptor in anaerobic conditions (26), because cyt c-550 can be reduced by ferredoxin II under in vitro conditions indicating the possible involvement of cyt c-550 in carbohydrate breakdown. The cyt c-550 involvement was predicted to be as a disposal of electrons in fermentative pathways, although the evidence of the reduced cyt c-550 involvement in transferring electrons in cyanobacterial hydrogenase (which is believed to be a part of anaerobic carbohydrate metabolism) was not found. This conclusion remains speculative.

Perhaps the first evidence which indicated that cyt c-550 might be a part of the PSII protein complex was obtained by Shen et al. (45). Biochemical analysis of the detergent-solubilized PSII complex in *Synechococcus vulcans* revealed two more extrinsic proteins in addition to MSP. The two extrinsic proteins were associated with the core complex in the stoichiometric amount which could be released with 1 M CaCl<sub>2</sub> or 1 M alkaline Tris. Further analysis of the two proteins indicated that they were different from the higher plant 17 and 23 KDa extrinsic proteins, and the N-terminal sequence of the 17 KDa protein indicated that it is homologous to the cyt c-550 [apoprotein]. Furthermore, the absorption



spectrum analysis of the 17 KDa protein indicated the presence of peaks at 407.5 , 522.3, and 549.1 nm wave lengths after reducing the protein with dithionite. These absorption spectra are typical spectra of a reduced cytochrome.

When the whole cell of *Synechococcus vulcanus* were completely fractionated into soluble and thylakoid membrane fractions using lysozyme treatment to lyse the cells, cyt c-550 was associated with the thylakoid membrane fraction (47). Further fractionations of detergent solubilization of the thylakoid membrane using lauryldimethylamine N-oxide (LDAO) treatment indicated the association of cyt c-550 with PSII fraction. It should be indicated that the presence of cyt c-550 is exclusively concentrated in the crude PSII fraction and the protein was absent in other fractions unlike what has been predicted in other studies (26).

Shen et al. (47) have indicated that cyt c-550 helps to stabilize the PSII complex and plays an important role in stabilizing oxygen evolution. This was concluded from studying *psbV* deletion and *psbV* interruption mutants. When *psbV* was genetically removed or interrupted, several physiological alterations were observed. For example, the photoautotrophic growth rate was doubled to 28 hrs for the mutants compared to 13 hrs for the wild type. The two mutants, moreover, exhibited 40% oxygen-evolving activity compared to the wild type in the presence of DCBQ and  $K_3Fe(CN)_6$  as electron acceptors. The ratio of chlorophyll to PSII was also increased to 660 for the interrupted *psbV* mutant and to 1100 for the *psbV* deletion mutant compared to the wild type 580. This indicates that the decrease in the oxygen-evolving activity is probably correlated with a decrease in the relative amount of PSII in the thylakoid membrane (the remainder of chlorophyll is associated with PSI in cyanobacterium).

In further studies on the growth rate of the double deletion mutant of MSP and cyt c-550 in *Synechocystis* sp. PCC6803 (44), it was found that the double deletion mutant and the *psbO* single deletion mutant exhibited similar growth rates in heterotrophic

conditions (doubling time was 9 hrs). Whereas the growth rate of the *psbO* deletion mutant was 60% of the wild type (doubling time was 26 hrs) in autotrophic growth, the double deletion mutant could not grow in autotrophic growth conditions (i.e. without glucose). The inability of the double deletion mutant to grow autotrophically indicated that *cyt c-550* is able to support the photoautotrophic growth in the *psbO* single deletion mutant.

Furthermore, the inability of double deletion mutants (*psbO* and *psbV*) to grow autotrophically was also correlated to the loss of an electron transport chain in PSII activity. Maximal rates of oxygen evolution of the  $\Delta psbO$  strain was 30% and the double deletion mutant was 8% compared to the wild type in the presence of DCBQ and  $K_3Fe(CN)_6$  as electron acceptors. These results indicated that the destabilizing effect caused by the loss of *cyt c-550* became more pronounced in the absence of MSP in *Synechocystis* sp. PCC6803 suggesting some sort of interaction between MSP and *cyt c-550*. Our work to explore the interaction between MSP and *cyt c-550* was pursued by introducing site-directed mutants in MSP in the absence of *cyt c-550*. These mutants were a valuable source of information regarding the relationship between MSP, *cyt c-550* and the PSII complex.

In protein reconstitution experiments (46), it was observed that *cyt c-550* binds to PSII in the absence of MSP and the 12 KDa extrinsic proteins in *Synechocystis* sp. PCC6803, although the binding of *cyt c-550* was enhanced by 10% in the presence of MSP. This finding contrasts with the previous studies of the 23 KDa extrinsic protein in plants in which the 23 KDa protein could not bind to PSII in the absence of MSP (33) (The 23 KDa in higher plants was hypothesized to be an equivalent of *cyt c-550* in cyanobacteria). These findings supported the differences between the PSII of higher plants and cyanobacteria. Despite these differences, one similar function of *cyt c-550* and the 23 KDa protein is that the absence of either protein results in a reduction in oxygen evolution and, in addition, destabilization of the PSII complex. Based upon the available evidence,

Shen et al. (46) have suggested a new model for the probable association of the three extrinsic proteins in cyanobacteria. A hypothetical model is shown in Figure 1.

### Expression of MSP

There are multiple processes which are important in the expression of MSP in plants and cyanobacteria. One process which was investigated extensively in plants is the regulation of protein expression of MSP by controlling the expression of mRNA encoding MSP. This process was explored by growing, for example, etiolated spinach in dark and white light conditions. By comparing the accumulation of MSP mRNA, it was discovered that mRNA of spinach MSP incubated under dark conditions accumulated one tenth of the mRNA accumulated under white light conditions (37). Although there were differences in mRNA accumulation of MSP, protein accumulation in dark and white light conditions was the same. The regulation of mRNA transcript of MSP was also investigated in etiolated barley, and it was found that the difference of mRNA accumulation in the dark was 50% of the accumulation under white light conditions (42).

Another process potentially controlling MSP expression in cyanobacteria and plants is the transportation of a precursor MSP across the thylakoid membrane. In plants, the N-terminal of the MSP protein carries two domains. The first domain helps to direct the precursor polypeptide from the plant cell cytoplasm into the stroma of the chloroplast which corresponds to the cytoplasm in cyanobacteria. The second domain directs the polypeptide from the stroma of the chloroplast into the thylakoid lumen. The N-terminal part of this domain -- the thylakoid transfer domain-- is variable in length, mostly a hydrophilic polypeptide, and has a net positive charge. The central polypeptide sequence of the thylakoid transfer domain is hydrophobic, and the secondary structure is predicted to be hydrophobic also and helical. On the other hand, the C-terminal part contains alanine residues in position -3 and -1 (relative to the cleavage site of the signal peptidase) and they are considered the recognition sites for the thylakoidal processing peptidase in plants (21).

On the other hand, cyanobacteria have only a thylakoid transfer domain which directs the pre-MSP to cross the thylakoid membrane. This thylakoid transfer domain of MSP in cyanobacteria is believed to be similar to the thylakoid transfer domain in plants.

The similarity between cyanobacteria and plants in the translocation of the precursor MSP across the thylakoid membrane is consistent with the endosymbiotic theory of the origin of the chloroplast in plants. The endosymbiotic theory posits that the ancestors of the chloroplast in eukaryotic cells were originally free-living cyanobacteria (21). Further evolutionary studies using cyanelles (photosynthetic organelles) in the eukaryotic alga *Cyanophora paradoxa* indicated that the *psbA* gene which encodes for the D1 protein is identical in length with cyanobacteria's counterpart and the sequence identity is closer to the *psbA* found in higher plants (23). This finding was another piece of evidence which appears to justify the assumption that the cyanelle is the evolutionary bridge between cyanobacteria and plastids in higher plants.

The translocation of MSP across the membrane in cyanobacteria is hypothesized to be similar to the mechanism in *E. coli*. This mechanism is mediated by a sec-related mechanism which requires ATP, a proton gradient across the thylakoid membrane, and the Sec A protein. The MSP in *Synechocystis* sp. PCC6803 is believed to possess a 28 amino acid leader peptide sequence. The leader sequence works as a signal peptide for MSP to cross the thylakoid membrane in the lumen (29). Furthermore, the amino acid signal of the MSP in *Synechocystis* sp. exhibits a 48-49 % homology with the plant's MSP. Our work is focused on exploring the expression of MSP heterologously in *E. coli*. The heterologous MSP protein, furthermore, will be used to conduct reconstitution experiments of PSII in vitro containing MSP site-directed and random mutants in *Synechocystis* sp. PCC6803.

Our work of identifying possible calcium-binding sites of MSP, exploring the interactions between MSP and cyt c-550, and expressing MSP heterologously using an *E. coli* expression system represent our main goals in this thesis.

## CHAPTER III

### MATERIALS AND METHODS

#### Strains and Plasmids

*Synechocystis* sp. PCC6803 is a naturally transformable unicellular cyanobacterium (51). In our work, we constructed a new control type *Synechocystis* sp. PCC6803 by transforming a *psbO* deletion *Synechocystis* sp. PCC6803 mutant (8) with a wild-type *psbO* gene. Henceforth this wild-type *Synechocystis* will be called SS6803. This gene was carried on a genomic *Synechocystis* fragment which has a kanamycin resistance cassette inserted at a downstream *Xba* I site previously determined to be neutral (8). The *psbV* *Synechocystis* deletion mutant was created by using a plasmid which was provided by Dr. Shen et al.(47). This plasmid has the *psbV* gene deleted and replaced by an erythromycin cassette. We transformed the *psbO* deletion mutant with this plasmid in order to delete the *psbV* gene. In further work, we transformed some of Dr. Qian's MSP site-directed mutants into the *psbO-psbV* double deletion *Synechocystis* mutants. Table 3.

In constructing recombinant plasmids, we used different strains of *E. coli*. Table 4 indicates all the *E. coli* strains which were used in this study and the recombinant vectors which were created in this work.

TABLE 3

*Synechocystis* sp. PCC6803 MUTANT STRAINS

Strains	Phenotype	Genotype	Reference
SS6803	Km <sup>r</sup>	kanamycin cassette is inserted at a neutral site near <i>psbO</i> wild type	This study
$\Delta$ psbO	Spec <sup>r</sup>	<i>psbO</i> is deleted and replaced by Spec cassette	8
$\Delta$ psbO- $\Delta$ psbV	Spec <sup>r</sup> Em <sup>r</sup>	$\Delta$ psbO strain was used to delete psbV and replaced by Em cassette (plasmid was supplied by Dr. Shen)	This study
$\Delta$ psbV-D159 N-R163L	Em <sup>r</sup> Km <sup>r</sup>	$\Delta$ psb- $\Delta$ psbV strain was transformed with pRBB81- D159N-R163L plasmid (created by Dr. Qian)	This study
$\Delta$ psbV-D159N	Em <sup>r</sup> Km <sup>r</sup>	$\Delta$ psbO strain was transformed with pRB81-D159N (created by Dr. Qian)	This study
$\Delta$ psbV-R163L	Em <sup>r</sup> Km <sup>r</sup>	$\Delta$ psbV strain was transformed with pRB81-R163L (created by Dr. Qian)	This study
D159N	Km <sup>r</sup>	$\Delta$ psbO was transformed with pRB81-D159N (created by Dr. Qian)	This study
R163L	Km <sup>r</sup>	$\Delta$ psbO was transformed with pRB81-R163L (created by Dr. Qian)	This study

TABLE 4

E. coli STRAINS AND RECOMBINANT PLASMIDS		
<i>E. coli</i> strains	Genotype	Reference
XL1- Red	endA1 gyrA96 thi-1 hsdR17 supE44relA1 lac mutD5 mutS mutT Tn10(Tet r)	Stratagene
BL21(DE3)	lamda derivative , pro. lacI , lacUV51, lacZ, T7 RNA Poly	Gift from Dr. Vijayakumar
DH5 $\alpha$	F' recAI	BRL
Plasmids		
pSSO5	6.5 kb <i>Hind</i> III fragment ( <i>psbO</i> -Km cassette) :: <i>Hind</i> III-Bluescript SK-	This study
pRB81	Km cassette and <i>psbO</i> gene	Dr. Burnap
pRB81-D159N	Aspartic acid changed to asparagine at 159 amino acid	Dr. Qian
pRB81- R163L	Arginine acid changed to leucine at 163 amino acid	Dr. Qian
pRB81-D159N- R163L	D and R changed to N and L as indicated above	Dr. Qian
$\Delta$ psbV-Em	<i>psbV</i> was deleted and replaced by Em cassette	Dr. Shen
pSSO39	<i>psbO</i> random mutant selected by calcium deficient medium and cloned back in <i>E. coli</i>	This study
pSSO43	<i>psbO</i> random mutant selected by calcium deficient medium and cloned back in <i>E.</i> <i>coli</i>	This study
pSSO55	<i>psbO</i> random mutant selected by digital imaging spectrum and cloned back in <i>E.</i> <i>coli</i>	This study



## Media and Buffers

*Synechocystis* sp. PCC6803 and other constructed mutants were grown on a rotary shaker in BG-11 media (51) supplemented with 5 mM glucose at 32 ° C with constant fluorescent light except the *psbV* deletion *Synechocystis* derivative mutants were grown on a rotary shaker in BG-11 media supplemented with 50 mM glucose. Stock solution for calcium-deficient medium was prepared as follows: 100X BG-11 stock solution lacking calcium: 0.17 M NaNO<sub>3</sub>, 0.03 M MgSO<sub>4</sub>, 0.006 M citric acid, 1/10 dilution of trace metal mix lacking calcium (50 ml of trace metal was added to 500 ml of 100X of BG-11). The trace metal mix was 46.3 mM H<sub>3</sub>BO<sub>3</sub>, 9.15 mM MnCl<sub>2</sub>, 0.77 mM ZnSO<sub>4</sub>·2H<sub>2</sub>O, 1.61 mM Na<sub>2</sub>MoO<sub>4</sub>·5H<sub>2</sub>O, 0.32 mM CuSO<sub>4</sub>·5H<sub>2</sub>O, and 0.17 mM Co(NO<sub>3</sub>)<sub>2</sub>·6H<sub>2</sub>O. One liter of calcium-deficient medium was prepared as follows: 10 ml of 100X BG-11 calcium-deficient stock solution, 5 ml of 1 M of Tes pH 8, 1 ml of 6 mg/ml ferric ammonium citrate, 1 ml of 189 mM Na<sub>2</sub>CO<sub>3</sub>, 1 ml of 175 mM K<sub>2</sub>HPO<sub>4</sub>. Moreover, we completed the volume to one liter of ddH<sub>2</sub>O and carefully poured 100 mls of mixture into the plastic-polycarbonate acid-washed 250 ml Erlenmeyer flasks and autoclaved for 30 min. at 121 ° C at 15 LB pressure. For the calcium-deficient medium experiments, we acid-washed plasticware with 120 mM HCL for 30 minutes minimum and the plasticware was rinsed with ddH<sub>2</sub>O prior to using.

Luria-Bertani (LB), TB, and 2X YT media were prepared according to (41). The many common buffers were used in this study such as: SSC, TE, 0.5 M EDTA (pH 8.0) and TBE were prepared as recommended by (41)

### Random Mutagenesis of the MSP of *Synechocystis* sp. PCC6803

A pRB81 plasmid was constructed by Burnap et al. (8). M. Qian deleted a *Hind*III site in the Kanamycin cassette of the pRB81 using site-directed mutagenesis. Furthermore, this plasmid was transformed to the *psbO* deletion *Synechocystis* sp. PCC6803 mutant and

a 6.4 kb *Hind*III fragment carrying MSP and a kanamycin cassette was cloned. The plasmid was named pSS05 and it was used to transform the *E. coli* mutator strain which has been developed by Stratagene Inc. This *E. coli* mutator strain is lacking three repair systems and, therefore, the plasmid will undergo error-prone replication (Table 4). These mutations in pSS05 include point mutations. The mutagenesis was done according to the manufacturer's instructions. Furthermore, enrichment of the mutants was done by transforming the random-mutated *psbO* into *Synechocystis* which lacks the MSP gene. The mutated culture was grown in a calcium-deficient medium which was supplemented with 150 µg/ml cycloserine. Cycloserine is an antibiotic which inhibits the synthesis of the cell wall. The mixture was kept at 32° C in fluorescent light for 6 hours and finally the cells were washed twice with BG11 calcium-deficient medium to remove the antibiotic and the Km<sup>r</sup> transformants (population enriched in mutants) were plated in BG11 with DCMU, glucose, and kanamycin.

The screening for calcium-dependent mutants was done by visual identification of the enriched calcium-dependent transformants grown under different conditions in 96 -well microtiterplates. Candidate mutant colonies were selected according to slow growth in the calcium-deficient medium and were inoculated into another two 96-well microtiterplates containing calcium-deficient medium and a master plate containing normal BG11 medium, respectively. The mutants which exhibited growth differences between the calcium-deficient microtiterplate versus the master normal BG11 microtiterplate were selected for further testing. These potential calcium-dependent mutants were tested again using a 10-ml plastic sterile falcon tube and by the same procedure. Finally, the calcium-dependent mutants were tested for the third time using 250-ml plastic-polycarbonate Erlenmeyer flasks (acid-washed) containing sterile calcium-deficient medium.

## Growth and Storage of Bacterial Strains and Transformation

All *Synechocystis* strains were grown photoheterotrophically using cool-white fluorescent lamps (approximately  $50 \mu$  Einstein's  $m^{-2} s^{-1}$ ) at  $32^\circ C$ . For growth and storage of *Synechocystis* stains, the cells were grown to mid-log phase and a 100-ml culture was centrifuged at 400 xg. The pellet was resuspended in 2 ml of BG11 supplemented with 5 mM glucose. The resuspended culture was adjusted to 16% (v/v) glycerol and stored at  $-80^\circ C$  for further use.

Transformation of *Synechocystis* sp. PCC6803 was done by incubating the mid-log culture at  $42^\circ C$  for one hour in a rotary shaker water incubator bath in order to heat shock the cells (we discovered that heat shocking the cells will increase the transformation frequency-unpublished data). The cells were harvested and resuspended at a density of approximately  $10^9$  cells/ml. 5-10  $\mu$ g of DNA was used to transform 300  $\mu$ l of the *Synechocystis* resuspended pellet in the presence of 15 mM  $CaCl_2$ . The transformation mixture was incubated in dim light with gentle agitation in 120 ml Falcon tubes at  $32^\circ C$  for six hours to allow DNA uptake. Afterward, 3 ml of BG11 liquid medium was added to the transformation mixture in 125 ml flasks which were then incubated for 24 hrs under illumination with rotary shaking. The 24-hr period will allow the integration of the transformed DNA into the chromosome and will allow enough time for the expression of antibiotic resistance. The transformation mixture was then plated on BG11 plates containing antibiotic, 0.1 mM of [(3-(3-4-Dichlorophenol)-1, 1- Dimethylurea] DCMU and 5 mM glucose and antibiotic. DCMU is a herbicide which blocks the electron transfer in PSII and as result will allow the transformants to grow at the same rate of non-transformants before challenging the transformation mixture with antibiotic selection. The transformants were visible in 7 to 10 days. For complete segregation of the mutant isolate from the wild type isolates, we streaked the colony from two to three times before using the transformants in physiological characterization.

*E. coli* strains were grown overnight in the assigned medium with aeration and the strains were kept in 16% (v/v) glycerol at -80° C for further use. The antibiotic concentrations used for different strains are shown in Table 5. The *E. coli* competent cells were prepared as recommended by Inoue et al.(22).

### Enzymes and Chemicals

T4 DNA ligase, restriction endonuclease and molecular weight standard were purchased from either New England Biolab (NEB) or Promega Laboratories. Lysozyme grade I was purchased from Sigma or USB. Media and agar for bacteria were purchased from Difco or USB. Agarose for gel electrophoresis was purchased from Fisher or International Biotechnologies, Inc. For cleaning the DNA, we used GeneClean or Wizard Prep and we followed the manufacturer's instructions.

### Gel Electrophoresis and Western Blotting Analysis

Acrylamide gel for SDS-PAGE contained a 12% polyacrylamide gel and the preparation of the gel was done according to the BioRad manufacturer's instructions. Western blotting analysis using cyanobacterial membrane or whole-cell lysate was conducted by using antibodies directed against MSP and the D1 protein which were gifts from Dr. Kuwabara and Dr. Ikeuchi, respectively. Antibody-antigen complexes were visualized using horseradish peroxidase conjugated goat anti-rabbit IgG for the MSP protein (8) and/or alkaline phosphatase-conjugated goat anti-rabbit IgG for the D1 protein.

For membrane isolation, we followed Gleiter et al. (18) and modified the procedure as follows: *Synechocystis* cells were grown in 500 ml Erlenmeyer flasks at 32° C in continuous light. The maximum oxygen-evolving rate ( $VO_{2,max}$ ) of the cells was measured prior to starting the membrane isolation in order to confirm the activity of the cells. The cells were incubated on ice for 30 min., spun at 4000 xg for 10 min., and resuspended with HMCS buffer pH 7 (50 mM HEPES, 10 mM MgCl<sub>2</sub>, 1 M sucrose, 5

TABLE 5  
ANTIBIOTIC CASSETTE MARKERS

Phenotype	Selection	Concentration for <i>Synechocystis</i>	Concentration for <i>E. coli</i>
Km <sup>r</sup>	Kanamycin	5 µg/ml	50 µg/ml
Em <sup>r</sup>	Erythromycin	1 µg/ml	750 µg/ml
Spec <sup>r</sup>	Spectinomycin	5 µg/ml	50 µg/ml
Amp <sup>r</sup>	Ampicillin	N/A	60 µg/ml
Cyc <sup>r</sup>	Cycloserine	N/A	150 µg/ml

mM CaCl<sub>2</sub>- total volume was 7 mls). The resuspended cells were kept on ice for 45 min. to let the cells equilibrate with the new HMCS buffer. Afterwards, the cells were mixed with glass beads (the bead size was 105 micron) in a 10 ml screw cap tube leaving a small airspace once the tube was closed. The cells were broken using a braun homogenizer for four minutes under a continuous stream of liquid CO<sub>2</sub>. The glass beads, unbroken cells, and debris were pelleted from the cell homogenate by centrifugation at 4000 xg for 3 min. The glass beads were extracted three times with fresh HMCS buffer and centrifuged three times at 1000 xg for 3 min. The membranes were resuspended to 25 ml total volume of HMCS pH 7 buffer and spun in the ultracentrifuge for one hour at 44,000 xg using 70 Ti rotor. Supernatant was discarded and the pellet was resuspended to 800 µg of chlorophyll/ml. The oxygen-evolving activity was measured to confirm the activity of the membranes. The membranes were aliquoted and kept at -80° C.

#### MSP-Binding Assay

For membrane-binding assay experiments we did the following. We used three treatments of urea for each sample in addition to two nonurea samples (controls) which were resuspended with HMCS and HS pH 7.2 (50 mM HEPES, 1.5 M sucrose) buffers respectively. Each treatment including the controls contained 25 µg of chlorophyll. The different urea treatments of each sample were .75 M, 2 M, 4 M Urea. Each treatment including the controls was treated with a .05% detergent of N-dodecyl maltoside and resuspended with 500 µl total volume of HMCS /HS buffer. All the samples were kept on ice for 30-45 minutes. Afterwards, the samples were spun for 7000 xg for 45 minutes at 4° C using a Vti rotor. Each treatment was divided into supernatant and pellet. The pellet was washed with HS buffer before resuspending it with 250 µl of HS buffer. In the preparation of the samples for SDS-PAGE and Western blot, each well contained .85 µg of chlorophyll.

### Flash O<sub>2</sub> Yield Measurement

The peak time of the release of oxygen under flashing light which is a part of the rising time of the mutants, was measured (four flashes per second for five seconds) polarographically. This was done by using a Bare platinum Joliot-type electrode with a AC-coupled transimpedance amplifier with 5 ms rise time in apparatus described by (6, 8). The platinum surface of the electrode was cleaned with CaCO<sub>3</sub> paste between measurements. Cell suspensions were incubated and allowed to dark adapt for 5 min. The platinum electrode was polarized to -0.7 V relative to the Ag/AgCl evolution by whole cells.

### Oxygen-Evolving Activity

Oxygen evolution by membranes and whole cells under continuous illumination was measured at 30° C by using 750 μM DCBQ/ 4.5 mM K<sub>3</sub>Fe(CN)<sub>6</sub> as the artificial acceptor system with a Clark-type concentration electrode in water-jacketed 2-ml cuvette under heat-filtered illumination transmitted through a red-pass filter (corning 2406) as described previously (8). The intensity of light impinging upon the cuvette was approximately 2000 μEinstein m<sup>-2</sup> s<sup>-1</sup>. The rate of oxygen-evolution was calculated by taking the slope of the oxygen release from 60 to 90 sec. upon continuous illumination of the sample tested. It should be indicated that dark respiration, photorespiration, and the Mehler reaction were not considered in the oxygen-evolution measurements (24). DCBQ works as an electron acceptor and the K<sub>3</sub>Fe(CN)<sub>6</sub> oxidize the DCBQ molecules.

### Heterologous Expression of MSP

We used pRB81 which carries *apsbO* gene as a model to express MSP heterologously in *E. coli*. This plasmid was transformed to a BL21(DE3) *E. coli* strain. The BL21(DE3) *E. coli* strain has the T7 RNA polymerase gene inserted in the

chromosome. Upon inducing T7 RNA polymerase transcription by IPTG, the enzyme will bind to the T7 promoter upstream of the *psbO* gene in the pRB81 construct (49). It should be indicated that we obtained the optimal expression of MSP at 28° C with a rotary shaker incubator (not at 37° C). The fractionation and localization of MSP expression in *E. coli* was done according to (41). For high yield heterologous expression of MSP, BL21(DE3) carrying pRB81 was grown in LB medium supplemented with an antibiotic overnight at 28° C. The next day, we inoculated the 100 ml LB medium with 3 ml of overnight culture supplemented with kanamycin. In order to induce the transcription of T7 RNA polymerase, we added IPTG to a concentration of 0.4 mM after the culture reached a density of  $A_{600}=0.7-1$ . The culture was incubated for 2-3 hours at 28° C and the cells were ready to be harvested. The culture was kept on ice for 10 min. Furthermore, we centrifuged the culture for 10 min. at 4000 x g at 4° C. The pellet was resuspended with 20% sucrose, 30 mM Tris pH 8, 1 mM EDTA and 1 mg/ml lysozyme and kept on ice or at room temperature for 20 -60 min. The cells were centrifuged for 3 min. at 4000 xg at 4° C. The supernatant was harvested and used for further investigation of MSP heterologous expression.

#### Cyanobacterial DNA Isolation

A 100 ml culture of *Synechocystis* was grown to late-log phase under antibiotic selection and continuous light on a rotary shaker at 32° C. The culture was pelleted by centrifugation at 300 xg for 10 min. and the pellet was resuspended with 10 ml 5X TE (50 mM Tris-HCl, 5 mM Na<sub>2</sub>EDTA, pH 7.6). The resuspended cells were pelleted again at 5800 xg for 10 min. The pellet was resuspended with 3 ml of 1.5 M KCl. The resuspended cells were incubated in a water bath at 65° C for 20 min. This treatment will inactivate the nuclease.

Furthermore, the cells were washed again with 14 ml of 5X TE buffer and the cells were pelleted by centrifugation 300 xg for 10 min. The pellet was resuspended with 3 ml



of 5X TE and the resuspended cells were treated with 1 mg/ml lysozyme for 30 min. at room temperature on a rotary shaker. The treated cells were incubated in the presence of 0.4 % SDS (w/v), 0.4% Sarkosyl (w/v), 20 mg/ml Proteinase K overnight at 50<sup>0</sup> C with gentle rocking.

The next day, the lysed cells were extracted with phenol/chloroform once and chloroform two times. DNA was precipitated by adding an equal volume of isopropanol for 30 min. The precipitated DNA was pelleted by centrifugation at 9600 xg for 30 min. at 4<sup>0</sup> C. The pellet was resuspended with 400 µL of TE containing 100 µg/ml RNase-free DNase and the resuspended DNA was kept at 37<sup>0</sup> C for 30 min. The DNA was extracted further by 1x phenol/chloroform and 2x chloroform. The DNA was precipitated with 2X of 100% ethanol and 1/4X of 3 M Na Acetate. The DNA was kept at -20<sup>0</sup> C for one hour. The DNA was pelleted further by centrifugation at 7000 xg for 20 min. The pelleted DNA was washed with 70% ethanol and the DNA was resuspended with 100 µl of TE.

### DNA Sequencing

Primer synthesis and automated DNA sequencing were done by the Recombinant DNA and Protein Resource Facility in the Department of Biochemistry and Molecular Biology at Oklahoma State University under the supervision of Dr. John Cushman. The nucleotide sequences were determined using a Perkin-Elmer 373A automated DNA sequencing system and using the Prizm<sup>TM</sup> Ready reaction Dye-deoxy<sup>TM</sup> terminator Cycle sequencing kit (Applied Biosystems Division). We sequenced both strands in different directions. The following primers were used to sequence the *psbO* gene: 1) Left end 5' GCATCCGTGTAAGTCTGG3', 2) Right end 5' CGCCAAACTGTTCAGCTC 3', 3) R163L 5'ATGACCCA(A/C/G/T)GGCTTTGGG3'.

## CHAPTER IV

### ISOLATING CALCIUM-DEPENDENT MUTANTS

#### Introduction

The extrinsic 33 KDa Mn-stabilizing protein is involved in water oxidation and it has been suggested that it stabilizes two of the four Mn atoms that are present at the catalytic center of the water-splitting enzyme [for complete review see (17)]. MSP binds to the intrinsic part of the PSII complex and this interaction probably involves ionic interactions and hydrogen bonding. The *psbO* gene has been cloned and sequenced in previous work (8, 38).

Further molecular genetic studies have indicated that deleting MSP from the *Synechocystis* sp. PCC6803 genome does not abolish the water-splitting reaction. However, this mutation alters the kinetics of the oxygen-evolving activity and makes cells more dependent upon calcium and chloride in the growth medium (9). The altered oxygen-evolving activity of  $\Delta psbO$  *Synechocystis* can be partially overcome and growth restored by the addition of  $Cl^-$  and  $Ca^{+2}$  to the liquid BG11 medium at a concentration higher than required by the wild type (8).

It was suggested that MSP of pea has sequence homology to a calcium-binding protein such as an intestinal calcium-binding protein (ICaBP) although the calcium-binding sequence in MSP is not conserved (52). The sequence form ICaBP that was examined is DKNGNGEVSFEFEQ and for the MSP of peas was EVSADGSVKFEEK. In addition, sequence analysis of more than 160 binding loops of calcium-binding proteins suggested that the loop sequence only partially determines affinity and specificity of calcium and metal

binding (48). The exact function of calcium in PSII is still not resolved. Several extraction-reconstitution experiments using calcium and other cations such as  $\text{Sr}^{+2}$ ,  $\text{K}^+$ ,  $\text{Cs}^+$ ,  $\text{Na}^+$ , and  $\text{Mg}^{+2}$  demonstrate that calcium is critical for oxygen-evolving activities (17, 52). Recently, calcium was also suggested to play an important role in photoactivation (39).

Yocum (52) suggested that the binding of MSP to the intrinsic protein of PSII might produce conformational changes altering the putative calcium binding site. These conformational changes might be in MSP itself or in the intrinsic proteins of PSII. This possibility is still to be tested. Alternatively, Seidler (42) has suggested the presence of MSP increases the local concentration of calcium present around the manganese cluster. Biochemical studies indicated that calcium protects the manganese cluster from being over-reduced or reduced manganese from being released from PSII. In this regard it should be noted that active-site manganese is thought to cycle between the +3 and +4 oxidation states during catalysis, but it is never in the +2 state except prior to assembly. Thus, reduction of active-site manganese to the +2 state causes release of the manganese from the active site.

Although strong evidence exists that MSP affects the calcium site of PSII, little is known about the mechanism of its influence. An understanding of this mechanism will help define the exact function of calcium involvement in photosynthetic electron transport.

Our goal is to localize possible calcium-binding sites in PSII and interaction sites of MSP as part of the overall strategy to study the structure and the functional relationships of this protein within the PSII complex. This chapter describes attempts to create calcium-dependent mutants after randomly mutagenizing a 6.4 kb *HindIII* fragment containing a *psbO* gene and other genes. Our results show that these mutants exhibited physiological alteration, although the sequence data unfortunately indicated the absence of any sequence alteration in the *psbO* gene itself.

## RESULTS

Previous observations indicated that when MSP was deleted from *Synechocystis* sp. PCC6803, the mutant exhibited a high requirement for chloride and calcium (8, 42). These results led to the hypothesis that MSP is involved with calcium binding in PSII. In order to explore the hypothesized mechanistic interaction between MSP and calcium, it was important to conduct random or site-directed mutagenesis to localize the possible calcium-interaction sites of MSP. Site-directed mutagenesis of a protein is a very efficient strategy to study function when the structure is determined or when the conserved sequence of the protein is recognized. Thus, the limitation of this strategy is clear when the conserved sequences of the *psbO* gene of *Synechocystis* sp. PCC 6803 do not have any sequence similarity with calcium-binding proteins, and in contrast, the non-conserved regions of the *psbO* gene have some sequence similarities to calcium protein-binding sequences (42).

Our goal of localizing possible calcium-binding sites and interaction sites of MSP using random mutagenesis was challenged by these problems. The first problem was that the plasmid pRB81 which harbors the *psbO* gene gave a low transformation frequency in the *psbO* *Synechocystis* deletion mutant. The second problem was selecting an efficient method to conduct random mutagenesis of the *psbO* gene. The third problem is to develop an efficient screening which is to be fully solved as described below.

### Cloning the 6.4 kb *Hind*III Fragment of the *psbO*-km Cassette from SS6803

In previous work, a *psbO* gene was cloned from *Synechocystis* sp. PCC6803 and the plasmid which carries the gene was named pRB81 (8) and when used to transform the

*ΔpsbO* deletion strain, it restores the expression of MSP. This plasmid, unfortunately, gives low transformation frequency in the *Synechocystis* mutant *psbO* deletion S425. In previous work (8), the *psbO* gene was deleted by replacing the 1.2 kb *AfIII-XbaI* fragment from the genome of the wild type *Synechocystis* with the spectinomycin cassette. The low transformation frequency is related to the relatively short flanking sequence (50 bp) on the left side (5' end of the *psbO* gene) of the integrated fragment containing the *psbO* gene. This results in low homologous recombination because it is believed that high frequency homologous recombination requires a 200-500 bp flanking sequence on each side of the target locus (19). The low transformation frequency of pRB81 hinders the efficiency of recovering random mutants and subsequently transformation of the *ΔpsbO* deletion mutant strain. Therefore, cloning the *psbO* gene with a large flanking sequence from both flanking sides of the gene was a requirement to increase the transformation frequency (Fig. 2).

Our attempt to clone the *psbO* gene with a large flanking sequence started by deleting a *HindIII* site located in the kanamycin cassette using site-directed mutagenesis (M. Qian unpublished data 31). The purpose of deleting the *HindIII* site within the kanamycin cassette was to allow us to clone a 6.4 kb *HindIII* fragment containing the *psbO* and kanamycin cassette. Restriction enzyme analysis was conducted to confirm the deletion of the *HindIII* site within the kanamycin cassette and the plasmid was named pRB81H. In further work, this plasmid was used to transform the deletion mutant S425 which has the *psbO* gene deleted (Fig.3).

Upon transforming pRB81H to the *Synechocystis psbO* deletion mutant S425, the transformants were selected on BG11 plates containing 5 mM glucose, 10 μM DCMU, 5 μg/ml kanamycin. The newly created strain of *Synechocystis* was named the SS6803 strain. It is considered the control strain which harbors a wild type *psbO* gene and appears phenotypically identical to the wild type except for kanamycin resistance due to the insertion of a kanamycin antibiotic cassette fragment which has a *HindIII* deleted site.

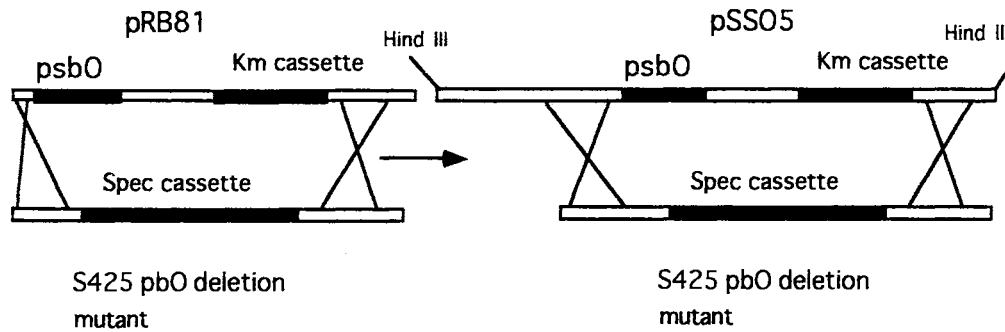


Figure 2: Homologous recombination of pRB81 and pSSO5 with S425 *psbO* deletion mutant. The left end (5' end of the *psbO* gene) of pRB81 is 50 bp and the integration of the fragment by double-crossing over is low in frequency. The left end of the pSSO5 is at least 2300 bp which increases the integration of the fragment by double-crossing over.

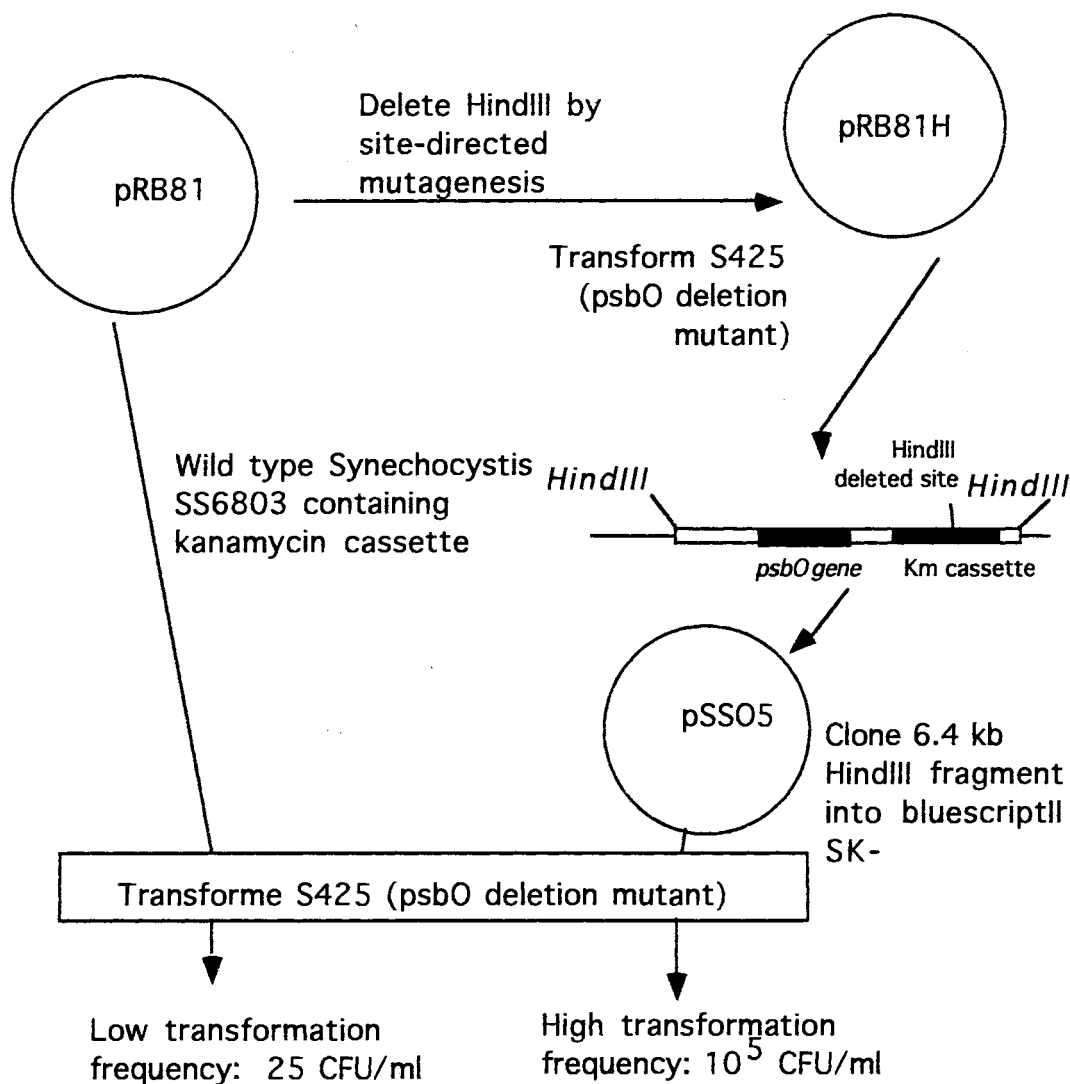


Figure 3: The cloning strategy for the 6.4 kb *Hind*III fragment containing the *psbO* gene and kanamycin cassette. pRB81 is 5.7 kb and contains 50 bp flanking sequences on the left side of the *psbO* gene and around 500 bp on the right. pRB81H is the same as pRB81 except for the deleted *Hind*III site in the kanamycin cassette. pSSO5 is 9.2 kb containing a long flanking sequence on both sides of the *psbO* gene.

Chromosomal DNA was isolated from SS6803, digested with *Hind*III, and a 6.4 kb *Hind*III fragment was cloned into a pBluescript II SK- plasmid. This plasmid was called pSS05 (Fig. 4). Restriction enzyme and DNA sequence analysis have confirmed the *psbO* and kanamycin cassette's physical measurements. The insert DNA of pSS05 also corresponded with the original physical map of the *Synechocystis* 6803 genome. pSS05 has at least 500 bp from each flanking sequence of the *psbO*-km fragment which maximizes the frequency of homologous recombination (Fig. 3)

We conducted transformation of the *psbO* deletion mutant with two plasmids, pRB81, and pSS05 again selecting for Km<sup>r</sup>. As illustrated in Figure 5, the transformation frequency has been improved from 25 (pRB81) to  $4 \times 10^5$  (pSS05) transformants per ml of viable cells using equal amount of transforming plasmid DNA. This transformation frequency of *Synechocystis* S425 by pSS05 represents the minimum value to conduct efficient random mutagenesis of the *psbO* gene (Fig. 5).

#### Random Mutagenesis of the *psbO* Gene

Random point mutagenesis was originally developed to overcome the limitations of mutating large segments of DNA because of time and money constraints. Random point mutagenesis is also an efficient strategy for creating suppressor mutants. For a complete reference of random mutagenesis see (32). Different protocols to random-mutagenize the *psbO* gene were explored and hydroxylamine random mutagenesis was our first attempt to mutate the *psbO* gene.

**Hydroxylamine mutagenesis.** This strategy involves a chemical reaction that damages bases so that the damaged site can no longer undergo Watson-Crick pairing. The strategy depends on treating a single-strand DNA with hydroxylamine and then allowing it to anneal with its complement in order to reform the vector in a transformation-competent



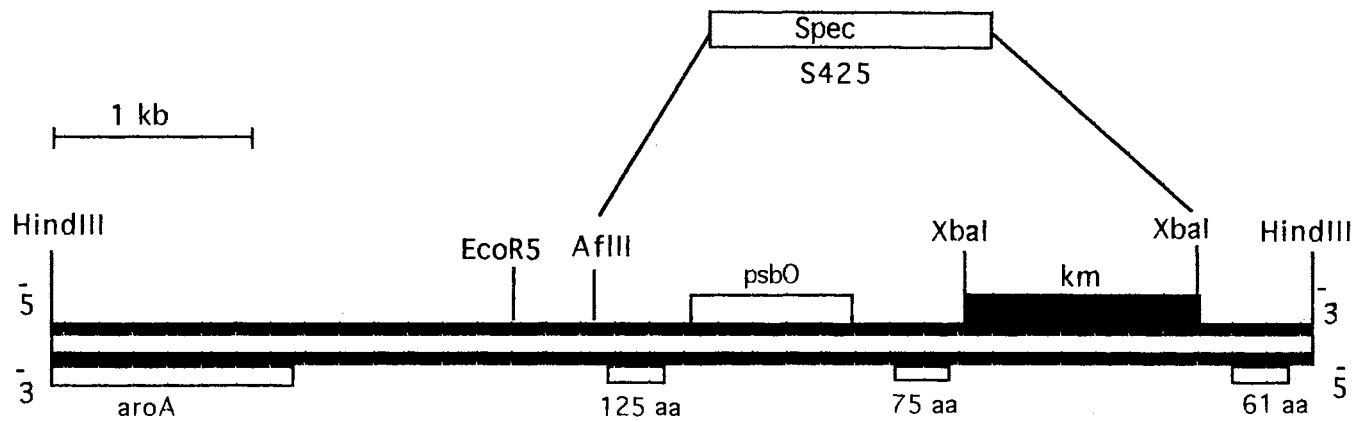


Figure 4: 6.4 kb *HindIII* fragment of pSSO5. *EcoR5* represents the site which was used to digest pSSO39 and pSSO43 in order to create 39C and 43C calcium-dependent mutants. 1.3 Kb *AfIII*-*XbaI* fragment was replaced with a spectinomycin cassette in order to create the S425 *psbO* deletion mutant (8). The figure shows the relative location of the three small polypeptides.

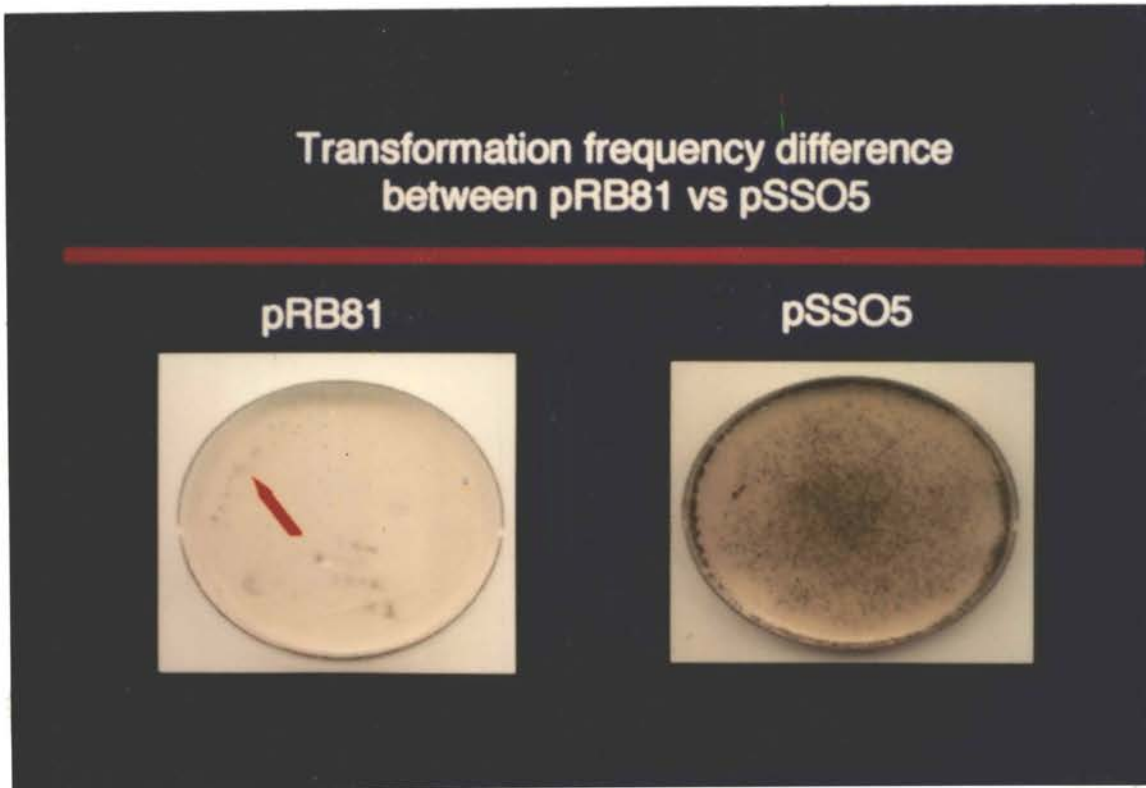


Figure 5: Transformation frequency difference between pRB81 vs pSSO5. Plate to the left represents transformation frequency using pRB81 with the S425 deletion mutant. Plate to the right represents the transformation frequency using the pSSO5 plasmid with S425 deletion mutants.

duplex form. Hydroxylamine is believed to react preferably with the cytosine (32).

pSS05 was treated with 1 M hydroxylamine (HA) for 5, 10, 20 min. and the DNA was cleaned with a spin bind column to wash the DNA from all the hydroxylamine and other contaminating molecules. We had more Km<sup>r</sup> transformants in HA treated DNA compared with non-treated DNA. These results were unexpected since we expected that mutagenesis would damage the Km<sup>r</sup> cassette in a fraction of the transforming DNA. This experiment was repeated three times and under different time intervals. One possible explanation for these results is that residual HA increased the transformation efficiency. A second possibility is that HA might increase kanamycin resistance spontaneous mutations. In any event, our conclusion is that hydroxylamine mutagenesis is not feasible in our hands. Therefore, a different strategy was proposed, see below.

***E. coli* Mutator Strain.** *E. coli* mutator strain XL-1 Red (endA1 gyrA96 thi-1 hsdR17 supE44 relA1 Lac mutD5 mutS mutT Tn10 (Tet)) was selected to randomly mutagenize the *psbO* gene. Therefore, we transformed pSS05 and pUC18 as a control into a mutator *E. coli* strain. We had 1500 cfu/ $\mu$ g of DNA compared to the DNA control (pUC18) 2500 CFU/ $\mu$ g of DNA. We selected 200 colonies from each plate and inoculated 5-10 ml of LB broth. After this passage through the mutator strain, the mutant plasmid population was isolated and transformed to *E. coli* XL1- Blue strain (recA1 endA1 gyrA96 thi-hsdR17 uspE44 relA1 lac [F' proAB lac Z $\Delta$  M15 Tn 10 (Tet)]) competent cells. The transformation frequency was  $1.5 \times 10^6$  cfu/ $\mu$ g of DNA (Fig. 6). The mutated plasmids

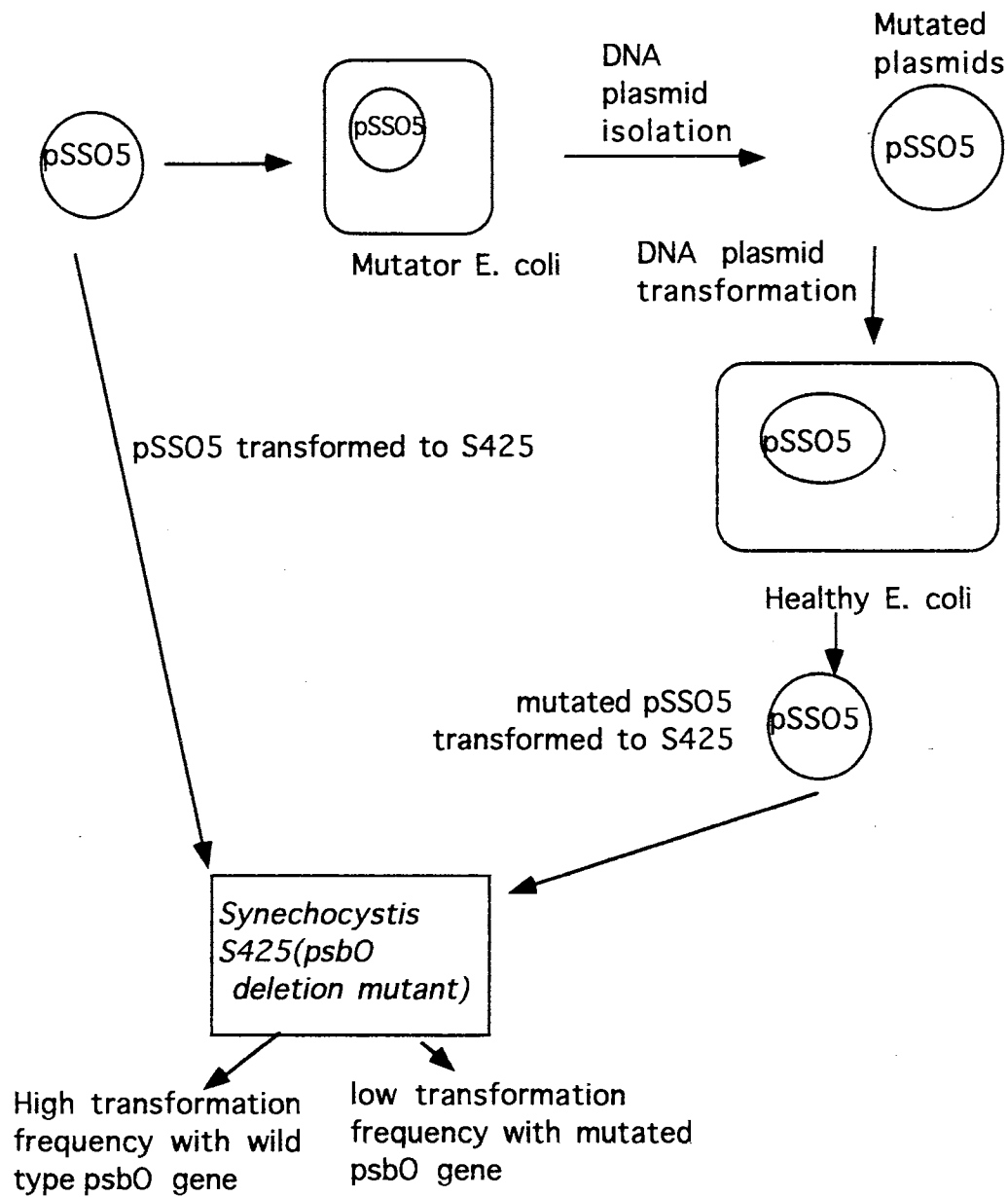


Figure 6: The strategy of conducting random mutagenesis of the 6.4 kb *Hind*III fragment using an *E. coli* mutator strain.

were then used to transform *psbO Synechocystis* deletion mutants. After having optimized the conditions to mutate MSP in *E. coli*, it was important to optimize the conditions for selecting calcium-dependent mutants.

#### Determination of the Calcium Requirement of the

#### *Synechocystis psbO* Deletion Mutant S425

Since calcium contamination is very difficult to eliminate, all equipment and glassware were acid-washed (see Material and Methods). Initial experiments involved testing the calcium requirements of the deletion S425 and wild type SS6803. We used 24-well micro-titerplates and tested the two strains at several different concentrations of calcium in the presence and absence of glucose. The calcium-depletion medium was supplemented with CaCl<sub>2</sub> at the following concentrations : 0, 0.3, 2.5, 12.5, 145, 245  $\mu$ M. Table 6 shows that the wild type SS6803 and the deletion mutant S425 grew at the same final cell density in the presence of 5 mM glucose. Thus, in the absence of glucose, only the wild type *Synechocystis* SS6803 grew in the calcium-depletion medium, whereas the deletion mutant S425 grew in 145 and 245  $\mu$ M of calcium-supplemented wells.

This indicated that the wild type SS6803 can grow in the absence or presence of added calcium while the deletion mutant S425 could not grow - at least in the presence of 145  $\mu$ M of calcium. In both strains, 5 mM of glucose overcame the effect of the calcium requirement. The glucose was not treated with Chelex 100 and therefore the glucose might be contaminated with calcium. This indicated that calcium is specifically involved not only in the stability of PSII but also in the viability of cells in the absence of MSP.

#### Enrichment of Calcium-Dependent Mutants

Our ultimate goal was isolating calcium-dependent mutants. Enriching for calcium-dependent mutants required testing the viability of the deletion mutant S425 and the

TABLE 6

CALCIUM DEPLETION -MEDIUM IN MICROTITER PLATES						
Strains	μM Calcium added					
	No added calcium	0.3	2.5	12.5	145.0	245.0
SS6803+ Glucose	xxxx	xxxx	xxxxx	xxxxx	xxxxx	xxxxx
SS6803	x	xx	xxx	xxxx	xxxxx	xxxxx
S425+Glucose	xx	xx	xx	xx	xx	xx
S425	none	none	none	none	xxx	xxxxx

Table 6: <sup>a</sup>Relative growth of 150 μl of calcium-depletion medium in microtiter plate for 6 days after incubation at 32° C and constant light. The microtiter wells were inoculated with 10 μl of the mid-log cells. The cells were washed twice with calcium-depletion medium prior to inoculation with SS6803 and S425. The following represent the densities of the cells in Microtiter plate using microtiter plate reader has 750 nm filter : None: <.00, X: .03-0.7, XX: .08-.25, XXX: 0.3-0.85, XXXX: 0.9-1.3.

wild type SS6803 in a calcium-depleted medium. Therefore, we did viable count experiments of SS6803 and S425. Figure 7 shows that the wild type SS6803 continued to grow until day six compared to S425 which did not grow through the six-day incubation. The viable count of SS6803 at the end of the six days was  $1.6 \times 10^7$  cfu/ml compared to the deletion mutant S425  $6 \times 10^6$  cfu/ml. This indicates that a calcium-depletion medium supported the growth of the wild type SS6803 and did not support the growth of S425. The viability test of S425 and SS6803 was always used to test the calcium-depletion medium every time we prepared a new batch of flasks (Figure 8).

Furthermore, we needed to see the effect of a calcium-depletion medium on the deletion mutant S425 and the wild type SS6803 in the presence of cycloserine. Cycloserine inhibits the cell wall synthesis of the growing cells and as a result the cells continue to grow until they burst. We used cycloserine to select against *Synechocystis* transformants which received an unaltered phenotype. Because the altered *Synechocystis* phenotype that requires calcium can not grow in the medium, it is unaffected by cycloserine.

We inoculated separate aliquots of the calcium-depletion medium containing 150  $\mu$ g/ml cycloserine with S425 and SS6803. Figure 9 shows that the deletion mutant S425, surprisingly, died in the 3-day period more than the wild-type SS6803. This indicated that the deletion mutant is more sensitive to the calcium-depletion medium supplemented with cycloserine than the wild type SS6803. We decided to treat the transformants with cycloserine for 6 hours (a shorter time than 3 days) to eliminate the possibility of losing all the transformants.

Possible explanation of the increased sensitivity of the deletion mutant than the wild type is that the deletion mutant is challenged with cycloserine and the harsh conditions of

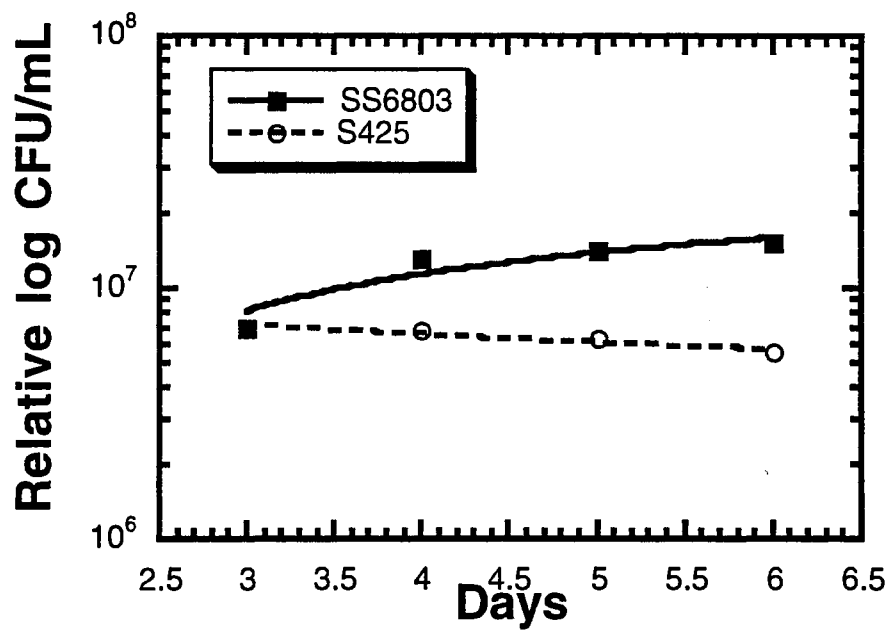


Figure 7: Viable count of the SS6803 wild type and S425 deletion mutants in calcium-depletion medium.





Figure 8: S425 deletion mutant inoculated in two plastic-polycarbonate flasks containing calcium-depletion medium. Flask to the right contains calcium-depletion medium supplemented with  $245 \mu\text{M}$  of  $\text{CaCl}_2$  and the flask to the left contains calcium-depletion medium without calcium.

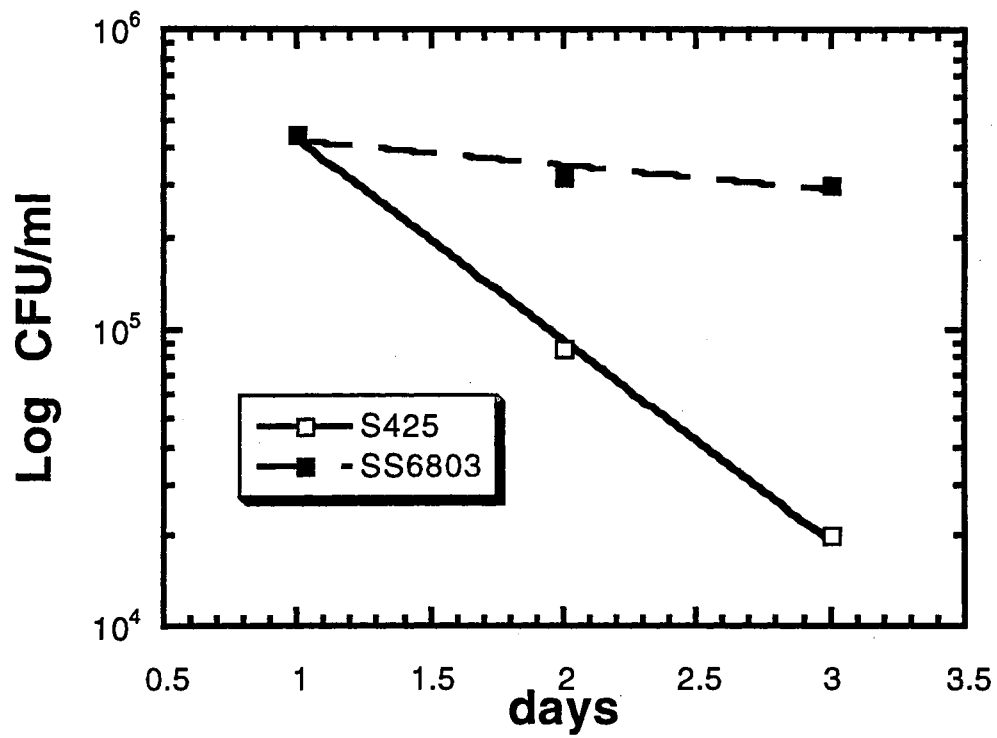


Figure 9: Viable count of the SS6803 wild-type and S425 deletion mutants in calcium-depletion medium supplemented with 150  $\mu$ g of cycloserine.

the calcium-depletion medium which help to kill most the cells at least in the first 24 hrs. More work is needed to test the viability of the deletion mutant and the wild type under different concentrations of cycloserine.

pSSO5 mutated plasmids (carrying a *psbO* gene) were mixed with the deletion mutant S425 and the transformation mixture for 24 hours. After 24 hours the transformation mixture was washed twice with calcium-depletion medium and the pellet was resuspended with calcium-depletion medium supplemented with cycloserine 150 µg/ml for six hours. Figure 10 shows the complete strategy of isolating calcium-dependent mutants.

After cycloserine treatment, cells in the transformation mixture were washed twice with calcium-depletion medium to remove the antibiotic cycloserine. The transformants were plated on BG11 plates containing 5 mM glucose, 10 µM DCMU and 5 µg/ml kanamycin. Forty-seven surviving transformant colonies were obtained from this procedure. The 47-transformant colonies were inoculated into separate wells of microtiter plates containing calcium-depletion medium supplemented with 2 mM of glucose. The colonies were kept in a 32<sup>0</sup> C incubator under constant light for one week. Each well represents one potential mutant. The potential calcium-dependent mutants were replica-transferred to a microtiter plate containing calcium-depletion medium and a second master microtiter plate containing calcium-depletion medium supplemented with 245 µM of calcium.

Sixteen mutant colonies which exhibited an altered growth rate in the calcium-depletion medium were compared to the master microtiter plate were analyzed further. They were inoculated in plastic tubes containing 5 ml of calcium-depletion medium and a control tube containing calcium-depletion medium supplemented with 245 µM of CaCl<sub>2</sub>. Out of the sixteen only nine showed alteration of the growth rate in the calcium-depletion

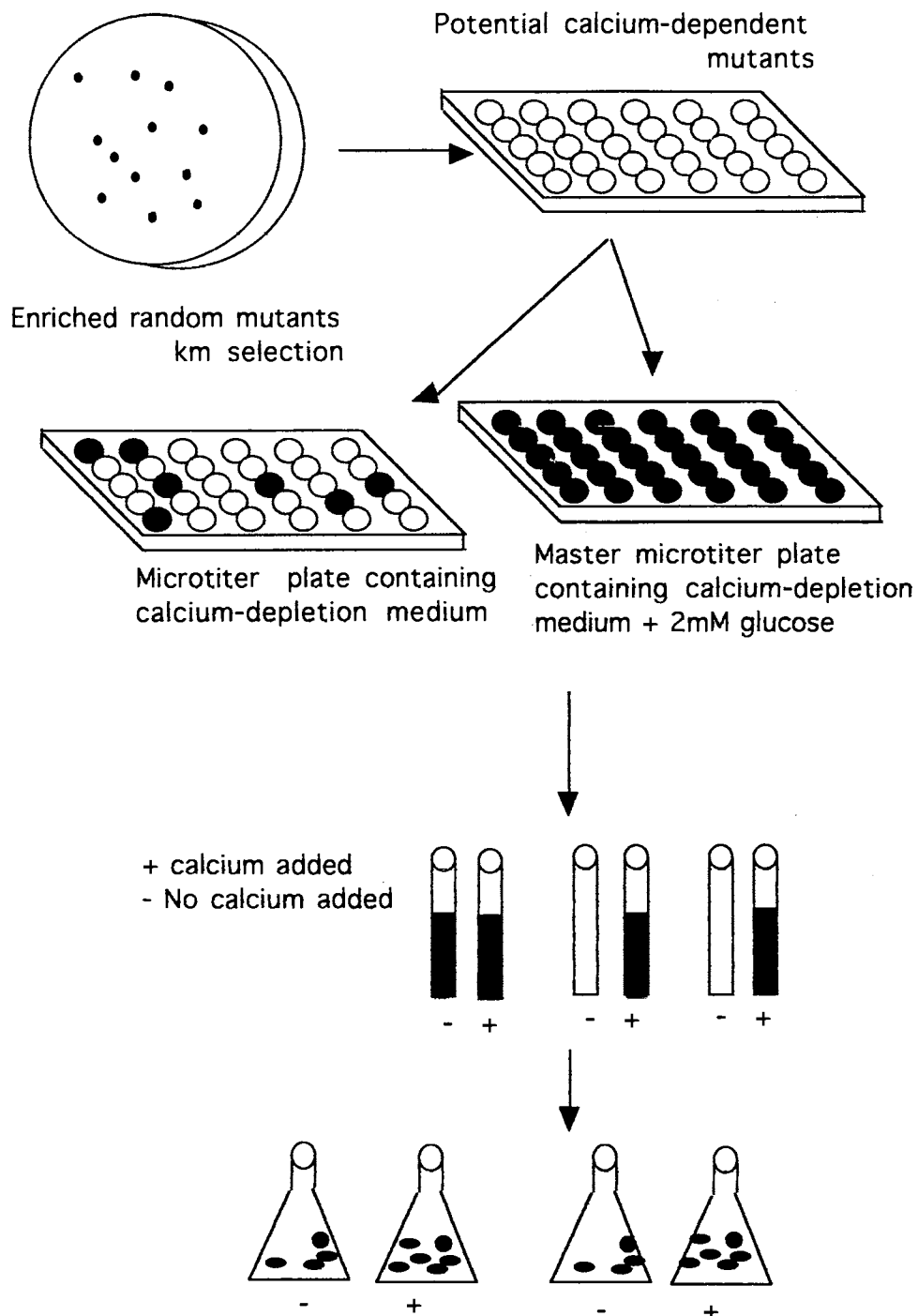


Figure 10: Selection strategy of isolating calcium-dependent mutants using microtiter plates, plastic tubes, and plastic-polycarbonate Erlenmeyer flasks.

medium compared to the master tubes (visual inspection). These nine potential mutants were tested again in an Erlenmeyer plastic-polycarbonate flask containing 100 ml of calcium-depletion medium and only two mutants showed alteration in growth in the calcium-depletion medium compared to the master flasks. These two random mutants were named 39A and 43A calcium-dependent mutants.

#### Growth Rate of Calcium-Dependent Mutants

The growth rate of the calcium-dependent mutants 39A and 43A, Wt SS6803 and S425 deletion mutants was measured in calcium-depletion medium. The mutants were grown in BG11 medium supplemented with 5 mM glucose. In mid-log culture the cells were washed three times with calcium-depletion medium. For each strain, three flasks of calcium-depletion medium were inoculated to  $A_{750} = 0.1$ . Figure 11 shows the mean of growth curves of all the strains 39A, 43A, SS6803, and S435. The doubling time of all the strains was calculated as follows:

$$\text{doubling time (dt)} = \frac{\text{Time}}{\text{Generations}}$$

$$\text{Time} = T_1 - T_0$$

Where  $T_1$  is the time at the end of log phase

$T_0$  is the time at the beginning of log phase

$$\text{Generations} = \frac{\log(N_1) - \log(N_0)}{0.30}$$

Where  $N_1$  is the cell density at the end of log phase

$N_0$  is the cell density at the beginning of the log phase

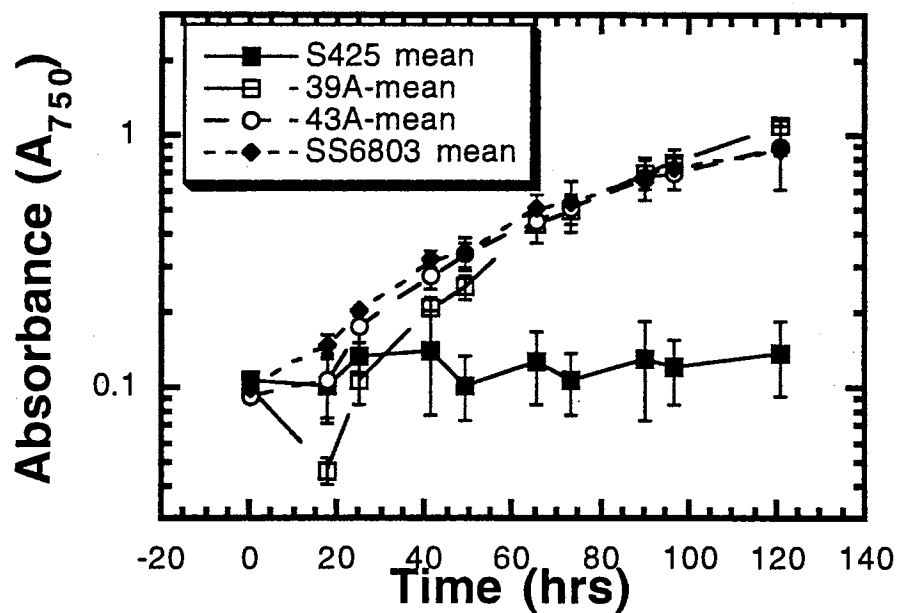


Figure 11: Growth curve of the random calcium-dependent mutants 39A, 43A in calcium-depletion medium. SS6893 is a wild type and S425 is a *psbO* deletion mutant. For each curve three samples were analyzed and the error bars represent the standard deviation. The following represent the beginning and the end of the log phases for each strain: 39A:  $T_0 = 41$ ,  $T_1 = 72$ ; 43A:  $T_0 = 25$ ,  $T_1 = 49$ ; SS6803:  $T_0 = 17$ ,  $T_1 = 41$ ; S425: no growth.

The doubling time (dt) of the strains was as follows: S425 No growth, 39A dt= 23 +/- 6.2 hrs , 43A dt= 27 +/- 5.4 hrs, SS6803 dt= 21 +/- 3 hrs

Our results indeed indicate that the doubling time for the wild type SS6803 (dt = 21 hrs) is lower than for the 39A (dt = 23 hrs) and 43A (dt = 27 hrs), although the differences in the mean values among the treatment groups are not great enough to exclude the possibility that the differences in the doubling time is due to random sampling; there are not statistically significant differences (  $P=0.564$  done according to one way anova methods). It should also be observed that the 39A and 43A mutants exhibited a pronounced increase in the lag phase in the first 24 hrs compared to the wild type SS6803. This observation indicates that the mutants take a longer time to adapt to the harsh new medium (calcium-depletion medium) compared to the wild type SS6803.

#### Cloning the 6.4 kb *Hind*III Fragment Containing

the *psbO* Gene from the 39A and 43A

#### Calcium-Dependent Mutants

The chromosomal DNA of the 39A and 43A calcium-dependent mutants was isolated and digested with *Hind*III. The digested chromosomal DNA was ligated to *Hind*III pBluescript SK- and 9.2 kb plasmids were recovered. The two plasmids were named pSSO39 and pSSO43, respectively.

pSSO39 and pSSO43 were found to have the 6.4 kb *Hind*III fragment. Restriction enzyme characterization of the two plasmids indicated that the vectors indeed have the *psbO* gene and the kanamycin cassette. The insert DNA of pSSO39 and pSSO43 corresponded with the original physical map of the *psbO* fragment. These plasmids used to transform the deletion mutant S425 and two strains of *Synechocystis* were named 39B and 43B, respectively. This step was performed to prove that the alteration of the physiology of the

mutants 39A and 43A is attributed to the change of the 6.4 kb *Hind*III fragment carrying the *psbO* gene.

**The MSP Binding of Calcium-Dependent Mutants.** It has been documented in our lab (39) and in other labs as well (36) that there are many probable protein-protein interactions between the MSP and remainder PSII protein complex. Figure 12 shows an immunoblot experiment where a whole cell fraction of MSP was found in the supernatant following high-speed centrifugation (18) in the two mutants 39A and 43A. Unlike the wild type SS6803, each mutant 39A and 43A MSP exhibited weakened binding and a fraction of the MSP was found in the supernatant (Figure 12, lanes designated S in both the mutants 39A and 39B) compared to the amount in the pellet (Figure 12, lanes designated P, in 39A and 43A). This suggests that each mutant harbors mutation(s) which causes weakened binding affinity of the MSP to its binding sites.

Similarly, using isolated active membranes of the 39A and 43A mutants, the MSP protein exhibited weakened binding in the presence of a low concentration of urea compared to the wild type SS6803. Figure 13 shows that upon increasing the urea concentration from zero to 4 M, the mutant 39A membrane released all of the MSP fraction in the supernatant at 0.4 M urea (Figure 13, 39A lanes designated S) and the 43A mutant released all the MSP at 2 M urea (Figure 13, 43A lanes designated S). These results confirmed that the 39A and 43A MSP binding was weakened compared to the binding of the wild type SS6803. Furthermore, the wild type MSP binding was not as severely weakened with increasing urea concentrations.

**Oxygen-evolving activities of random mutants using whole cells and membranes.** A water-jacketed (30 ° C) polygraphic oxygen electrode chamber was used to measure the liberation of oxygen during photosynthetic reaction. It is sensitive to detect



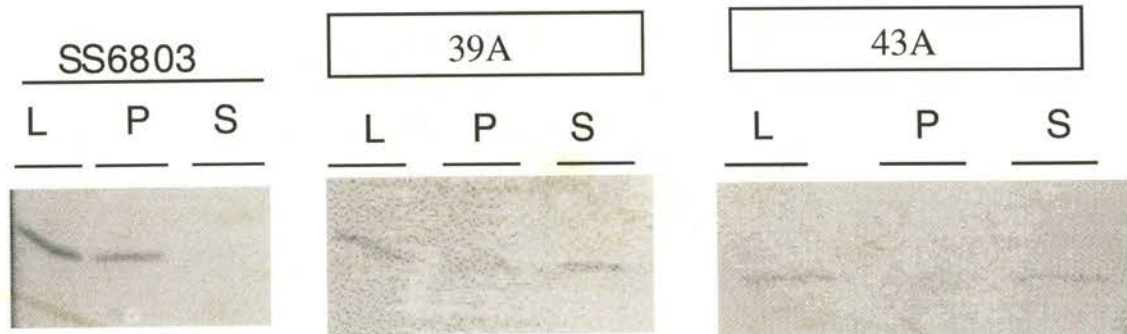


Figure 12: Immunoblot analysis of the MSP in whole cell containing lysate, pellet and post centrifugal supernatant in lanes designated L, P, S respectively. Samples analyzed: SS6803 wild type control, 39A, and 43 calcium-dependent mutants.

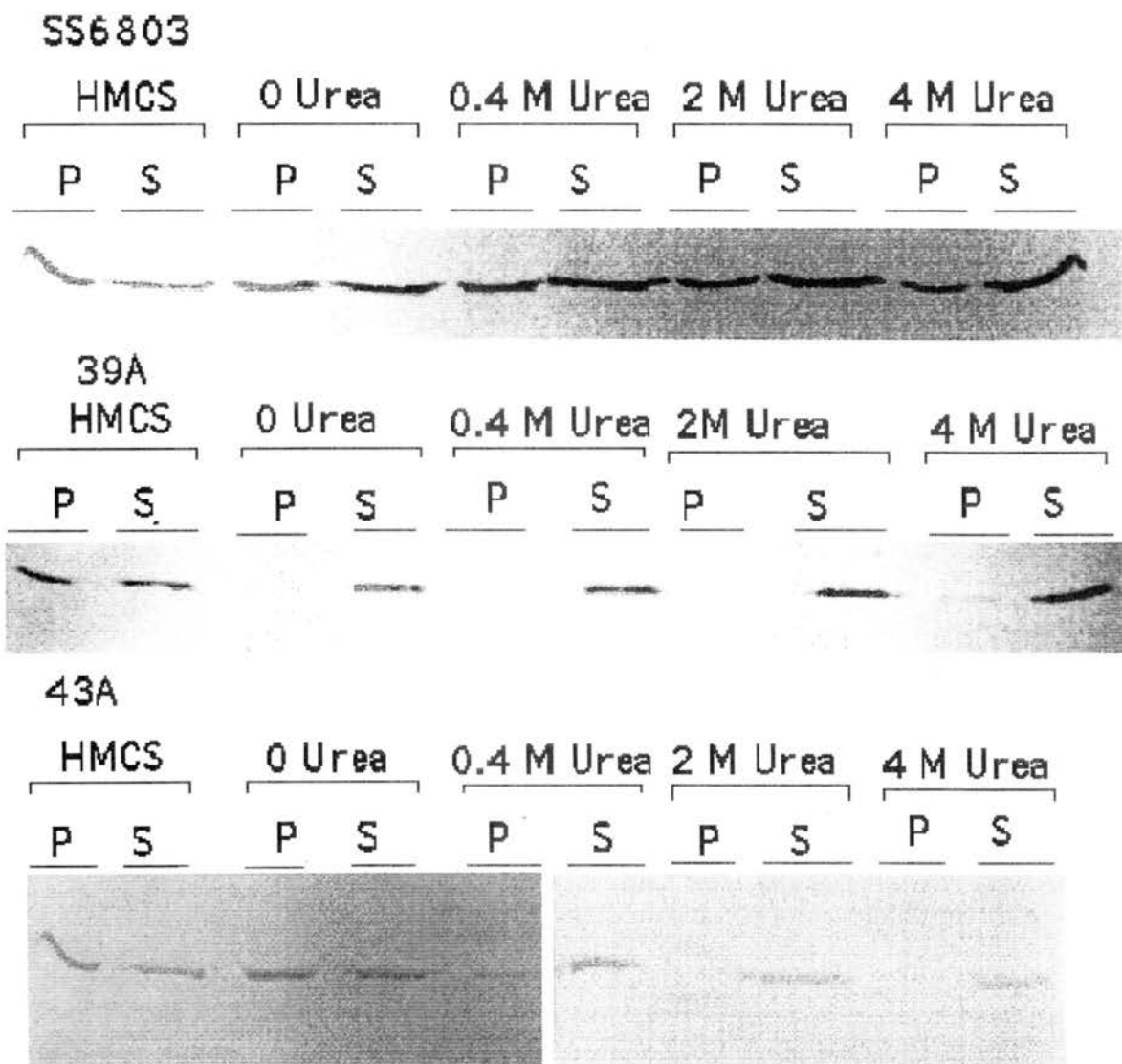


Figure 13: Immunoblot analysis of MSP in membrane containing pellet and post-centrifugal supernatants in lanes designated P and S, respectively. Samples were resuspended in HMCS buffer pH 7 without any urea which is designated as lane HMCS (50 mM HEPES, 10 mM MgCl<sub>2</sub>, 5 mM CaCl<sub>2</sub>, and 1 M sucrose). Samples which contain different concentrations of urea (designated as Zero, .4, 2, and 5 M urea) were resuspended in HS pH 7 (50 mM HEPES, 1 M sucrose). Samples analyzed: SS6803 wild type, 39A and 43A calcium-dependent mutants.

changes of 0.01  $\mu\text{M}/\text{ml}$  oxygen. The tested cells were washed with pH 7 HN buffer and incubated at room temperature on a rotary shaker under constant illumination prior to measurement.

The oxygen-evolving activities were measured by dispensing 6  $\mu\text{g chl mL}^{-1}$  of active cells into 1.7 ml of NH buffer containing 750  $\mu\text{M}$  DCBQ and 4.5 mM  $\text{k}_3\text{Fe}(\text{CN})_6$ . The amount of oxygen signal was recorded by a computer.

Figure 14 shows the mean of the maximal light saturated rates of  $\text{O}_2$  evolution oxygen ( $\text{VO}_{2,\text{max}}$ ) of whole cells of the 39A, 39B, 43A and 43B mutants. The  $\text{VO}_{2,\text{max}}$  of the 39A and 39B random mutants was 89 and 82% (respectively) compared to the wild type SS6803 (100%). However, the  $\text{VO}_{2,\text{max}}$  of 43A and 43B was 75 and 73% (respectively) compared to the wild type SS6803. Moreover, it should be noted that the calcium-dependent mutants were more light-sensitive than the wild type SS6803. This was observed by wide range fluctuation of the  $\text{VO}_{2,\text{max}}$  (wider error bar) compared with the wild type. Photoinhibition might be possible reason for greater variability of the  $\text{VO}_{2,\text{max}}$  of the random mutants (Fig. 15).

The 39A / 39B and 43A / 43B calcium-dependent mutants have not only exhibited lower  $\text{VO}_{2,\text{max}}$  compared to the wild type SS6803, but they also showed somewhat faster decline in the activity upon illumination, as has been reported previously (44, 47), Figure 15. This loss of  $\text{O}_2$  evolution activity during illumination may imply that the PSII complex in the mutant cells is sensitive toward photoinhibition. This observation is a typical phenomenon in mutants which suffer impairments at their donor side of PSII. Dark respiration, photorespiration and Mehler reaction might also be a possible reason which might increase the sensitivity of the cells for photoinhibition as well (24), please see Material and Methods).

To confirm the alteration of  $VO_{2,max}$  activities of the calcium-dependent mutants, active membranes of mutants were isolated. Figure 16 shows the active membrane  $VO_{2,max}$  of 39A, 39B, 43A, and 43B, which were 55, 50, 62, 90 %, respectively, compared to the wild type SS6803. It is also interesting to observe that upon isolating active membranes from the calcium-dependent mutants, the mutants exhibited more loss of activity than the wild type SS6803, Fig. 17. Figure 17 shows the percent of  $VO_{2,max}$  recovered upon isolating the active membrane from whole cells. The recovery of  $VO_{2,max}$  membrane activity of 39A, 39B, 43A, and 43B was 57, 75, 77, 69 %, respectively, while the recovery of  $VO_{2,max}$  activity upon isolating the wild type SS6803 membrane was 99%. This confirms the instability of the calcium-dependent mutants.

**Spectroscopic Characterization.** Our work also included spectroscopic characterization of calcium-dependent mutants. The absorption spectrum of the whole cells and the active isolated membranes was measured to see the purity of the active membranes. Figure 18 (39A, 39B, 43A and 43B) shows the spectra of the whole cells and the active membranes for each mutant. The spectra of active membranes of all samples reveal a significant reduction in the absorbance in the region of the spectrum where phycocyanin absorbs maximally (around 620) compared to the whole cells. This suggests that the active membranes were free from any biliproteins and all the oxygen-evolving activities were produced by active membranes rather than samples which might be contaminated with live cells. Biliprotein contamination indicates the presence of whole-cell photosynthetic pigments. Biliproteins are photosynthetic-pigment containing proteins which are a part of the light harvesting complex (LHC) in the whole cell and the LHC's are located on the outer membrane of the thylakoid.

**The kinetics of oxygen release.** It was mentioned in the previous work that deleting MSP retarded the oxygen release from the S<sub>3</sub>-state (9). Further work by Shen et al. (unpublished data) also indicated that deleting cyt c-550 slightly retarded the S<sub>3</sub>-[S<sub>4</sub>]-S<sub>0</sub>

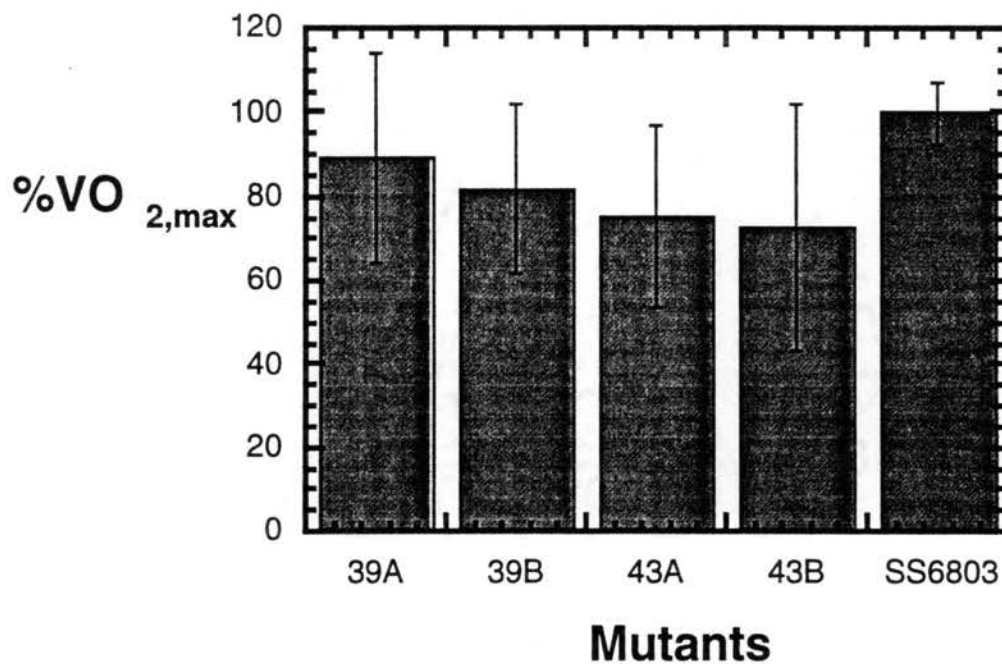


Figure 14: Maximal light-saturated rate of O<sub>2</sub> evolution (VO<sub>2,max</sub>) of whole cells expressed as a percentage of the rate observed for the wild type SS6803. The average wild type rate (100%) was determined to be 677  $\mu\text{mol of O}_2 (\text{mg of chl})^{-1} \text{h}^{-1}$  under continuous saturating illumination as was measured at 30° C with addition of 750  $\mu\text{M}$  DCBQ and 4.5 mM K<sub>3</sub>Fe(CN)<sub>6</sub> and with samples at a concentration of 6  $\mu\text{g}$  of chlorophyll ml<sup>-1</sup>. The error bars represent the standard deviation of maximal rates. The mean was an average of 4-6 readings. The cells were grown in BG11 medium supplemented with 5 mM Glucose.

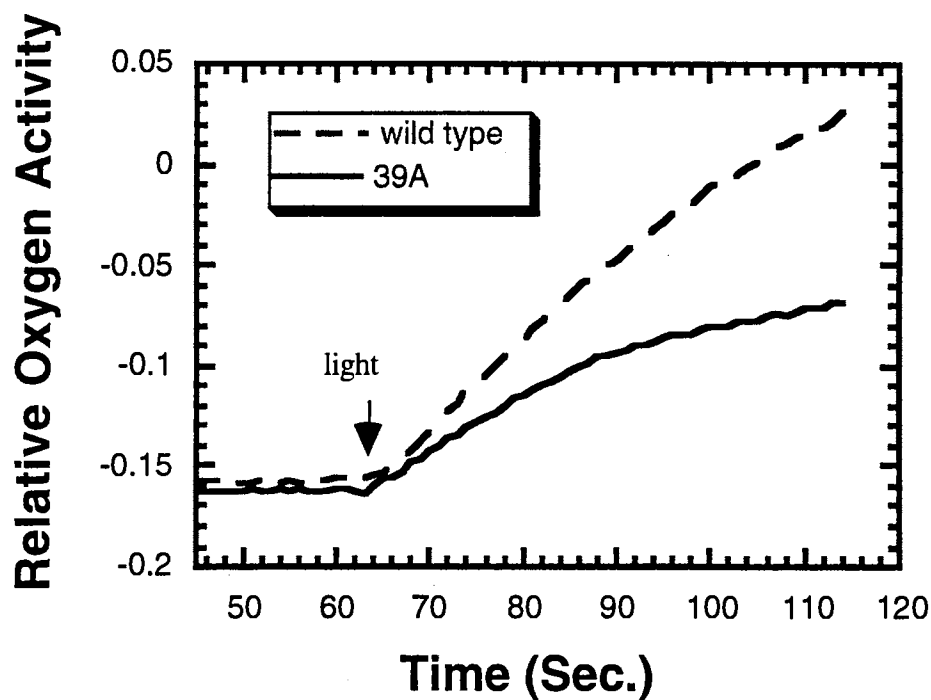


Figure 15: Oxygen-evolving activities of the wild type SS6803 and calcium-dependent mutant. The graph shows that the 39A calcium-dependent mutant was photoinhibited compared to the wild type. The cells were grown in BG11 medium supplemented with 5 mM glucose. The oxygen-evolving activities were measured in continuous illumination at 30° C with addition of 750  $\mu$ M DCBQ and 4.5 mM  $K_3Fe(CN)_6$  as electron acceptors and with samples at a concentration of 6  $\mu$ g of chlorophyll ml<sup>-1</sup>.

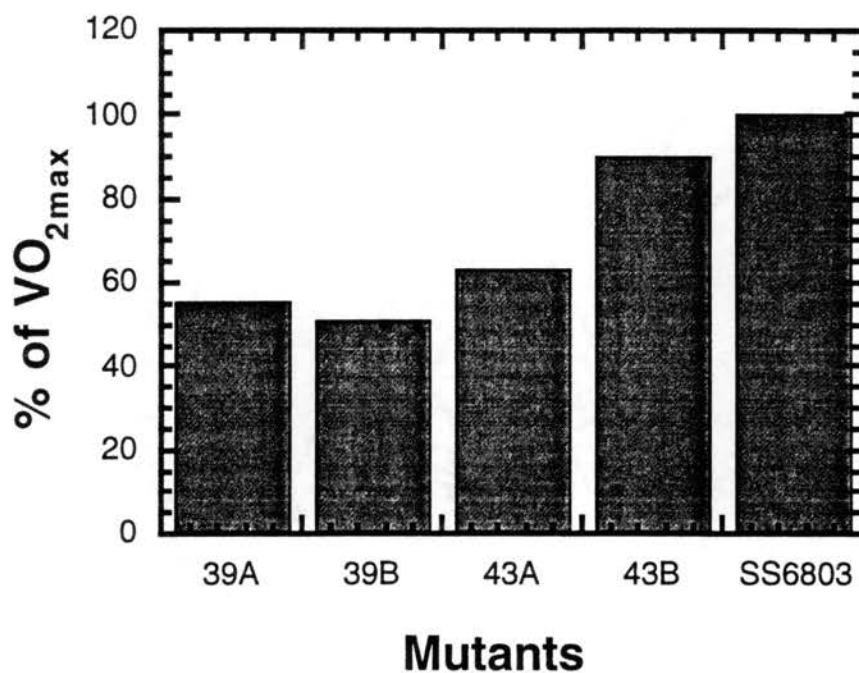


Figure 16: The mean of the maximal rate of  $O_2$  evolution ( $VO_{2,max}$ ) of membrane expressed as a percentage of the rate observed for the wild type SS6803. The wild-type rate (100%) was determined to be  $620 \mu\text{mol } O_2 (\text{mg chl})^{-1} \text{ h}^{-1}$  under continuous saturating illumination at  $30^\circ \text{C}$  with addition of  $750 \mu\text{M}$  DCBQ and  $4.5 \text{ mM}$   $K_3\text{Fe}(\text{CN})_6$  and with samples at a concentration of  $10 \mu\text{g chl.ml}^{-1}$ . The cells were grown in BG11 medium supplemented with  $5 \text{ mM}$  glucose. The  $VO_{2,max}$  of each random mutant represents one measurement of successful active membrane isolation.

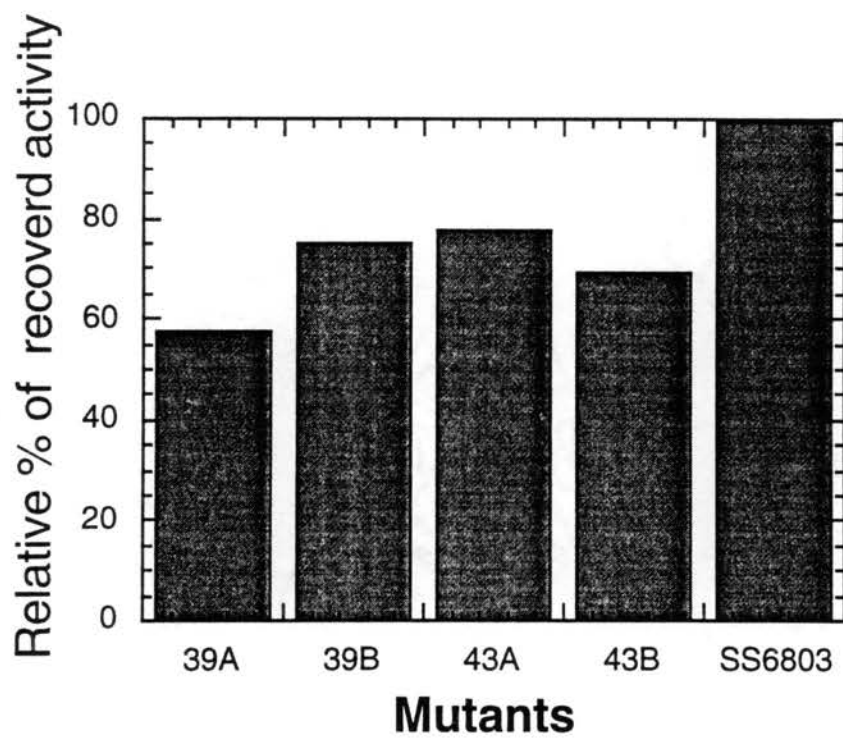


Figure 17: Maximal recovery of oxygen evolution,  $VO_{2, \text{max membrane}}/VO_{2, \text{max Cells}}$  isolated membranes. Samples analyzed: 39A, 39B, 43A, 43b and wild type SS6803.



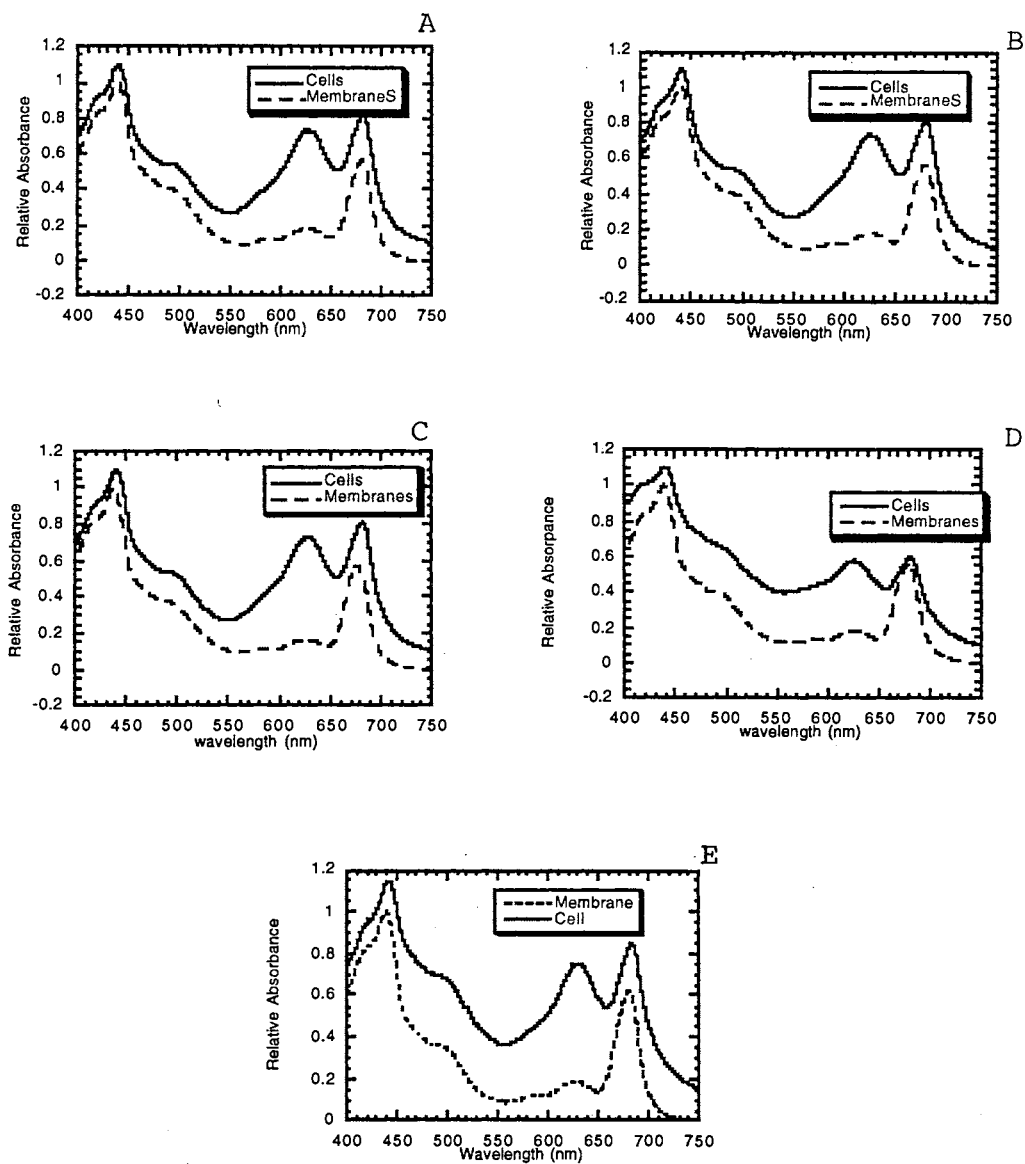


Figure 18: Absorption spectra of the whole cells and cell membranes of the A: 39A, B: 39B, C: 43A, D: 43B calcium-dependent mutants and E: the wild type SS6803.

transition whereas the deletion of 12 KDa (*psbU*) did not elicit any alteration in oxygen release in the S<sub>3</sub>-state. In this work we measured the oxygen release from the S<sub>3</sub>-state by placing 5 µg Chl mL<sup>-1</sup> of the sample onto the surface of a bare platinum electrode by centrifugation at 5,000 x g for 5 min. at 25<sup>o</sup> C in the dark. Sample were illuminated with saturating, single turn-over xenon flashes. The oxygen signal generated was digitized and recorded by a computer.

Figure 19, A shows an example of the recorded amperometric signal of the 39B calcium-dependent mutant. Four flashes per second for five seconds were directed toward the sample and the result oxygen signal was recorded. Since the rise time of oxygen signal depends on the rate of oxygen release from the S<sub>3</sub> state and the diffusion process of molecular oxygen out of the cells, Figure 19B shows the enlargement of one signal to illustrate the rise time (the length of time it takes the curve to peak). Figure 20 shows that the rise time of the oxygen signals of 39A, 39B, 43A, 43B are all between 9-13 ms, similar to that observed for our wild type SS6803 and previous work as well. This suggests that there is no alteration in the rise time of the calcium-dependent mutants. Because the rise time of the mutants is similar to the wild type, our measurements do not distinguish between the rise time and the diffusion process. Thus, Shen et al. (43) indicated that there is significant difference in the rise time of  $\Delta psbV$  compared to the wild type using bare platinum electrode (in our lab). This suggests that the rise time measurements are most likely representative of the oxygen release from the S<sub>3</sub> state rather the diffusion of the oxygen.

**Sequence analysis.** After conducting all the physiological characterizations of the calcium-dependent mutants (39A, 39B, 43A, 43B), it was important to conduct sequence analysis of the *psbO* gene in the pSSO39 and pSSO43 plasmids. Surprisingly, our sequence data revealed that the *psbO* gene located in pSSO39 and pSSO43 did not have any sequence alteration (Fig. 21). This conclusion was reached after sequencing the *psbO*

gene completely in two directions using three different primers. The meaning of these results will be explained in detail in the discussion section.

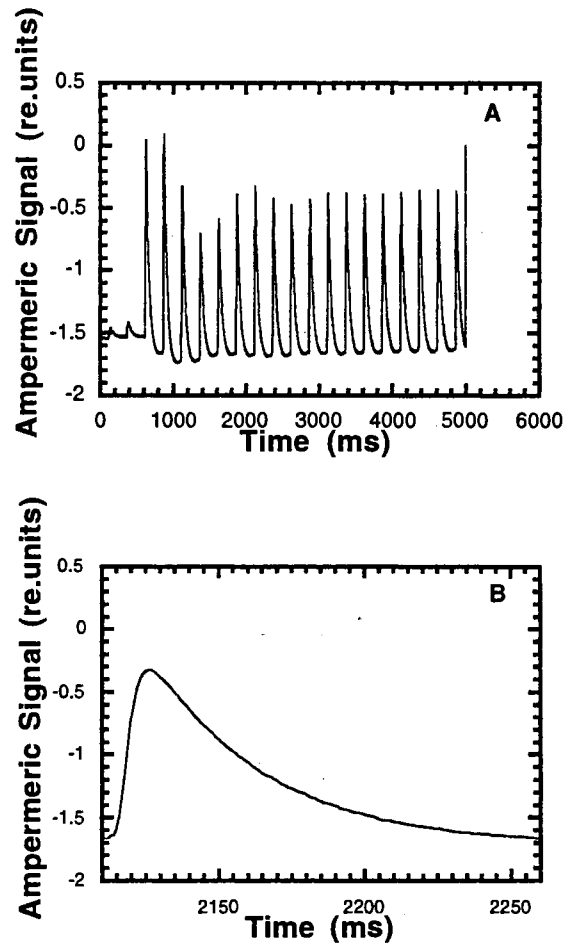


Figure 19: Time- resolved O<sub>2</sub> release signal from the bare platinum oxygen electrode (mutant 39B). The cells were collected onto the surface of the electrode and then subjected to illumination with 20 flashes at 4 Hz. A: entire O<sub>2</sub> trace. B: single flash showing kinetics.

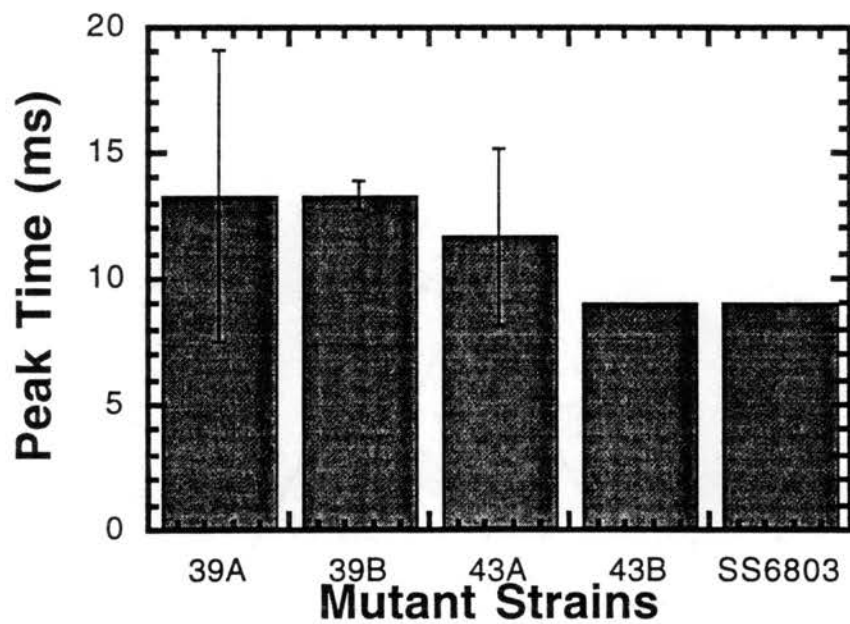


Figure 20: Rise time of the calcium-dependent mutants which measures the kinetic release of oxygen upon flashing the sample with light. The peak time represents the mean and the error bar represents the standard deviation of the rise time. Sample analyzed: 39A, 39B, 43A, 43B and wild type SS6803.

psbO (wt)	1	M R F R P S I V A L L S V C F G L L T F L Y S G S A F A V D K S Q	33
psbO39	1	M R F R P S I V A L L S V C F G L L T F L Y S G S A F A V D K S Q	33
psbO43	1	M R F R P S I V A L L S V C F G L L T F L Y S G S A F A V D K S Q	33
psbO (wt)	34	L T Y D D I V N T G L A N V C P E I S S F T R G T I E V E P N T K	66
psbO39	34	L T Y D D I V N T G L A N V C P E I S S F T R G T I E V E P N T K	66
psbO43	34	L T Y D D I V N T G L A N V C P E I S S F T R G T I E V E P N T K	66
psbO (wt)	67	Y F V S D F C M E P Q E Y F V K E E P V N K R Q K A E Y V K G K V	99
psbO39	67	Y F V S D F C M E P Q E Y F V K E E P V N K R Q K A E Y V K G K V	99
psbO43	67	Y F V S D F C M E P Q E Y F V K E E P V N K R Q K A E Y V K G K V	99
psbO (wt)	100	L T R Q T T S L E Q I R G S I A V G A D G T L T F K E K D G I D F	132
psbO39	100	L T R Q T T S L E Q I R G S I A V G A D G T L T F K E K D G I D F	132
psbO43	100	L T R Q T T S L E Q I R G S I A V G A D G T L T F K E K D G I D F	132
psbO (wt)	133	Q P I T V L L P G G E E V P F F F T V K N F T G T T E P G F T S I	165
psbO39	133	Q P I T V L L P G G E E V X F F F T V K N F T G T T E P G F T S I	165
psbO43	133	Q P I T V L L P G G E E V X F F F T V K N F T G T T E P G F T S I	165
psbO (wt)	166	N S S T D F V G D F N V P S Y R G A G F L D P K A R G L Y T G Y D	198
psbO39	166	N S S T D F V G D F N V P S Y R G A G F L D P K A R G L Y T G Y D	198
psbO43	166	N S S T D F V G D F N V P S Y R G A G F L D P K A R G L Y T G Y D	198
psbO (wt)	199	N A V A L P S A A D K F R T N K K E T P L G K G T L S L Q V T Q V	231
psbO39	199	N A V A L P S A A D K F R T N K K E T P L G K G T L S L Q V T Q V	231
psbO43	199	N A V A L P S A A D K F R T N K K E T P L G K G T L S L Q V T Q V	231
psbO (wt)	232	D G S T G E I A G I F E S E Q P S D T D L G A K E P L D V K V R G	264
psbO39	232	D G S T G E I A G I F E S E Q P S D T D L G A K E P L D V K V R G	264
psbO43	232	D G S T G E I A G I F E X E Q P S D T D L G A K E P L D V K V R G	264
psbO (wt)	265	I F Y G R V D T D V	274
psbO39	265	I F Y G R V D T D V	274
psbO43	265	I F Y G R V D T D V	274

Figure 21: Deduced sequence alignments of the *psbO* protein of the psbO39 (pSSO39), psbO43 (pSSO43), and wild type. The X represents a possible error of the sequence. The errors were checked visually and the errors were confirmed to be an error of the DNA editing software (Edit View).

## Discussion

In this work, we describe the isolation and analysis of altered calcium-dependent mutants of *Synechocystis* sp. PCC6803. We used random mutagenesis to generate mutations in the 6.4 kb *Hind*III fragment containing the *psbO* locus and phenotypic enrichment and screening to isolate calcium-dependent mutants in order to identify possible calcium-binding sites in MSP. Alteration in calcium-binding sites of MSP might exhibit elicited calcium requirements and, therefore, might give more information on the role of calcium in oxygen-evolving activities of PSII in *Synechocystis* sp. PCC6803.

Two mutants with increased autotrophic calcium requirements were recovered after transforming the mutagenized 6.4 kb *Hind*III fragment to *psbO* deletion mutants S425. The *Hind*III fragment carries the *psbO* gene, kanamycin cassette, ORFX, *aroA* and different hypothetical small polypeptides (Fig. 5). Cycloserine enrichment and microtiter plates were used to isolate calcium-dependent mutants. These calcium-dependent mutants 39A and 43A exhibited the following: (a) No alteration of doubling time in the absence of calcium with a significant lag prior to exponential growth; (b) weak protein-binding of MSP with PSII; (c) decreased oxygen evolution comparable to some of the MSP site-directed mutants; (d) unaltered kinetic oxygen release from the S<sub>3</sub> state; (e) unaltered DNA sequence of the *psbO* gene.

As documented in previous studies, adding calcium to the MSP deletion strain S425 causes the recovery of growth and partial restoration of oxygen-evolving activities (8). The 39A and 43A calcium-dependent mutants exhibited a large increase in the lag phase of batch culture growth compared to the wild type SS6803 when the measurements were performed in the calcium-depletion medium. This alteration of the growth rate in the calcium-depletion medium is not statistically significant ( $P=0.564$ , it should be lower than 0.05 in order to be statistically significant) and as pronounced as in the MSP deletion mutant S425 (9) and

other mutants such as the  $\Delta psbO$ - $\Delta psbV$  mutant (47), which fail to grow at all under similar conditions.

One of the important functions for calcium in the *Synechocystis* PSII complex is the maintenance of normal oxygen evolution. Several studies indicated that calcium-binding site(s) in PSII of cyanobacteria have low affinity compared to the higher plants. This low-affinity for calcium in cyanobacteria might be related to the higher concentration of calcium in the cyanobacteria compared to chloroplasts (4). It is possible that a prolonged lag in growth of the two mutants in the calcium-depletion medium in the first 24 hours might indicate the decreased affinity of calcium-binding sites in PSII. Subsequently, calcium released from lysed cells in the medium supported further cell and recovery at a normal growth rate. However, this interpretation is unlikely since cell densities several-fold greater than the initial density are achieved, implying that release calcium would not be great enough to support relatively high final yields of cells. Therefore, the long lag may relate to a transient effect. The long lag phase might also be related to the photoinhibition of the cells during growth in a calcium-depletion medium. It should be noted that the two mutants exhibit a photoinhibition effect compared to the wild type (Fig. 15). According to this hypothesis calcium may be necessary to protect PSII from photoinhibition.

Previous biochemical analysis has indicated that MSP, cyt c-550, and other proteins may also be critical for the binding of the proteins to the reaction center (39, 47). In this work, in vitro binding assays of fractionated cell lysate as shown in Figures 12 demonstrated that the two mutants 39A and 43A exhibited weaker binding to PSII following cell lysis. This weakened binding using cell lysates was observed because a major fraction of MSP was found in the supernatant compared to the amount in the pellet. Similarly, using purified membranes (Fig. 13), the MSP protein fraction exhibited weakened binding in the presence of a low concentration of urea compared to the wild type SS6803. This weaker binding indicated destabilization of PSII.



The altered of the MSP binding of the two mutants 39A and 43A is correlated with altered oxygen-evolving activity. Figure 14 demonstrates that 39B and 43B as well as 39A and 43A exhibited a decrease in oxygen-evolving activities.

Transformation with the recloned 6.4 kb *HindIII* fragment, which caused the low oxygen-evolving activities of 39A and 43A mutants, results in the same alterations of oxygen-evolving activities in the 39B and 43B mutants which indicates that the phenotypes are due to the same alteration in the corresponding 6.4 kb *HindIII* DNA fragments. This might decrease the possibility that the alteration of oxygen-evolving activities and protein binding of the 39A and 43A mutants might be attributed to ectopic mutations somewhere in the chromosome other than in the 6.4 kb *HindIII* fragment.

Normal kinetics of oxygen release during S<sub>3</sub>-[S<sub>4</sub>]-S<sub>0</sub> transition were observed in the wild type SS6803 and in the deletion mutant of the 12 KDa extrinsic proteins encoded by *psbU* (43). Similarly, Figure 20 shows that the peak of the oxygen signal for both the wild type and calcium-dependent mutants occurs in 9-13 ms immediately following the third flash. These results indicate that the mutants had normal oxygen release kinetics during the S<sub>3</sub>-[S<sub>4</sub>]-S<sub>0</sub> transition.

#### Sequence Analysis of 39A and 43A Calcium-Dependent Mutants

After the cloning of the 6.4 kb *HindIII* fragment from the 39A and 43A mutants, sequence analysis of the corresponding two plasmids pSSO39 and pSSO43 was conducted. It was surprising that the sequence data of the *psbO* gene of the two mutants in two directions revealed a wild type sequence for both putative mutants. Figure 21 shows the alignment sequence of the two mutants 39A and 43A compared to the wild type. The absence of the *psbO* sequence alteration in the 39A/ 43A mutants and the presence of physiological alteration at least in the doubling time, VO<sub>2,max</sub>, protein binding suggests the presence of mutation(s) somewhere in the 6.4 kb *HindIII* fragment. This potential

mutation(s) which should be located outside of the *psbO* sequence 1) affects the activity of PSII or 2) affects another protein that modulates MSP binding and PSII or 3) affects the ionic concentrations (perhaps calcium or chloride) and this modifies MSP binding and PSII function. This raises the possibility of a potential undiscovered polypeptide(s) which might interact with PSII. This hypothetical protein might physically interact with the PSII complex. Alternatively, it exerts its effects indirectly by providing a factor necessary for the stable functioning of the complex.

Figure 4 shows that there are three hypothetical proteins located up and downstream of the *psbO* sequence. Sequencing these fragments might reveal the location of point mutations. In previous work (8), the *psbO* gene was deleted by replacing the 1.3 kb *AflIII-XbaI* fragment from the genome of the wild type *Synechocystis* by the spectinomycin cassette and this strain was named S425. Furthermore, when the 6.4 kb *HindIII* fragment carrying the *psbO* gene and kanamycin integrate by double-crossing over, the homologous recombination of the fragment can be in any location beyond the 1.3 kb *AflIII-XbaI* in both ends of the 6.4 kb *HindIII* fragment (Figure 2).

Narrowing down the search for the location of these potential mutants might help to restrict the sequence work to fragments which encode for small polypeptides only. Therefore, digesting pSSO39 and pSSO43 with *EcoR5* will eliminate the possibility of the 2.3 kb carrying *trnQ* and *aroA* genes from integrating in the chromosome when transforming the digested mixture to the *psbO* deletion mutant. This will allow only the *psbO* gene, kanamycin cassette and 473 bp above the *AflIII* site (see Figure 4) to integrate by homologous recombination.

The remaining fragment after digesting the pSSO39 and pSSO43 with *EcoR5* will harbor three hypothetical polypeptides 61, 75 and 125 amino acids. This will not only help narrow the possible locations of the mutants, but also generate new mutants 39C and 43C

which, hypothetically, should have the same physiological alteration as 39A/39B and 43A/43b, respectively.

The constraints of time and money did not allow us to pursue this further. Therefore, 39C and 43C were created and further analysis needs to be conducted.

It should be indicated that some of the random mutants which were created by mutating the 6.4 kb *Hind*III fragment using the same strategy of mutator *E.coli* strain did not have any sequence alteration. These random mutants were selected by our collaborators Dr. Pascal Meunier and Dr. Louis Sherman using a Digital Imaging Spectrophotometer (unpublished data). These random mutants exhibited physiological alteration despite the fact that an unaltered sequence of the *psbO* gene was observed although of physiological alterations. Our collaborators are investigating these mutants further in order to localize the actual point mutations in the 6.4 kb *Hind*III mutated fragment.

## CHAPTER V

### INTERACTION BETWEEN MSP AND CYTOCHROME C-550

#### Introduction

Cyt c-550 is a 17 KDa extrinsic protein which is reported to interact weakly physically with the 33 KDa MSP in the PSII complex (44, 47). Both proteins are proven to be important for the stabilization of PSII in *Synechocystis*. Deletion of either protein separately causes 60-70% reductions in the rate of oxygen evolution (44). Shen et al. (47) have shown that deleting both cyt c-550 and MSP from *Synechocystis* simultaneously produces a mutant which can not grow without glucose and evolves oxygen at a rate of 8% of the wild type. In the same study, it was demonstrated that MSP enhances the binding of cyt c-550 by 10%.

In this work we have explored the interaction of MSP and cyt c-550 by introducing site-directed mutants in MSP in the absence of cyt c-550. Three set of mutations were introduced into MSP in a strain that has already had the *psbV* gene encoding for cyt c-550 deleted. The first mutant: Asp159 of MSP was changed to Asn in the absence of cyt c-550. The second mutant: Arg163 of MSP was changed to Leu in the absence of cyt c-550. The third mutant: Asp159 -Arg163 of MSP was respectively changed to Asn and Leu in the absence of cyt c-550. Our data indicated that Asp159Asn - $\Delta$  cyt c-550 and Arg163Leu- $\Delta$  cyt c-550 could not grow without glucose, yet they exhibited 44-64% oxygen-evolving activity compared to the wild type, whereas the Asp159Asn -Arg163Leu- $\Delta$  cyt c-550 mutant could grow without glucose and exhibited 72% oxygen-evolving activity compared to the wild type. These results point to an intramolecular interaction

between the Asp159 and Arg163 residues of MSP and an unusual interaction between the *psbO* and *psbV* loci.

## Results

Shen et. al. (47) demonstrated a pronounced destabilization of oxygen-evolving activity in the double deletion mutant  $\Delta psbO$ - $\Delta psbV$ . Furthermore, the inability of the double deletion mutant  $\Delta psbO$ - $\Delta psbV$  to grow autotrophically indicated the concerted action of the two proteins in the support of the autotrophic growth of *Synechocystis*. Consistent with the absolute requirement of PSII function for autotrophic growth, we explored the effects of combining our most severe site-directed mutants in MSP in the  $\Delta psbV$  background.

### Introduction of Site-directed Mutants of the MSP in the Absence of Cyt c-550

The *psbV* was deleted using a plasmid which was provided by Shen et al. (47). In this  $\Delta$  c-550 plasmid the *psbV* was replaced by an erythromycin cassette. Using the  $\Delta$  c-550 plasmid to transform the *psbO* deletion mutant S425, a new genetically-engineered mutant containing the double deletion of *psbO* and *psbV* was recovered. The double deletion mutant *psbO* -*psbV* was streaked three times on BG11 plates containing 5 mM glucose, 10  $\mu$ M DCMU, 5  $\mu$ g spectinomycin and 1  $\mu$ g erythromycin. To confirm the *psbV* deletion, the recovered mutant was tested on autotrophic BG11 medium. The mutant  $\Delta psbO$  - $\Delta psbV$  could not grow autotrophically confirming the previous work of Shen et al. (47). This indicated that *psbV* was indeed deleted. Other work testing presence using heme staining techniques corroborated this.

Further work included the introduction of site-directed mutants of *psbO* in the absence of *psbV*. M. Qian (unpublished data) has produced many site-directed *psbO* mutants at different highly conserved amino acid positions. In this work, we used three site-directed mutants which exhibited phenotypic alteration upon transforming a *psbO* deletion mutant S425 (Dr. Qian- unpublished data). These mutants are shown in Table 7

and the hypothetical interaction between the two amino acids Asp159 and Arg163 are shown in Figure 22A, 22B.

The plasmids which contain the MSP site-directed mutants were introduced to the  $\Delta psbO \Delta psbV$  *Synechocystis* mutant by transformation. The new mutants were recovered and streaked three times on BG11 plates containing 5 mM glucose, 10  $\mu$ M DCMU, 5  $\mu$ g kanamycin and 1  $\mu$ g erythromycin to ensure separation from the wild type chromosome. The following mutants were created:  $\Delta psbV$ -Arg163Leu-Asp159Asn,  $\Delta psbV$ -Arg163Leu,  $\Delta psbV$ -Asp159Asn.

#### Growth in the Absence of Glucose

Figure 23 shows the autotrophic growth curve of  $\Delta psbV$ -Asp159Asn-Arg163Leu,  $\Delta psbV$ -Asp159Asn, and  $\Delta psbV$ -Arg163Leu.  $\Delta psbV$ -Asp159Asn and  $\Delta psbV$ -R153L could not grow in the absence of glucose whereas  $\Delta psbV$ -Asp159Asn-Arg163Leu was able to grow in the absence of glucose. The inability to grow autotrophically caused by the mutation of  $\Delta psbV$ -Asp159Asn or  $\Delta psbV$ -Arg163Leu was suppressed or compensated by the second mutation of Arg163Leu or Asp159Asn, respectively. We also tested the two single mutant strains' ability to grow in the absence and presence of glucose. Figure 24 shows that the two mutants  $\Delta psbV$ -Asp159Asn, and  $\Delta psbV$ -Arg163Leu grew very well in the presence of glucose confirming initial observation of the glucose-dependence growth in these mutants.

In order to determine whether the inability of  $\Delta psbV$ -Asp159Asn and  $\Delta psbV$ -Arg163Leu to grow in the absence of glucose is related to the deletion of the *psbV* gene, we next examined the abilities of the two mutants Asp159Asn and Arg163Leu to grow autotrophically. Figure 25 shows that Asp159Asn, Arg163Leu, and Asp159Asn-

Table 7

SITE-DIRECTED MUTANTS OF MSP	
R163L	A change of the 163 arginine (R) amino acid (basic) to non-polar side chain amino acid Leucine
D159N	A change of the 159 aspartic acid (D)(acidic) to neutral amino acid asparagine (N)
D15N-R163L	The two mutans are together

Table 7: These Mutants were created by M.Qian using site-directed mutagenesis.



ANABAENA	1	TRD--ILTYEQI-----RGTGLANKCPQITE	TSRGS	IPLDS	SKSYVL
ARABIDOPS	1	EGAPKRLTYDEIQSKTYMEVRGTGTANHSPTI	-DGGSE	TF9	FKPGR
CHLAMYDOM	1	AGSANALTFDEIQGLTYLVKGGSIANTCPVI	-ESGTT	NLKE	LKAGSYKL
PEA	1	EGAPKRLTFDEIQSKTYLEVKGGTGTANQCPTI	-DGGVDS	F9	FKPGR
POTATO	1	EGVPKRLTFDEIQSKTYMEVRGTGTANQCPTI	-DGGVDS	F9	FKPGR
S6803	1	DKS--QLTYDDI-----VNTGLANVCPEISS	FTRGT	IEVE	PNTRYFV
S7942	1	DIG--TLTYDQI-----KDTGLANKCLS	LKE	S	ARGTIPLEAGKRYAL
SELONG	1	AKQ--TLTYDDI-----VGTGLANKCPTLDD	TARGAYP	IDSS	QTYRI
SPINACH	1	EGG--KRLTYDEIQSKTYLEVKGGTGTANQCPTV	-EGGVDS	F9	FKPGR
WHEAT	1	EGAPKRLTFDEIQSKTYMEVRGTGTANQCPTI	-DGGVDS	F9	FKPGR
consensus		EGA KR yda QSKTYMEVKGt T CPTi DGG ESF FKPGR L			
ANABAENA	41	KELCLEPTNFFVKEEPAKRRQTAEFVAGKLLTRY	TS	TIDQV	9CDLKFND
ARABIDOPS	49	KKFCFEPTSFVVRADS	VSKNAPPEFQNTKLM	TRLTY	TLDEIEGPF
CHLAMYDOM	50	ENFCLEPTSFVVEESQFRGGTEFVKTKLM	TRLTY	TLDAM	SGSFKVGS
PEA	49	KKLCLEPTSFVVRSEGVTKNTPLAFQNTKLM	TRLTY	TLDEIEGPF	FEVSAD
POTATO	49	KKFCLEPTSFVVRKAEVSKNSAPDFQTKLM	TRLTY	TLDEIEGPF	FEVSPD
S6803	41	SDFCMEPQEFVKEEPAKRRQKAEYVGRVLT	BQTT	SLQIRGS	IAVGAD
S7942	41	TDLCLEPQEFFVKEEPAKRRQKAEFVPGRVLT	TRY	TS	SLDQVYCDLAKAD
SELONG	41	AKLCLEPTTFVVEEPAKRRQKAEFVPTKLVT	RETT	SLDQI	QCELEKVN9D
SPINACH	48	KKFCLEPTKFAVKAEGISKNSGPDFQNTKLM	TRLTY	TLDEIEGPF	FEVSSD
WHEAT	49	KKFCLEPTSFVVRKAEIQKNEPPRFQTKLM	TRLTY	TLDEIEGPF	LEVRRR
consensus		RKF La TSFT Ea VN N Ef T lm L Ytldeie PFEV D			
ANABAENA	91	SLTFVEEKDGLDFQAI	TVQLP	GGERV	PFLFTIKNLVAQTQ
ARABIDOPS	99	GSVNFKEEDGIDYAAAV	TVQLP	GGERV	PFLFTIKQLDASGKP
CHLAMYDOM	100	GSSELKEDDGI	YAAAVTVQLP	GGERV	AFLFTIKQFDGKGL
PEA	99	GSVNFKEEDGIDYAAAV	TVQLP	GGERV	PFLFTIKQLVASGKP
POTATO	99	GTVKFEEKDGI	YAAAVTVQLP	GGERV	PFLFTIKQLVASGKP
S6803	91	GTLTFKERDGI	DFQPI	TVLLP	GGEVPPFFFTVKNFTGTTEP
S7942	91	GTVSFTEKRGSI	DFQAI	TVLLP	GGEVPPFLFTVRGLVASTSEPATSINTST
SELONG	91	SLTFVEEDGIDFQPI	TVQLP	MAGGERI	PLLFTVRNLVASTQPNVTSTITS
SPINACH	98	GTVKFEEKDGI	YAAAVTVQLP	GGERV	PFLFTIKQLVASGKP
WHEAT	99	RTLKFEEKDGI	YAAAVTVQLP	GGERV	AFLFTIKQLVATGKP
consensus		GsV F RD i yAAV QLP RvPFL i QLVA	SGKP		D
		(D)Asp159Asn(N)		(R)Arg163Leu(L)	
ANABAENA	141	DFEGTFKVP	SYRGS	SFLDP	KGRGGVVS
ARABIDOPS	141	SFTGKFLVP	SYRGS	SFLDP	KGRGGST
CHLAMYDOM	142	GIRGDFLVP	SYRGS	SFLDP	KGRGGST
PEA	141	SFSGDFLVP	SYRGS	SFLDP	KGRGAST
POTATO	141	SFSVDFLVP	SYRGS	SFLDP	KGRGGST
S6803	141	DFVGDFFNVP	SYRGS	SFLDP	KARGLYT
S7942	141	DLRGGFRVP	SYRTS	NFLDP	KARGLT
SELONG	141	DFKGEFNVP	SYRTAN	NFLDP	KGRGLAS
SPINACH	140	SFSGDFLVP	SYRGS	SFLDP	KGRGGST
WHEAT	141	SFRP-FLVP	SYRGS	SFLDP	KGRGGST
consensus		SF GDFL GsS g GSt dN V l	AGGRG	DEEEL	KE V

Figure 22A: Amino acid sequence of MSP and the conserved sequence in *Anabaena*, *Arabidopsis*, *Chlamydomonas*, *Pea*, *Potato*, *Synechocystis* sp. PCC6803, *Synechococcus* sp. PCC7942, *Selong*, *Spinach*, and *Wheat*. The figure shows the site-directed mutants of Manganese Stabilizing Proteins (D)Asp159Asn(N), (R)Arg163Leu(L). The green color shows the conserved sequences.

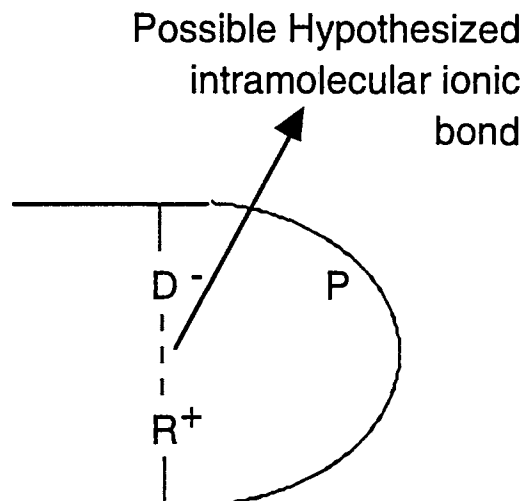


Figure 22B: Possible interaction between the Asp and Arg in the turn which formed by the Pro. It is quite possible that the Asn 159 and Leu163 in the absence of cyt c-550 disrupted the turn and the presence of the two mutant simultaneously somehow kept the turn intact in the absence of cyt c-550.

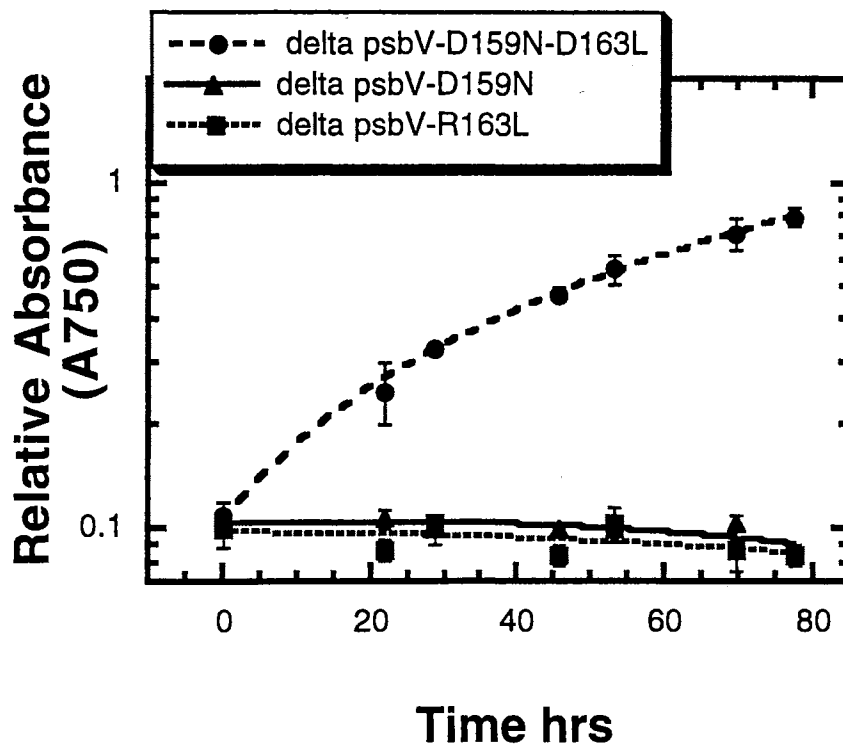


Figure 23: Growth rate of delta *psbV*-D159N-R163L, delta *psbV*-D159N, and delta *psbV*-R163L mutant strains in BG11 at 30° C in the absence of glucose. The absorbance readings represent the mean of three readings and the error bars represent the standard deviation.

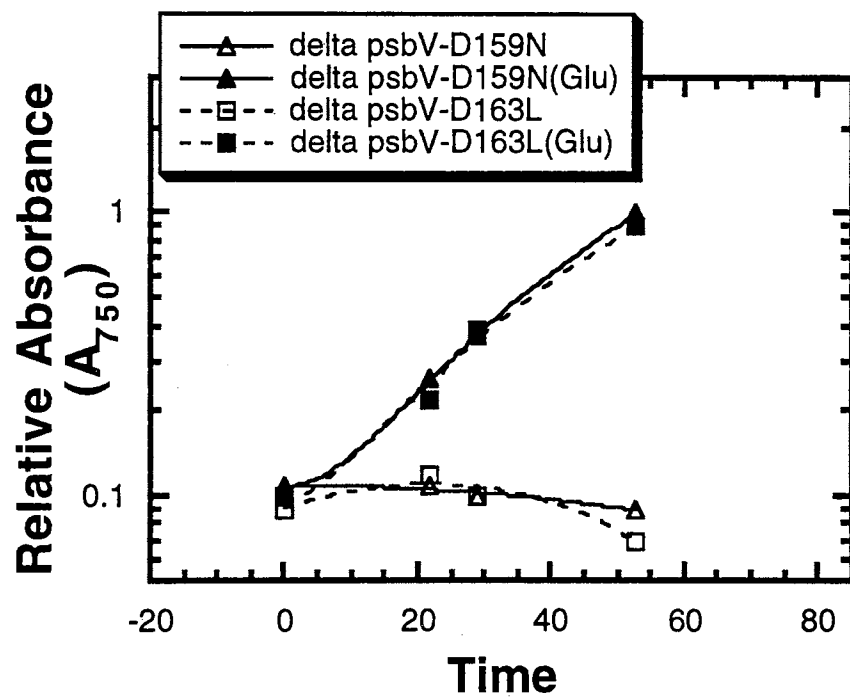


Figure 24: Growth rate of delta *psbV*- D159N and delta *psbV*-R163L mutant strains in BG11 at 30° C in the presence and absence of glucose.

Arg163Leu grew autotrophically suggesting that the inability of the two mutants  $\Delta psbV$ -Asp159Asn and  $\Delta psbV$ -Arg163Leu to grow autotrophically involves the absence of *psbV*.

To demonstrate that autotrophic growth depends on the involvement of the mutations Asp159Asn and Arg163Leu located on the *psbO* gene as well as absence of the *psbV* gene, we tested the ability of the *psbV* mutant (harboring wild type MSP) to grow autotrophically. Figure 26 shows that the  $\Delta psbO$  (S425),  $\Delta psbV$  and wild type SS6803 mutant strains grew autotrophically, but  $\Delta psbV$ - $\Delta psbO$  did not, indicating that the site-directed mutants Asp159Asn and Arg163Leu in the absence of the  $\Delta psbV$  are specifically involved in the support of the autotrophic growth of the *psbV* deletion mutants.

We conclude that *psbV* and the point mutations Asp159Asn and Arg163Leu are together involved in the support of autotrophic growth and one of them (Asp159Asn or Arg163Leu) suppresses the other in the absence of the *psbV* gene.

#### Immunoblot Analysis of the Mutants

Figure 27 shows an immunoblot experiment detecting the expression of MSP in all the mutant strains using polyclonal MSP spinach antibodies. As expected, the MSP was expressed in all the strains except the  $\Delta psbO$ - $\Delta psbV$  and  $\Delta psbO$  S425 mutants. This suggested that the inability of  $\Delta psbV$ -Asp159Asn and  $\Delta psbV$ -Arg163Leu to grow autotrophically is not simply caused by an absence of MSP.

Previous biochemical studies(47) indicated that upon deleting *psbV*, the PSII stability of PSII in the *Synechocystis* cells decreased (data not shown), and this was reflected by a decrease in the steady-state cellular concentration of PSII as indicated by immunoblot analysis of D1.

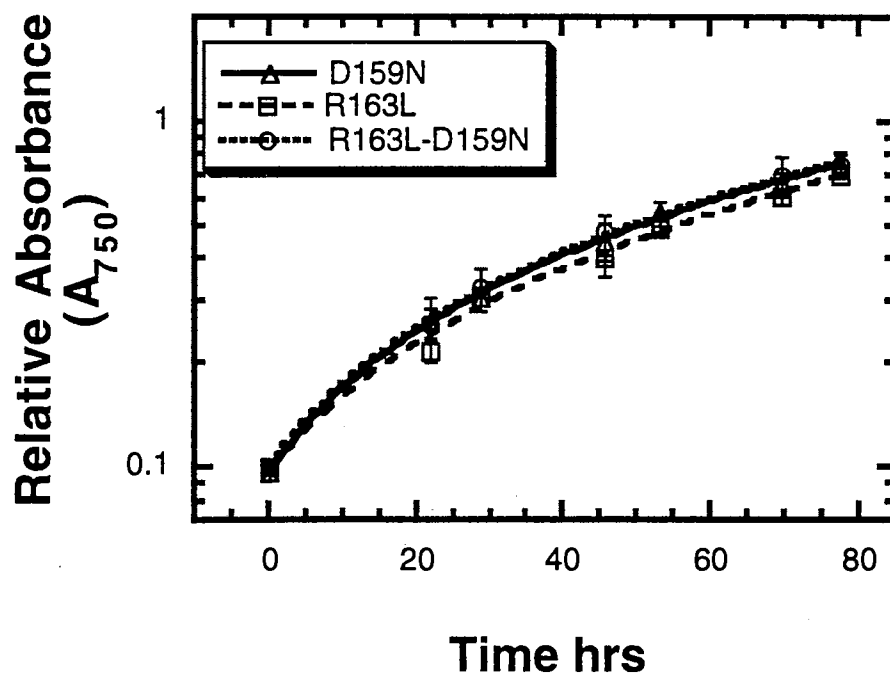


Figure 25: Growth rate of D159N, R163L, and D159N-R163L mutant strains in BG11 at 30°C in the absence of glucose. The absorbance readings represent the mean of three readings and the error bars represent the standard deviation.

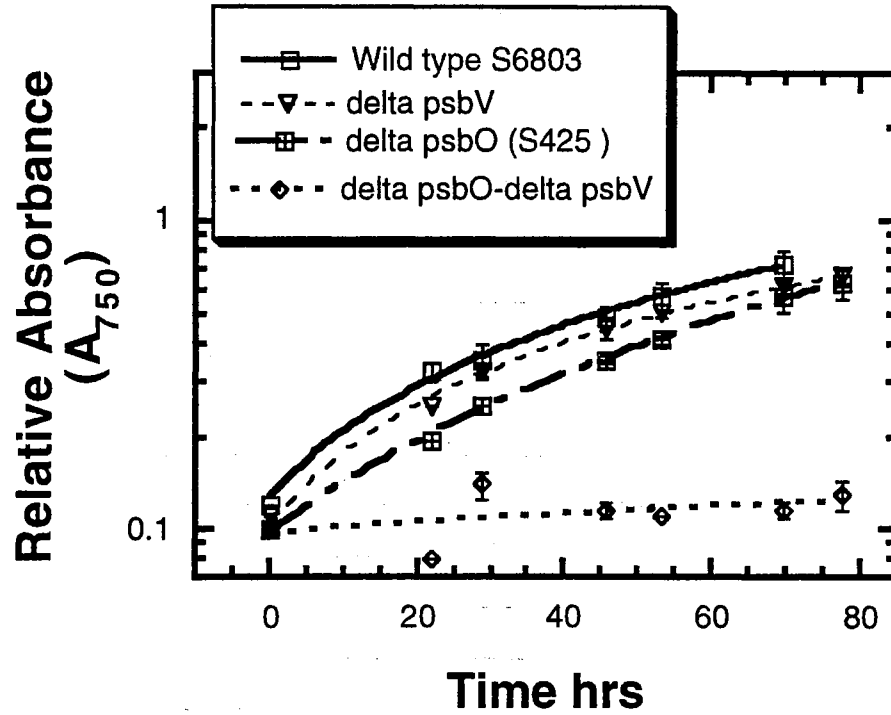


Figure 26 Growth rate of wild type , delta *psbV*, delta *psbO* (S425), and delta *psbO* delta *psbV* mutant strains in BG11 at 30°C in the absence of glucose. The absorbance readings represent the mean of three readings and the error bars represent the standard deviation.

## MSP Antibodies

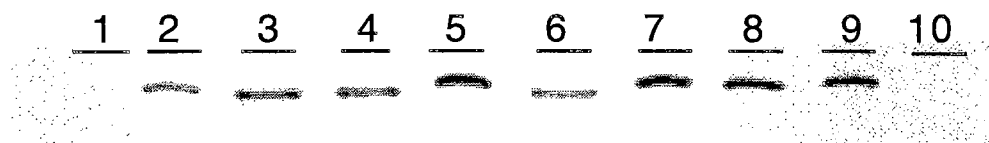


Figure 27: Immunoblot analysis of Anti-MSP in whole cell lysate. Sample analyzed: 1-  $\Delta psbV$ - $\Delta psbO$ , 2-  $\Delta psbV$ , 3-  $\Delta psbV$ -D159N-Arg163Leu, 4-  $\Delta psbV$  Arg163Leu, 5-  $\Delta psbV$  Asp159Asn, 6-Arg163Leu, 7-Asp159Asn, 8-Asp159Asn-Arg163Leu, 9-Wild type SS6803, 10-  $\Delta psbO$  (S425). Samples equivalent to 0.02  $\mu$ g of chlorophyll were loaded in each lane.



### Characterization of Oxygen Evolution ( $VO_{2, \max}$ )

Table 8 shows the maximal rates of  $O_2$  evolution ( $VO_{2, \max}$ ) in the presence of DCBQ and  $K_3Fe(CN)_6$  as an electron acceptor. The  $VO_{2, \max}$  of the  $\Delta psbV$ -Asp159Asn and  $\Delta psbV$ -Arg163Leu were 44% and 64%, respectively, compared to the  $VO_{2, \max}$  72% of the  $\Delta psbV$ -Asp159Asn-Arg163Leu. In agreement with the autotrophic growth curves, the lower  $VO_{2, \max}$  caused by the mutation of the  $\Delta psbV$ -Asp159Asn or the  $\Delta psbV$ -Arg163Leu was suppressed or compensated for by the higher  $VO_{2, \max}$  of the second mutation of Arg163Leu or Asp159Asn. This indicated that the introduction of the second mutation Asp159Asn or Arg163Leu in the background of  $\Delta psbV$ -Asp159Asn or  $\Delta psbV$ -Arg163Leu produced a marginal increase in the maximal rate of  $O_2$  evolution, to about 73% of the wild-type level.

### Comparison Effect of Stress-Inducing Agents on the Phenotype of Wild Type SS6803, $\Delta psbV$ and $\Delta psbO$

The combined results of the growth and oxygen evolution measurements were surprising since failure to grow autotrophically in PSII mutants is usually associated with a decrease in  $VO_{2, \max}$  to levels below 15% that of the wild type. Instead, the non-autotrophic mutants  $\Delta psb$ -Asp159Asn and  $\Delta psbV$ -Arg163Leu evolved oxygen at 44-64%. This suggests that something besides lowered PSII activity is impairing autotrophic growth. To begin to explore this hypothesis, we examined the effect of reagents of oxidative stress on cell growth since we hypothesize that mutations in MSP cause the production of toxic intermediates of  $H_2O$  oxidation and that absence of cyt c-550 aggravates that condition.

TABLE 8

OXYGEN-EVOLVING ACTIVITIES OF THE psbV  
DERIVATIVE MUTANTS

Strain	VO <sub>2,max</sub>
D159N	92
R163L	79
D159N-R163L	80
Δ psbV-D159N	44
Δ psbV-R163L	64
Δ psbV-D159N-R163L	72
ΔpsbV	56
ΔpsbV- ΔpsbO	14
Wild type (SS6803)	100

Table 8: Maximal high-saturated rate of O<sub>2</sub> evolution (VO<sub>2,max</sub>) expressed as a percentage of the rate observed for the wild type SS6803 (the VO<sub>2,max</sub> represents an average of the best 4-6 measurements). The average wild type rate was 633 μmol O<sub>2</sub> (mg chl)<sup>-1</sup> h<sup>-1</sup> under continuous saturating illumination at 30° C with the addition of 750 μM DCBQ and 4.5 mM K<sub>3</sub>Fe(CN)<sub>6</sub>, and with samples at a concentration of 10 μg chl. ml<sup>-1</sup>.

Stress-reducing agents were tested on the two strains. Table 9 shows the inhibition zone on BG11 plates of the two mutants  $\Delta psbO$  and  $\Delta psbV$  together with wild type SS6803 after adding  $H_2O_2$ , catalase, glutathiol and methyl viologen (MV).

The  $\Delta psbV$  mutant is more sensitive to  $H_2O_2$  than the  $\Delta psbO$  (S425) mutant and the wild type SS6803. In contrast, the  $\Delta psbO$  mutant is more resistant to the effect of MV than the  $\Delta psbV$  mutant and the wild type SS6803. Other chemicals such as glutathione did not have any detectable effect on the three strains. This suggests an interesting phenotypic effect of  $H_2O_2$  and MV on the two mutants  $psbV$ ,  $psbO$ , and the wild type SS6803.

TABLE 9

EFFECT OF STRESS OXIDATIVE-INDUCING AGENTS			
	SS6803	$\Delta$ -psbV	$\Delta$ -psbO
H <sub>2</sub> O <sub>2</sub>	18 mm	25 mm	15 mm
Glutathione	none	none	none
Methyl Viologen	34 mm	34 mm	15 mm

Table 9: Inhibition zone of the different chemicals which were added as follow: 0.15 % H<sub>2</sub>O<sub>2</sub>, 5  $\mu$ g catalase, 0.5 mM glutathione, and 20 mM MV. The strain cells were grown to the mid-log and 100  $\mu$ l of the culture was mixed with 3 ml of 0.7% agar layer on the top of 3.5-cm BG11 petri dish medium. The plates were incubated at 32<sup>0</sup> C at constant light.

## Discussion

Previous work has indicated that after the deletion of *psbO* and *psbV* from the wild type *Synechocystis* sp. PCC6803, the mutant could not grow photoautotrophically (47). In contrast, the *psbO* deletion mutant and the *psbV* deletion mutant could grow without glucose (44 Fig. 26). Thus, the *psbO* and *psbV* genes together support the photoautotrophic growth in *Synechocystis*.

In this work we have analyzed genetically-engineered mutants which have their amino acid Asp159 and Arg163 replaced by asparagine and leucine, respectively, in MSP in the absence or presence of cyt c-550. Our results indicated that after replacement of Asp159 by Asn in the absence of MSP, the mutant could not grow without glucose. Similarly, when Arg163 was changed to Leu in MSP in the absence of cyt c-550, the mutant also could not grow without glucose. However, when the two mutants Asp159Asn-Arg163Leu were put together in the absence of cyt c-550, the mutant grew photoautotrophically similar to the wild type. It seems that the two amino residues asparagine in the location of 159 and leucine in the location 163 not only interact but also suppress each other (Fig. 22B).

The sequence alignment of MSP, Figure 22, shows that Asp159 and Arg163 are highly conserved and furthermore are located in a highly conserved region. The aspartate and arginine amino acids are very close to each other and are separated by proline, lysine and alanine. The Pro residue can not assume an  $\alpha$  helical conformation or contribute a backbone hydrogen bond. Thus, the presence of Pro between Asp and Arg is likely to form a turn and, therefore, the two amino acids may interact ionically with each other.

In the absence of cyt c-550, changing one residue such as Asp or Arg to Asn or Leu of MSP, respectively, will decrease the hypothesized ionic interactions. Consequently, this causes conformational change to MSP folding or destabilization of PSII. This change

appears as an inability of the two mutants to grow without glucose in the  $\Delta psbV$  background. Our explanation of this is that these two sites, Asp 159 and Arg 163, either bind to cyt c-550 or are involved in the MSP interactions with cyt c-550.

It is interesting that the three mutants Asp159Asn, Arg163Leu and  $\Delta psbO$  in the absence of cyt c-550 all show the inability to grow photoautotrophically. This indicated that the effect of the two site-directed mutants Asp159Asn and Arg163Leu in the absence of cyt c-550 caused damage or lesion to PSII similar to the deletion of *psbO*. The inability of the two mutants to grow without glucose might be related to weak binding of MSP in such a way that MSP was totally unstable (as if it is deleted) and as a result, the stabilization of photosystem II or other proteins was affected.

In previous work, it was shown that any PSII mutant with 20% or higher of oxygen-evolving activities was able to grow autotrophically, whereas mutants with 20% or lower could not support autotrophic growth. For example, when Asp170 of D1 of PSII was replaced by Cys, Tyr, Arg, Met, Ala, Ser, and Phe, the mutants'  $VO_2, \max$  was 0-20% (in the presence of 0.3 mM DCBQ and 1 mM  $K_3Fe(CN)_6$  as an electron acceptor) and the mutants could not support the autotrophic growth of the cells ((16, 35). It seems that low oxygen-evolving activity (20%) is the minimum amount to support non-autotrophic growth of the cells

In striking contrast to these results, three mutants Asp159Asn, Arg163Leu, and  $\Delta$  MSP in the absence of cyt c-550 could not grow without glucose, yet the oxygen-evolving activities were 44-72% compared to the wild type in the presence of 0.75 mM DCBQ and 4.5 mM  $K_3Fe(CN)_6$  as an electron acceptor. The high rate of oxygen evolution of our mutants and the inability to grow autotrophically emphasize the uniqueness of our mutants. One explanation of this discrepancy is that the effect of the three mutants might be located somewhere other than in PSII such as in PSI or even in the Calvin cycle.

In order to explore this possibility, it is important to measure the photosynthesis electron transport whole chain activities by measuring the oxygen activity of the three mutants in the presence of  $\text{NaHCO}_3$ . The difference of  $\text{VO}_{2, \text{max}}$  of the three mutants in the presence of DCBQ/ $\text{K}_3\text{Fe}(\text{CN})_6$  and  $\text{NaHCO}_3$  as electron acceptors will indicate if the damage is located in PSII or somewhere else. For example, if the  $\text{VO}_{2, \text{max}}$  in the presence of DCBQ/ $\text{K}_3\text{Fe}(\text{CN})_6$  is high and  $\text{VO}_{2, \text{max}}$  is zero or less than 10% in the presence of  $\text{NaHCO}_3$ , this means that the major damage of our mutants might not be located in the PSII, but rather it might be located in another protein complex such as PSI. We have conducted preliminary work (with the help of J. Coker) which involved measuring the  $\text{VO}_{2, \text{max}}$  of two mutants ( $\Delta \text{cyt c-550 Asp159Asn}$ ,  $\Delta \text{cyt c-550 Asp159Asn-Arg163Leu}$ ) in the presence of DCBQ/ $\text{K}_3\text{Fe}(\text{CN})_6$  and  $\text{NaHCO}_3$  as electron acceptors separately. Indeed, the  $\Delta \text{cyt c-550 Asp159Asn}$  mutant has virtually no oxygen-evolving activities in the presence of  $\text{NaHCO}_3$ , whereas the mutant has 40% oxygen-evolving activity in the presence of DCBQ/ $\text{K}_3\text{Fe}(\text{CN})_6$ . In contrast, when  $\text{VO}_{2, \text{max}}$  of the  $\Delta \text{cyt c-550 Asp159Asn-Arg163Leu}$  mutant was measured in the presence of  $\text{NaHCO}_3$ , the oxygen-evolving activity was 40% which is similar to the oxygen-evolving activity in the presence of DCBQ/ $\text{K}_3\text{Fe}(\text{CN})_6$ . This indicates that PSII is relatively stable and the damage of the mutants might be in PSI or somewhere in the Calvin cycle.

The phenotype and the oxygen-evolving activities of the  $\Delta \text{psbO-}\Delta \text{psbV}$  mutant are comparable to the same mutant which was created by Shen et al.(47) . The latter  $\Delta \text{psbO-}\Delta \text{psbV}$  mutant could not grow without glucose (similar to our mutant) and the oxygen-evolving activities were 8% (our mutant was 15%) compared to the wild type in the presence of 0.5 mM DCBQ (our concentration was 0.75 mM) and 1 mM  $\text{K}_3\text{Fe}(\text{CN})_6$  (our concentration was 4.6 mM). This difference may be related to the amount of DCBQ and  $\text{K}_3\text{Fe}(\text{CN})_6$  added to the reaction during  $\text{VO}_{2, \text{max}}$  measurements or differences in culture conditions.

Immunoblot analysis of the MSP protein in all the mutants (Fig. 27) indicated a normal level of MSP expression. In contrast, the low D1 accumulation in the *psbV* deletion derivative mutants (data not shown) was consistent with the previous observation by Shen et al. (47) that D1 accumulation decreases in PSII of the  $\Delta psbV$ - $\Delta psbO$  mutant. This differential impact on these two proteins is consistent with the interpretation that the mutations cause the destabilization of the intrinsic portion of PSII, as has been shown for other PSII mutations. Further experiments (e.g. pulse-labeling of proteins) would be required to prove this hypothesis.

Table 9 indicates that  $\Delta psbV$  was the most sensitive to  $H_2O_2$  and MV (the wildtype was sensitive to MV similar to  $\Delta psbV$ ) suggesting that possible involvement of cyt c-550 in detoxification of radicals. Table 9 also indicates that the  $\Delta psbO$  mutant was the most resistant to  $H_2O_2$  and MV. Previous work indicated that MSP works as a barrier between PSII and the surroundings on the lumenal side compared to the wild type (9, 39). This was suggested because the  $\Delta psbO$  mutant was discovered to have faster photoactivation. The  $\Delta psbO$  mutant resistance to  $H_2O_2$  and MV in the absence of the MSP may indicate greater accessibility of proteolytic enzymes to photodegraded D1 or D2, such that the turnover of D1 and D2 is more efficient than when MSP is present. Accurate quantitative studies of the D1 and D2 in the presence of  $H_2O_2$  and MV are required to prove this hypothesis. The  $\Delta psbO$  mutant resistance to  $H_2O_2$  and MV in the absence of MSP may also be explained by the hypothesized greater accessibility of the Mn cluster to  $H_2O_2$  molecules, causing  $H_2O_2$  to be oxidized by the Mn cluster and decreasing the effect of  $H_2O_2$ .



## CHAPTER VI

### HETEROLOGOUS EXPRESSION OF MSP

#### Introduction

The MSP of *Synechocystis* sp. PCC6803 consists of 274 amino acids including a 28 amino acids leader sequence. This leader sequence works as a signal peptide for MSP to cross the thylakoid membrane to the lumen. The thylakoid lumen can be considered topologically identical to the cell periplasmic space and that the thylakoids represent highly convoluted invaginations of the cytoplasmic membrane. The signal peptide of MSP *Synechocystis* sp. MSP exhibits 48-49% homology to higher plant MSP (42). The processing mechanism of the leader sequence of the exported protein is also similar to the *E. coli* processing mechanism (20, 40, 42). Similarly, the leader sequence of the MSP protein of wheat is recognized and proteolytically cleaved by *E. coli* leader peptidase (20).

*Arabidopsis* MSP expressed heterologously in *E. coli* restored spinach oxygen-evolving complex activity (2). Reconstitution of the spinach oxygen-evolving complex with native MSP or *Arabidopsis* MSP respectively restored 67% and 58% of the steady-state rate of oxygen evolution lost following MSP extraction. This indicated that the reconstitution of the heterologous subunit is 87% as effective as the native MSP to the spinach oxygen-evolving complex.

I expressed the heterologous MSP in *E. coli* in order to conduct reconstitution experiments of the heterologous MSP with the oxygen-evolving complex in some of the *Synechocystis* site-directed MSP mutants. This will ultimately help us study the oxygen-

evolving activity of PSII in vitro rather than in vivo. My work included isolating and purifying heterologously expressed MSP. Our data demonstrate the expression of MSP of *Synechocystis* in *E. coli* and the fact that the heterologously expressed protein is exported to the periplasmic space of *E. coli* where it may be purified in the future. Our expression system was also used to monitor the expression of MSP of some of the site-directed mutants which were generated in our lab (M. Qian-unpublished data).

## Results

Figure 28 shows Western blot analysis. Three different subcellular fractions of *E. coli* were collected and analyzed. Lanes 5, 6, and 7 respectively show the periplasmic, cytoplasmic, and membrane fraction of *E. coli* after inducing the cells at ( $A_{600}=0.7$ ) by 0.4 mM IPTG for 2.5 hrs. This suggests that MSP is heterologously expressed in *E. coli* BL21 (DE3) and is exported to the periplasmic space of *E. coli*, indicating that the leader sequence of the MSP (28 amino acids) protein is recognized by the *E. coli* translocation machinery. Lanes 8, 9, and 10 show the same as in lanes 5, 6, and 7, but the *E. coli* culture was induced with 0.4 mM of IPTG at the beginning of the growth cycle. It appears that the IPTG inhibited the growth rate of the cells.

These data are not a quantitative study of the MSP expression and the decrease of MSP expression in lanes 8, 9, and 10 represents a decrease of cell growth rather than a decrease of protein expression. Nevertheless, the expression system worked very well without the need to clone the *psbO* gene in an expression vector. Thus the maximum expression, which gave a very high yield of heterologous MSP, was conducted at 28° C instead of 37° C.

Further work was continued to optimize the heterologous expression of MSP. Figure 29 shows the periplasmic fraction of heterologous MSP expression at different time intervals. Lanes 3, 4, and 5 show zero, one hour, and three hours of 0.4 mM IPTG induction. This indicates that the induction of heterologous MSP expression increases gradually for two hours (visual observation only). Further increased increment of MSP expression was not detectable after two hours of induction (Fig. 30).

In addition, our expression system is a good model to explore the expressions of MSP site-directed mutants which were generated by M. Qian (unpublished data).

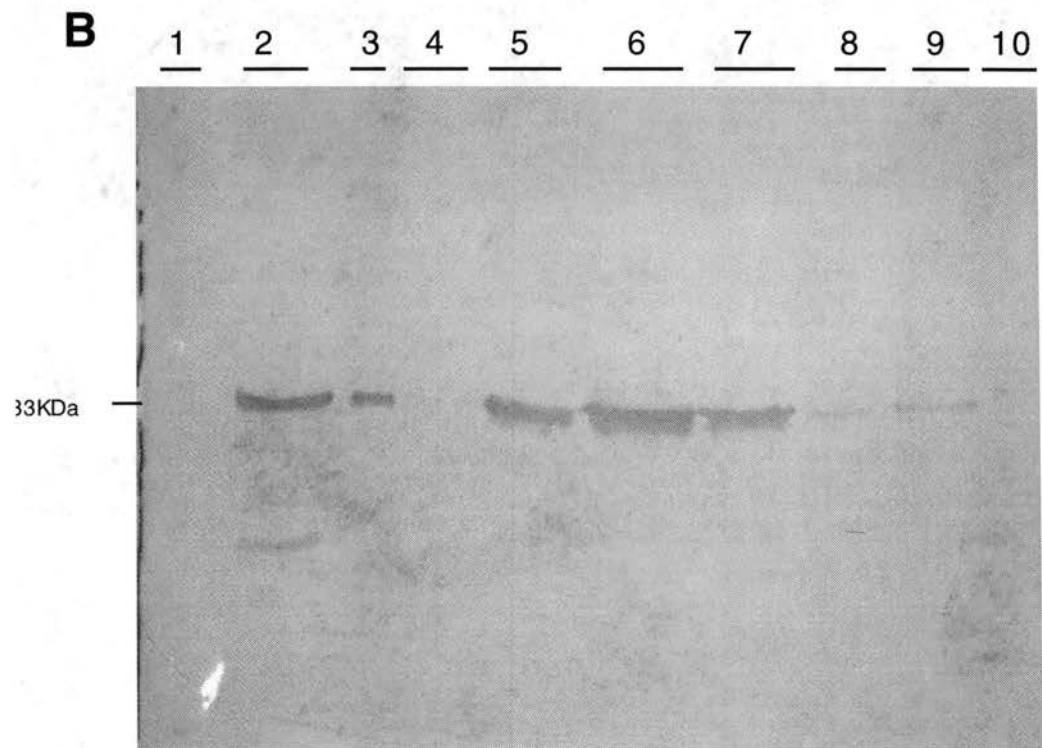
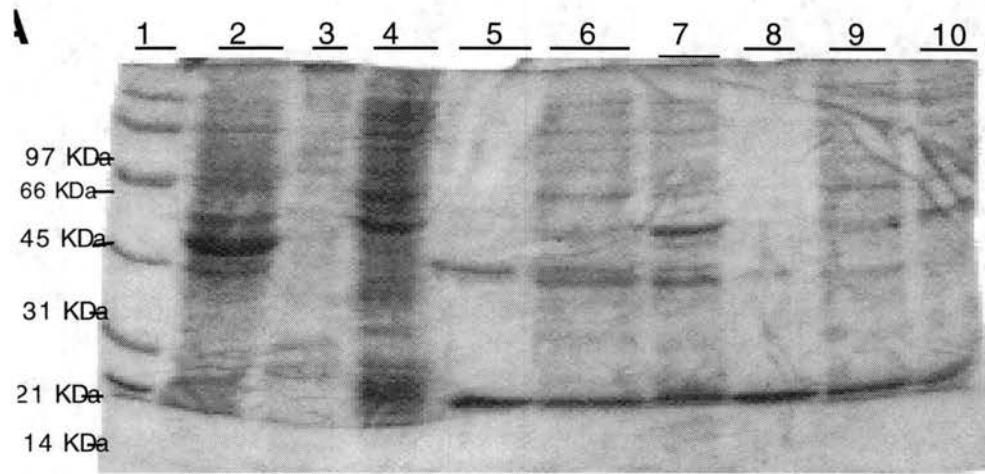


Figure 28: Immunoblot analysis of heterologous MSP. Panel A shows a Coomassie stained SDS-Page gel and panel B shows the Western blot of the same gel. Sample analyzed: Lane 1-Protein standard, Lane 2- Periplasmic fraction of MSP (2 hrs IPTG induction- positive control), lane 3- Native MSP (*Synechocystis* membrane), lane 4- Periplasmic fraction of *E. coli* BL21 (DE3) cells do not have MSP (negative control). Lane 5, 6, 7 include the periplasmic, cytoplasmic, and membrane fraction of MSP, respectively. The culture was induced when the cells reached to  $A_{600}=7-1$  with 0.4 mM IPTG and the culture was incubated in 28° C for 2.5 hrs. Lane 8, 9, and 10 include the periplasmic, cytoplasmic, membrane fraction of heterologous MSP, respectively. The cells were induced immediately (without any incubation period) with 0.4 mM IPTG and the culture was incubated in 28° C for 2.5 hrs.

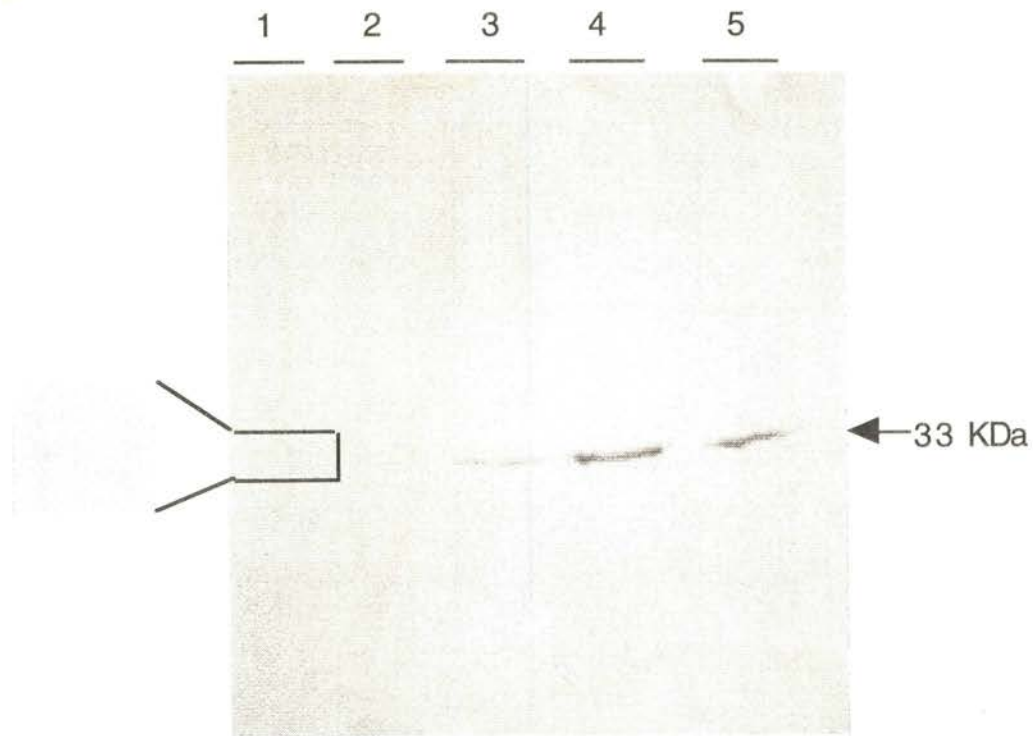


Figure 29: Immunoblot analysis of heterologous MSP at different time intervals. Sample analyzed: Lane 1- Native MSP (*Synechocystis* membrane), lane 2- Periplasmic fraction of *E. coli* BL21 (DE3) cells does not have MSP (negative control). Lanes 3, 4, 5 include the periplasmic fraction of MSP with zero, 1, 2 hrs induction, respectively. The culture was induced when the cells reached to  $A_{600}=0.7-1$  with 0.4 mM IPTG and the culture was incubated at  $28^{\circ}\text{C}$  for 2.5 hrs.

Heterologous Expression of the site-directed mutants will be a good test for uncovering a second site or unwanted mutation. Figure 30 shows a Western blot analysis of a periplasmic fraction of heterologously expressed MSP of some of the selected site-directed MSP mutants generated in our lab. Lanes 4, 5, 6, 7, 8, and 9 include the periplasmic fraction of Asp10His, Arg163Leu, Asp159Asn, Glu209stop, Asn138Lys, and Asp159Asn-Arg163Leu, respectively. These results indicated that all the site-directed mutants expressed MSP heterologously except the nonsense mutation Glu290stop.

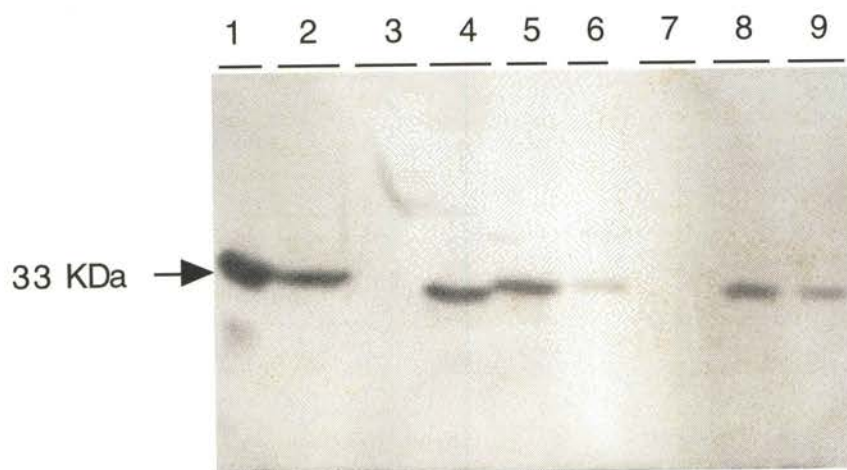


Figure 30: Immunoblot analysis of heterologous MSP. Sample analyzed: Lanes 1, 2, 3, 4, 5, 6, 7, 8, and 9 represent MSP heterologous wild type *E. coli*, MSP native wild type *Synechocystis*, Asp10His, Arg163Leu, Asp159Asn, Glu290stop, Asn138Lys, and Asp159Asn-Arg163Leu, respectively. The culture was induced when the cells reached to  $A_{600}=0.7-1.0$  with 0.4 mM IPTG and the culture was incubated at 28° C for 2.5 hrs.



## Discussion

Our data using Western blot analysis suggests that when we heterologously express the *psbO* gene in *E. coli* BL21 (DE3), the protein is exported to the periplasmic space indicating that the leader sequence of the MSP protein is recognized by the *E. coli* translocational machinery (7). Figure 28 shows that the recombinant MSP is expressed in the three fractions: periplasmic, membrane, and cytoplasm. Our system worked very well without the need to clone a *psbO* gene in an expression system such as pET vector.

We concluded that expressing pRB81 (Bluescript Sk-) carrying the *psbO* gene can be achieved at 28° C rather than 37° C (data not shown). One simple explanation is that the process of the translocation of the preMSP across the membrane in *E. coli* was not as efficient at 37° C as at 28° C. Betts et al. (2) indicated that cells grown with vigorous aeration and induced with 0.4 mM IPTG accumulated preMSP to very high levels, but were deficient in their ability to process the protein. We propose that the inability to observe a detectable mature heterologous MSP in the periplasmic space fraction at 37° C might be related to the accumulation of preMSP and the inability of the preMSP to be translocated across the membrane.

The optimal induction of MSP heterologous expression was not rigorously defined in this study. It only provided an indication of the best time to harvest the heterologously expressed MSP. The system works very well to monitor the expression of MSP heterologously in some of the site-directed mutants (Fig. 28). This helped to exclude the presence of any stop mutation up or downstream of the intended site-directed mutants which might be located in the *psbO* gene. However, this system is not sensitive enough to detect some of the missense mutations which might alter the *psbO* sequence, but will not alter the expression of MSP heterologously.

Our work also included purifying heterologous MSP from *E. coli* using  $(\text{NH}_4)_2\text{SO}_4$  precipitation. We used different concentrations of  $(\text{NH}_4)_2\text{SO}_4$  and we concluded that a 40-60 % cut is the optimal condition to concentrate the MSP heterologous protein without losing it (data not shown). Preliminary experiments to achieve further purification were done by using DEAE column. Purifying the heterologous MSP protein further is a remaining goal.

Finally it should be noted that in this work we did not study the molecular weight of the heterologous MSP. Such a study needs N-terminal protein sequencing and this was beyond the scope of this work.

## CHAPTER VII

### CONCLUSIONS AND RECOMMENDATIONS

#### Isolating Calcium-Dependent Mutants

In this work we have been able to isolate and analyze calcium-dependent mutants of *Synechocystis* sp. PCC6803. We used an *E. coli* mutator strain to randomly mutagenize a 6.4 kb *Hind*III fragment containing the *psbO*, Kanamycin cassette, *trnQ*, *aroA*, and three small polypeptides. Two calcium-dependent mutants were isolated using calcium-depletion medium enrichment and screening. Our data indicate that these two mutants exhibited alteration in the lag growth phase, oxygen-evolving activity, and protein binding to PSII compared to the wild type. However, sequence analysis of the *psbO* gene in the calcium-dependent mutants 39A and 43A indicated the absence of any sequence alteration compared to the wild type.

The alteration of the physiology of the two mutants might be related to the location of the point mutation(s) located out of the *psbO* sequence limits. Instead of sequencing a 6.4 kb *Hind*III fragment, it was important to select a strategy which localized the putative mutation on a sub-fragment. Therefore, a restriction enzyme such as *Eco*R5 was used to digest the pSSO39 and pSSO43 plasmids. This enzyme cuts at a location which is 427 bp from the *Afl*III restriction enzyme site representing the left end of the spectinomycin cassette, which replaces the *psbO* gene in the *psbO* deletion mutant S425, (Fig. 4). Digesting the two plasmids with *Eco*R5, will also eliminate the possibility of the 2.3 kb carrying *trnQ* and *aroA* genes from integrating in the chromosome after transforming the *psbO* deletion mutants (Fig. 2).

We have been able to create the two mutants again using the above strategy and they were named 39C and 43C. These two mutants should have the *psbO*, kanamycin, and three polypeptide proteins integrated and should have replaced the spectinomycin of the *psbO* deletion mutants. Hypothetically, these mutants should exhibit the same phenotypic alteration of the 39A/39B and 43A/43B, respectively, if the point mutation(s) is located in the sequence of any of the three small polypeptides.

Further sequence analysis should be conducted further on the DNA fragments which encode for the small polypeptides only. This might give the precise location of the mutation.

#### Interaction between MSP and Cytochrome c-550

In this work we have been able to create site-directed mutants in MSP in the absence of cyt c-550. These mutants were as follows:  $\Delta$  cyt c-550 Asp159Asn,  $\Delta$  cyt c-550 -Arg163Leu and  $\Delta$  cyt c-550 -Asp159Asn-Arg163Leu. The first two mutants could not grow without glucose, but exhibited 44-64% oxygen-evolving activity compared to the wild type. Thus, when the two site-directed mutants were together, as in the  $\Delta$  cyt c-550 -Asp159Asn-Arg163Leu, the mutant could grow without glucose and the oxygen-evolving activities were 72% compared to the wild type. This indicated that each mutant suppressed or countered the effect of the other.

It is interesting that these mutants have high oxygen-evolving-activities since failure to grow autotrophically in PSII mutants is usually associated with a more dramatic decrease in  $VO_{2,max}$ . Our hypothesis is that the effects of our two mutants were hidden in the presence of cyt c-550 and only when cyt c-550 was genetically removed, were the full effects of the mutations revealed. Since oxygen evolution was not fully impaired, it appears that the affected locus is elsewhere. Preliminary experiments suggest that  $CO_2$  fixation is impaired. Therefore, it will be interesting to explore the precise role of cyt c-550

and the possible interaction(s) of this protein with other protein(s) which might play a role in the whole electron transport chain and the calcium cycle of photosynthesis.

### Heterologous Expression of MSP

We have been able to establish an *E. coli* expression system for MSP using the Bluescript plasmid. Heterologous MSP was not only produced by *E. coli*, but it was also exported to the periplasmic space. This helped to increase the purity of the recombinant MSP. The developed expression system can also be used to test the presence of any nonsense mutations which are located up or downstream of *psbO* site-directed mutants. Furthermore, the recombinant protein needs to be purified and concentrated in order to reconstitute polypeptide depleted PSII in vitro. It will be interesting to compare the restoration of oxygen-evolving activity in vitro by adding recombinant or native MSP.

## REFERENCES

1. **Bakou, A., C. Buser, G. Dandulakis, G. Brudvig, and D. Ghantoakis.** 1992. Calcium binding site(s) of Photosystem II as probed by lanthanides. *Biochimica et Biophysica Acta*. **1099**:131-136.
2. **Betts, S. D., T. M. Hachigian, E. Pichersky, and C. F. Yocum.** 1994. Reconstitution of the spinach oxygen-evolving complex with recombinant *Arabidopsis* manganese-stabilizing protein. *Plant Molecular Biology*. **26**:117-130.
3. **Boussac, A., J. L. Zimmermann, and A. W. Rutherford.** 1989. EPR signals from modified charge accumulation states of the oxygen evolving enzyme in calcium deficient photosystem II. *Biochemistry*. **28**:8984-8989.
4. **Bricker, T. M.** 1992. Oxygen evolution in the absence of the 33-kilodalton manganese stabilizing protein. *Biochemistry*. **31**:4623-4628.
5. **Brudvig, G. W., W. F. Beck, and J. C. de Paula.** 1989. Mechanism of photosynthetic water oxidation. *Annu. Rev. Biophys. Biophys.Chem.* **18**:25-46.
6. **Burnap, R., H. Koike, G. Sotiropoulou, L. A. Sherman, and Y. Inoue.** 1989. Oxygen evolving membranes and particles from the transformable cyanobacterium *Synechocystis* sp. PCC6803. *Photosynth. Res.* **22**:123-130.
7. **Burnap, R., H. Koike, G. Sotiropoulou, L. A. Sherman, and Y. Inoue.** 1992. Oxygen yield and thermoluminescence characteristics of a cyanobacterium lacking the manganese-stabilizing protein of photosystem II. *Biochemistry*. **31**:7404-7410.

8. **Burnap, R., and L. A. Sherman.** 1991. Deletion mutagenesis in *Synechocystis* sp. PCC6803 indicates the Mn-stabilizing protein of photosystem II is not essential for O<sub>2</sub> evolution. *Biochemistry*. **30**:440-446.
9. **Burnap, R. L., M. Qian, and C. Pierce.** 1996. The manganese-stabilizing protein of photosystem II modifies the in vivo deactivation and photoactivation kinetics of the H<sub>2</sub>O oxidation complex in *Synechocystis* sp. PCC6803. *Biochemistry*. **35**:874-882.
10. **Burnap, R. L., M. Qian, J. R. Shen, Y. Inoue, and L. A. Sherman.** 1994. Role of disulfide linkage and putative intramolecular binding residues in the stability and binding of the extrinsic manganese-stabilizing protein to the photosystem II reaction center. *Biochemistry*. **33**:13712-13718.
11. **Cammarata, K. V., and G. M. Chebuae.** 1987. Studies on 17, 24 KDa depleted photosystem II membrane. Evidences for high and low affinity calcium sites in 17, 24 KDa depleted PSII membranes from wheat versus spinach. *Plant Physiol*. **84**:587-595.
12. **Carpenter, E. J.** 1983. Marine fixation by marine *Oscillataria "Trichodesmium"*, p. 65-104. *In* E. J. Carpenter and D. G. Capore (ed.), *The world's oceans, in nitrogen in the marine environment*. Academic Press, New York.
13. **Carr, N. G., and M. Wyman.** 1986. Cyanobacteria: Their biology in relation to oceanic picoplankton. *Ca. Bull. Fish. Aquat. Sci.* **214**:159-204.
14. **Chauvat, F., P. Rouet, H. Bottin, and A. Boussac.** 1989. Mutagenesis by random cloning of an *Escherichia coli* kanamycin resistant gene into genome of cyanobacterium *Synechocystis* PCC6803: Selection of mutants defective in photosynthesis. *Mol. Gen. Genetic.* **216**:51-59.

15. **Cheniae, G. M., and I. F. Martin.** 1971. Photoactivation of the manganese catalyst of O<sub>2</sub> evolution. 1. Biochemical and kinetic aspects. *Biochimica et Biophysica Acta.* **253**:167-181.
16. **Chu, H.-A., A. P. Nguyen, and R. J. Debus.** 1995. Amino acid residues that influence the binding of manganese or calcium to photosystem II. 2. The carboxy-terminal domain of the D1 polypeptide. *Biochemistry.* **34**:5859-5882.
17. **Debus, R. J.** 1992. The manganese and calcium ions of photosynthetic oxygen evolution. *Biochimica et Biophysica Acta.* **1102**:269-352.
18. **Gleiter, H., E. Haag, J. R. Shen, Y. Inoue, W. F. Vermaas, and G. Reger.** 1994. Functional characterization of mutant strains of the cyanobacteria *Synechocystis* sp. PCC6803 lacking short domains within the large, lumen-exposed loop of the chlorophyll protein CP47 in photosystem II. *Biochemistry.* **33**:12063-12071.
19. **Grindley, N. D., and R. R. Reed.** 1985. Transpositional recombination in prokaryotes. *Annu. Rev. Biochem.* **54**:863-896.
20. **Halpin, C., P. D. Elderfield, H. E. James, R. Zimmermann, B. Dunbar, and C. Robinson.** 1989. The reaction specificities of the thylakoidal processing peptidase and *Escherichia coli* leader peptidase are identical. *The EMBO Journal.* **8**:3917-3921.
21. **Hensyl, W. R. (ed.).** 1989. Oxygenic photosynthetic bacteria, vol. 3. Williams & Wilkins, Baltimore, MD 21202, USA.
22. **Inoue, H., H. Nojima, and H. Okayama.** 1990. High efficiency transformation of *Escherichia coli* with plasmids. *Gene.* **96**:23-28.



23. **Janssen, I., J. Jakowistich, C. B. Michalowski, H. J. Bohnert, and W. Loffelhardt.** 1989. Evolutionary relationship of *psbA* genes from cyanobacteria, cyanelles and plastids. *Current Genetics*. **15**:335-340.
24. **Kana, T. M.** 1992. Relationship between photosynthetic oxygen cycling and carbon assimilation in *Synechococcus* WH7803 (cyanobacteria). *J. Phycol.* **28**:304-308.
25. **Kaneko, T., S. Sato, H. Kotani, A. Tanaka, E. Asamizu, Y. Nakamura, N. Miyajima, M. Hirosawa, M. Sugiura, S. Sasamoto, T. Kimura, T. Hosouchi, A. Matsuno, A. Muraki, N. Nakazaki, K. Naruo, S. Okumura, S. Shimpo, C. Takeuchi, T. Wada, A. Watanabe, M. Yamada, M. Yasuda, and S. Tabata.** 1996. Sequence analysis of the genome of the unicellular cyanobacterium *Synechocystis* sp. strain PCC6803. II. Sequence determination of the entire genome and assignment of potential protein-coding regions. *DNA Research*. **3**:109-136.
26. **Krogmann, D. W.** 1991. The low-potential cytochrome c of cyanobacteria and algae. *Biochimica et Biophysica Acta*. **1058**:35-37.
27. **Kura-Hotta, M., S. Katoh, and K. Satoh.** 1986. Functional linkage between phycobilisome and reaction center in two phycobilisome oxygen-evolving photosystem II preparations isolated from the thermophilic cyanobacterium *Synechococcus* sp. *Arch. Biochem. Biophys.* **249**:1-7.
28. **Kuwabara, T., M. Miyao, T. Murata, and N. Murata.** 1985. The function of 33-kilodalton protein in the photosynthetic oxygen-evolution system studied by reconstitution experiments. *Biochimica et Biophysica Acta* **806**:283-289.
29. **Kuwabara, T., K. J. Reddy, and L. A. Sherman.** 1987. Nucleotide sequence of the gene from the cyanobacterium *Anacystis nidulans* R2 encoding the Mn

Stabilizing protein involved in Photosystem II water oxidation. Proc. Natl. Acad. Sci. USA :8230-8234.

30. **Matsunaga, T., H. Takeyama, and N. Nakamura.** 1990. Characterization of cryptic plasmid from marine cyanobacteria and construction of a hybrid plasmid potentially capable of transformation of marine cyanobacteria *Synechococcus* sp. and its transformation. Applied Biochemistry and Biotechnology. **24/25**:151-160.
31. **McClary, J. A., F. Witney, and J. Geisselsoder.** 1989. Efficient site-directed in vitro mutagenesis using phagemid vector. BioTechniques. **7**:282-289.
32. **Michael, S.** 1985. In vitro mutagenesis. Ann. Rev. Genet. **19**:423-62.
33. **Miyao, M., and N. Murata.** 1984. Effect of urea on photosystem II particles. Evidence for an essential role of the 33 kilodalton polypeptide in photosynthetic oxygen evolution. Biochimica et Biophysica Acta. **765**:253-257.
34. **Nakatani, H. Y.** 1984. Photosynthetic oxygen evolution does not require participation of polypeptide of 16 and 24 kilodaltons. Biochem. Biophys. Res. Commun. **120**:299-304.
35. **Nixon, P., and B. Diner.** 1992. Aspartate 170 of the Photosystem II reaction center polypeptide D1 is involved in the assembly of the oxygen-evolving manganese cluster. Biochemistry. **31**:942-948.
36. **Odom, W. R., and T. M. Bricker.** 1992. Interaction of cpa-1 with the manganese-stabilizing protein of photosystem II identification of domains cross-linked by 1 ethyl-3-(3-dimethylaminopropyl)-carbodiimide. Biochemistry. **31**:5616-5620.
37. **Palomares, R., R. G. Herrmann, and Oelmüller.** 1993. Post-transcriptional and post-translational regulatory steps are crucial in controlling the appearance and stability

of thylakoid polypeptides during the transition of etiolated tobacco seedlings to white light. *European Journal of Biochemistry*. **217**:345-352.

38. **Philbrick, J. B., and B. A. Zilinskas.** 1988. Cloning, nucleotide sequence and mutational analysis of the gene encoding the photosystem II manganese-stabilizing polypeptide of *Synechocystis* 6803. *Mol. Gen. Genet.* **212**:418-425.

39. **Qian, M., S. F. Al-Khalidi, C. Putnam-Evans, T. M. Bricker, and R. L. Burnap.** 1997. Photoassembly of the photosystem II (Mn)<sub>4</sub> cluster in site-directed mutants impaired in the binding of the manganese-stabilizing protein. *Biochemistry*. **36**:15244-15252.

40. **Rabinson, C., and R. B. Klossgen.** 1994. Targeting of the proteins into and across the thylakoid membrane - a multitude of mechanisms. *Plant Molecular Biology*. **26**:15-24.

41. **Sambrook, J., E. F. Fritsch, and T. Maniatis.** 1989. *Molecular cloning : A laboratory manual*, 2 ed. Cold Spring Harbor Laboratory, Cold Spring Harbor, New York.

42. **Seidler, A.** 1996. The extrinsic polypeptides of photosystem II. *Biochimica et Biophysica Acta*. **1277**:35-60.

43. **Shen, J.-R., M. Qian, Y. Inoue, and R. L. Burnap.** 1998. Functional characterization of *Synechocystis* sp. PCC6803 delta *psbU* and *psbV* mutants reveals important roles of cytochrome c-550 in cyanobacteria oxygen evolution. *Biochemistry*. (In press).

44. **Shen, J. R., R. L. Burnap, and Y. Inoue.** 1995. An independent role of cytochrome c-550 in cyanobacteria I photosystem II as revealed by double-deletion mutagenesis of the *psbO* and *psbV* genes in *Synechocystis* sp. PCC 6803. *Biochemistry*. **34**:12661-12668.

45. **Shen, J. R., M. Ikeuchi, and Y. Inoue.** 1992. Stoichiometric association of extrinsic cytochrome c-550 and 12 KDa protein with a highly purified oxygen-evolving photosystem II core complex from *Synechococcus vulcanus*. FEBS lett. **301**:145-149.
46. **Shen, J. R., and Y. Inoue.** 1993. Binding and functional properties of two new extrinsic components, cytochrome c-550 and a 12-KDa protein, in cyanobacteria photosystem II. Biochemistry. **32**:1825-1832.
47. **Shen, J. R., W. Vermaas, and Y. Inoue.** 1995. The role of cytochrome c-550 as studied through reverse genetics and mutant characterization in *Synechocystis* sp. PCC6803. J. Biol. Chem. **270**:6901-6907.
48. **Silva, A. C. and Reinach. F. C.** 1991. Calcium binding induces conformational changes in muscle regulatory protein. TIBS. **5076**:53-57
49. **Studier, F. W., A. H. Rosenberg, J. J. Dunn, and Dubendorff. J. W.** 1990. Use of T7 RNA polymerase to direct expression of cloned genes, p. 60-89. *In* D. V. Goeddel (ed.), Methods in Enzymology, vol. 185. Academic Press Inc., San Diego, CA 92101-4495.
50. **Tamura, N., and G. Cheniae.** 1987. Photoactivation of the water-oxidizing complex in Photosystem II membranes deleted of Mn and extrinsic proteins. I. Biochemical and kinetic characterization. Biochimica et Biophysica Acta. **890**:179-194.
51. **Williams, J. G. K.** 1988. Construction of specific mutations in Photosystem II photosynthetic reaction center by genetic engineering methods in *Synechocystis* 6803. Meth. Enzymol. **167**:766-778.
52. **Yocum, C. F.** 1990. Calcium activation of photosynthetic water oxidation. Biochimica et Biophysica Acta. **1059**:1-15.

2

VITA

Sufian F. Al-Khaldi

Candidate for the Degree of

Doctor of Philosophy

Thesis: GENETIC ANALYSIS OF PHOTOSYNTHESIS *psbO* AND *psbV*  
GENES IN CYANOBACTERIA *Synechocystis* SP PCC6803

Major Field: Microbiology & Cell and Molecular Biology

Biographical:

Personal Data: Born in Kuwait, December 18, 1962, the son of Fawzi Al-Khaldi and Entisar Shaat.

Education: Graduate from Abdullah Al-Salem High School , Kuwait, in 1980: received BS in Microbiology from the University of Baghdad, Iraq, in 1985; 1992 received MS in Microbiology and Molecular Genetics from Oklahoma State University, USA, completed the requirements for the Doctor of Philosophy in May 1998.

Professional Experience: Clinical Microbiologist at Ibn Sina Hospital, Kuwait, 1986-1990; Teaching Assistant, Oklahoma State University Jan. 1990-Dec. 1997.

Professional Organization: American Society for Microbiology